NATIONAL ADVISORY COMMITTEE FOR AERONAUTICS

TECHNICAL NOTE 2926

STATIC FORCE-DEFLECTION CHARACTERISTICS OF SIX AIRCRAFT TIRES UNDER COMBINED LOADING

By Walter B. Horne

Langley Aeronautical Laboratory
Langley Field, Va.

Washington
May 1953

NATIONAL ADVISORY COMMITTEE FOR AERONAUTICS

TECHNICAL NOTE 2926

STATIC FORCE-DEFLECTION CHARACTERISTICS OF SIX AIRCRAFT TIRES UNDER COMBINED LOADING

By Walter B. Horne

SUMMARY

Static force-deflection tests were made on six aircraft tires ranging in size and ply rating from a diameter of 56 inches and a ply rating of 32 to a diameter of 27 inches and a ply rating of 10. These tests included the vertical loading of all six tire specimens and, for five of the tire specimens, combined vertical loading and side loading and combined vertical loading and torsional loading. The vertical loading combined with the fore-and-aft (longitudinal) loading of one tire specimen and the distortion of the center or equatorial line of this tire under side loading were also determined. The tire deflections, vertical-load center-of-pressure shifts, and the increases in tire pressure resulting from the different loadings were measured.

The lateral spring constants for all tire specimens generally decreased with increasing vertical tire deflection; whereas, the torsional and fore-and-aft spring constants were found to increase with increasing vertical tire deflection. Increasing the inflation pressure tended to increase the torsional stiffness of the tires. The vertical-load center-of-pressure shifts due to side and fore-and-aft loadings were found to average 75 percent and 25 percent, respectively, of the side and fore-and-aft tire deflections. An approximate 8-percent increase in tire pressure over the initial inflation pressure was noted for each tire when subjected to 50 percent of the maximum vertical tire deflection.

INTRODUCTION

Existing experimental data on aircraft-tire behavior under dynamic and static conditions are limited in scope and quantity and, for the most part, cover only the smaller tire sizes. This lack of data has been felt by those engaged in research on landing problems, such as wheel shimmy and landings with yaw. Experimental values of the tire parameters for the larger tire sizes are also needed for comparison with present theories on tire stiffness so that the validity of these theories

for the larger range of tire size may be determined. In order to help fulfill this need, a program has been started to determine values of the essential tire parameters under static, kinematic, and dynamic conditions. This paper presents the results of the static force-deflection tests of the program. Six aircraft tires ranging in size and ply rating from a diameter of 56 inches and a ply rating of 32 to a diameter of 27 inches and a ply rating of 10 were tested. This range in tire size covers most aircraft tires in current usage.

The tests made included the following types of loading: vertical, combined vertical and side, combined vertical and torsion, and combined vertical and fore-and-aft (longitudinal) for different tire inflation pressures. The quantities measured included tire deflection, change in tire pressure, and shift of the vertical-load center of pressure resulting from these loadings. The distortion of the center or equatorial line of the tire under side loading was measured for one tire.

The maximum vertical load applied to each tire specimen was limited to twice the rated load of the tire at its rated inflation pressure with the following exceptions: the 56-inch, 32-ply-rating tire (a later addition to the test) was limited to 90,000 pounds by the test fixture, which was designed to meet the load requirements of the 56-inch, 24-ply-rating tire; the two 27-inch, 10-ply-rating tires were loaded up to tire bottoming. The maximum side load, torsional moment, and fore-and-aft load applied on a tire specimen were limited to values that either produced a noticeable crease in the deflected tire wall or were slightly below the slip point for the vertical load used.

APPARATUS

The combined load testing machine at the Langley Aeronautical Laboratory which is capable of applying six components of load on a test specimen, singly or in various combinations, was used in the investigation. The maximum loading rates of the machine in terms of tire deflection are limited to the following values: 2 inches per minute for the vertical and side loads and approximately 3 inches per minute for the fore-and-aft (longitudinal) load. A tire specimen mounted in the machine is shown in figure 1. Even though the tire is shown mounted in a horizontal position, all references to tire deflection and loads are made as if the tire were mounted in its normal vertical position. For the first three parts of the test the wheels were allowed freedom in roll but in the fore-and-aft test the wheel was locked to the test fixture.

Vertical, side, and fore-and-aft tire deflections were determined by measuring the displacements with steel scales. The torsion angle was

determined from the angular deflection of a sensitive protractor mounted on the wheel rim. The tire pressures were determined by using Bourdon tube gages.

The tires tested in this investigation are listed in the following table:

Tire	Diameter (in.)	Specifications given in reference 1			Manufacturer
		Size	Type	Ply rating	
A	56	56 × 16	VII (extra high pressure)	32	IV
B	56	56 × 16	VII (extra high pressure)	24	III
C	45	15.50-20	III (low pressure)	14	III
D	44	44	I (smooth contour)	10	III
E-1	27	27	I (smooth contour)	10	II
E-2	27	27	I (smooth contour)	10	IV

Figure 2 shows the deflated and inflated cross-sections of five of the tires tested. These profiles were made from plasticine casts and are believed accurate to $\pm\frac{1}{8}$ inch. Table I lists the specifications for the tire specimens, taken either from reference 1 or by direct measurements. Figure 3 shows the relative size and tread pattern of five of the tire specimens. The sixth specimen, a 27-inch tire with a block tread, is not shown in figure 3 (nor in table I or fig. 2) but is of the same size and ply rating as tire E-1.

PRECISION OF DATA

The instruments used in these tests give measurements that are believed accurate within the following limits:

Vertical load, percent	±1.0
Side load, percent	±1.0
Fore-and-aft load, percent	±1.0
Moment about vertical axis, percent	±1.0
Vertical tire deflection, in.	±0.02
Side tire deflection, in.	±0.02
Fore-and-aft tire deflection, in.	±0.02
Torsion angle, deg	±0.1
Lateral shift of vertical-load center of pressure, percent	±10.0
Fore-and-aft shift of vertical-load center of pressure, percent	±10.0
Tire pressure, lb/sq in.	±3.0

TEST PROCEDURE

The tire-wheel combinations tested were mounted in the test fixture and instrumented as shown in figure 1 for the 44-inch tire. Each tire was tested over a range of inflation pressure. The tests were divided into four parts: vertical-load tests and tests combining vertical load with side load, torsion load, and fore-and-aft load.

The loading procedure for the vertical-load tests was as follows: The vertical load was applied in increments, cumulatively, up to the maximum vertical-load value and was then reduced by increments to zero. The vertical tire deflection and the tire pressure were noted at each value of vertical load. This loading procedure is hereinafter referred to as the cumulative loading procedure.

The loading procedure was begun in the side-load tests by first applying an initial vertical load to the tire specimen. The vertical tire deflection and the tire pressure due to this load were noted. With this vertical load held constant, side load was applied in increments up to the point where a large crease in the tire wall developed or tire slippage appeared imminent and was then decreased in increments to zero. Side deflection, vertical tire deflection, tire pressure, and moments were measured at each increment of side load. The vertical load was then removed, a new zero established, and this procedure repeated for the next higher vertical load. This type of vertical loading is hereinafter referred to as the step loading procedure.

In the torsion tests, an initial vertical load was applied to the tire as in the side-load tests. Then a torsional moment was applied and the resulting torsional displacement was measured with the sensitive protractor. The loading procedure for the torsion tests was similar to that of the side-load tests. Measurements of torsion angle, vertical tire deflection, and tire pressure were taken at each value of torsional moment.

The test for the fore-and-aft loading was conducted on only tire A, the 56-inch tire with a ply rating of 32. In this test, an initial vertical load was applied to the tire as in the previous tests, and fore-and-aft loads were then applied. The loading procedure used in this test was similar to the side-load and torsion-load test procedures. Measurements of fore-and-aft tire deflection, vertical tire deflection, moments, and tire pressure were made at each value of fore-and-aft load.

In some supplementary tests, tire creep, which is defined as the change of deflection with time under constant load, was investigated for several inflation pressures by holding the vertical load constant at each test point until the change in vertical tire deflection was not more than 0.01 inch for two consecutive measurements taken 2 minutes apart. The

time to reach a vertical-load value from the preceding load value was not measured. However, a rough estimate of this time can be made by dividing the tire deflection between the test points in question by the maximum speed of the vertical loading piston, 2 inches per minute. The time taken to record data at each test point was approximately 30 seconds. On the average, 4 to 6 minutes were required for the tire specimen to stabilize at the larger tire deflections.

The shift of the vertical-load center of pressure under side or fore-and-aft loading was determined from the moment measurements made during the respective tests. Figure 4(a) illustrates a loading sequence for the test of combined vertical and side loads and indicates the vertical-load center-of-pressure shift. A similar diagram for the test of combined vertical and fore-and-aft loads is shown in figure 4(b).

Some tire-contact (referred to herein as "footprint") area measurements were made of the 56-inch, 24-ply-rating tire under vertical load for several inflation pressures. Each measurement was obtained from the imprint left by the tire on a piece of stiff cardboard that had been placed between the tire and the concrete test platen (see fig. 1).

The lateral distortion of the tire center or equatorial line due to side loading was measured at several points near the center of contact along the circumference of the 56-inch, 32-ply-rating tire only.

The characteristics of the test setup were such that small values of side load, side tire deflection, torsional moment, and so forth were sometimes encountered after the initial value of vertical load was applied. These loads or deflections are probably due to a combination of tire strain from a previous loading, a slight amount of play in the test setup, or some interaction of loads in the weighing unit. The presence of these small initial deviations should be considered in the use of the figures.

RESULTS AND DISCUSSION

A large number of plots resulted from the present investigation and an index to the principal data plots has been made to aid in the use of the data and is presented as table II.

Vertical Load

The vertical-load—vertical-tire-deflection characteristics of the tire specimens are shown in figures 5 to 9. The differences between the short-dashed-line and solid-line curves shown in these figures for

some inflation pressures represent the amount of creep measured before the tires reached equilibrium under constant vertical load. On the average, this creep ranged between 1 and 2 percent of the tire deflection. The time required to reach equilibrium averaged 4 to 6 minutes for most load points. The low values of tire creep measured are attributed to the slow maximum loading rate of 2 inches tire deflection per minute used in the tests.

The comparison between cumulative and step loading procedures is also presented in these figures. The step-loading data resulted from measuring the vertical tire deflection due to a particular vertical load immediately prior to the combined loading of a tire specimen. The vertical load for combined loads was increased continuously on the tire until the desired load value was reached; whereas in the vertical-load tests (no combined loads), the vertical load was applied in increments, cumulatively, until the desired load value was reached. The difference in the loading procedures lies in the time required to reach a given vertical load. The cumulative loading procedure averaged 4 to 5 minutes longer than the step loading procedure in the cases of maximum vertical load. The data shown in the figures indicate that the step loading procedure results in only a slightly stiffer vertical-load—vertical-tire-deflection characteristic than that shown for the cumulative loading procedure.

Figure 9 contains additional data for the 27-inch tires to make possible tire-hysteresis or energy-loss calculations over a large range of tire deflection. In order to present these data conveniently, the loading curves in figure 9 are displaced along the abscissa. The zeros located beneath the vertical-tire-deflection scale indicate the initial point for each loading.

Test results are compared in figures 6, 7, and 8 with data from manufacturer I for 56-inch (24-ply-rating), 45-inch, and 44-inch tires, respectively. These tires were supplied by manufacturer III. Figure 10 shows the comparison of test data (cumulative loading) with data from manufacturer II (the manufacturer of tire E-1) for the two 27-inch tires tested. These comparisons indicate that variations ranging up to 13 percent in vertical load for a given vertical tire deflection exist between tires of the same type and ply rating.

Figures 11 to 15 show the variation of tire pressure with vertical tire deflection and with vertical load for the two loading procedures used. These figures show a tendency for the pressure rises resulting from step loading to be slightly higher than those due to cumulative loading. This result offers an explanation for the differences in vertical-load—vertical-tire-deflection data (see figs. 6 to 9) between step and cumulative loading procedures. The more lengthy cumulative loading has a smaller pressure increase because a greater amount of the

heat of compression is dissipated through the tire walls. This smaller pressure rise shows up as a larger vertical tire deflection in the case of the cumulative loading procedure.

The pressure rise occurring at 50 percent of the maximum tire deflection for all tests averaged approximately 8 percent of the initial inflation pressure for the different tire specimens. Maximum vertical tire or bottoming deflection is arbitrarily defined as the distance between the rim edge and the ground line of the undeflected tire at its rated inflation pressure. The values of maximum vertical tire deflection used in this paper for the different tire specimens are listed in the following table:

Tire	Maximum vertical tire deflection (in.)
56-inch, 32-ply-rating	11.75
56-inch, 24-ply-rating	11.50
45-inch, 14-ply-rating	10.69
44-inch, 10-ply-rating	10.10
27-inch, 10-ply-rating	6.44

Figure 16 presents data on footprint area and the comparison of these data with effective footprint area which is defined as the vertical load divided by the sum of the initial inflation pressure and the pressure rise. Fairly close agreement is shown between measured and effective footprint-area curves up to the limit of data for comparison, which is about 50 percent tire deflection.

Combined Vertical and Side Loads

Figures 17 to 21 show the side-load—side-tire-deflection characteristics for five of the tire specimens for different vertical loads and test inflation pressures. Considerable apparent hysteresis is indicated in these curves. Also shown in these figures are the lateral shift of the vertical-load center of pressure and the increase in vertical tire deflection plotted against side tire deflection. The accuracy of the values for center-of-pressure shift at small deflections is uncertain since these values were derived from the small difference of two large numbers.

The trends of the side-load data obtained from the tire specimens are shown in figures 22 to 24. Figure 22 shows the variation of the lateral spring constant with percent of maximum vertical tire deflection and initial inflation pressure for five of the tire specimens.

The lateral spring constant is defined in this paper as the slope of the side-load—side-tire-deflection curve at a side deflection of 0.5 inch. This figure indicates that the lateral spring constant for a tire generally decreases with increasing vertical tire deflection and increases with increasing inflation pressure. Figure 23 shows the effects of vertical tire deflection and inflation pressure on the ratio of the lateral shift of the vertical-load center of pressure resulting from side load to the side tire deflection. The ratios were measured at side deflections equal to 0.5 inch. This figure shows that the lateral shift of the vertical-load center of pressure for the tire specimens decreases slightly with increasing vertical tire deflection and averages approximately 75 percent of the side tire deflection. The effect of inflation pressure is difficult to ascertain because of the scatter of the data. Figure 24 shows the effects of vertical tire deflection and inflation pressure on the ratio of the increase in vertical tire deflection resulting from side load to the side tire deflection. This ratio appears to be independent of initial vertical load and inflation pressure, a fact which indicates that the increase in vertical tire deflection due to side load is dependent only on the amount of side deflection for a given tire. Each tire type appears to have a distinctive value for this ratio regardless of tire size or ply rating.

The distortion of the equatorial line of the tire under side load was determined for different vertical loads and initial inflation pressures for the 56-inch, 32-ply-rating tire. The results are shown in figure 25 in the form of curves for which the lateral displacement of the tire equatorial line relative to the wheel rim are plotted against station location in degrees and in inches of circumferential displacement (on the unloaded tire) from the center of the contact area. The measured footprints of the 56-inch, 24-ply-rating tire under side load disclosed that, for the side loads used, the tire equatorial line was straight within the limits of the contact area. (A slight curving of the tire equatorial line was observed near each end of the footprint but this curved region appeared to be less than 5 percent of the contact length.) The lengths of the measured footprints were found to be less than the geometric chords corresponding to the vertical tire deflections. These contact lengths agreed closely, however, with data shown in reference 2. An empirical equation for contact length given in reference 2 was used to compute the approximate 1/2 contact lengths, marked "A", shown on the curves of figure 25.

Combined Vertical and Torsion Loads

The variation of torsional moment with torsion angle at different vertical loads and initial inflation pressures is shown in figures 26 to 30 for five tire specimens. These curves show large amounts of apparent hysteresis similar to that of the side-load curves. Also shown

in these figures are the variations of the changes in vertical tire deflection due to torsional moment with torsion angle for the specimens. Positive values of the change in vertical tire deflection indicate increasing vertical tire deflection.

The trends of the data given in figures 26 to 30 are shown in figure 31 where the torsional spring constants of the tire specimens are plotted against percent of maximum vertical tire deflection. The torsional spring constant is defined herein as the slope of the torsional-moment—torsion-angle curve at a torsion angle of 1°. The torsional spring constant for each tire increases with increasing vertical tire deflection. Increasing the tire inflation pressure appeared to increase the torsional stiffness of the tire. The variation appears linear in the test range. No attempt was made to determine the variation of the ratio of the change in vertical tire deflection resulting from torsional moment to the torsion angle for the specimens since most of these curves were erratic and not linear. The amount of added vertical tire deflection is rather small and is considered insignificant.

Combined Vertical and Fore-and-Aft Loads

Figure 32 shows the variation of fore-and-aft load with fore-and-aft tire deflection for different vertical loads and initial inflation pressures. Also shown plotted against fore-and-aft tire deflection are the variations of the vertical-load center-of-pressure shift due to fore-and-aft load and the increase in vertical tire deflection due to fore-and-aft load. This type of loading was conducted on the 56-inch, 32-ply-rating tire only. The trends of the curves shown in figure 32 are shown in figure 33. Here the fore-and-aft spring constant, the ratio of fore-and-aft center-of-pressure shift resulting from fore-and-aft load to the fore-and-aft tire deflection, and the ratio of the increase in vertical tire deflection resulting from fore-and-aft load to the fore-and-aft tire deflection are plotted against percent of maximum vertical tire deflection. The values of the parameters used in figure 33 were determined from the average slope occurring near zero fore-and-aft tire deflection in figure 32.

The fore-and-aft spring constant appears to be about three times the magnitude of the lateral spring constant at 50 percent of the maximum vertical tire deflection. The fore-and-aft spring constant increases with increasing vertical tire deflection and with increasing tire inflation pressure. The fore-and-aft shift of the vertical-load center of pressure due to fore-and-aft loads appeared to be about 25 percent of the fore-and-aft tire deflection and was independent of vertical tire deflection over the range of the tests. The increase in vertical tire deflection due to the fore-and-aft load appears to be about 10 percent of the fore-and-aft tire deflection.

CONCLUSIONS

Tests were made in the combined load testing machine at the Langley Aeronautical Laboratory to determine the static force-deflection characteristics of six aircraft tires. The results of these tests which included the vertical loading of the six tire specimens, combined vertical loading and side loading and combined vertical loading and torsional loading of five tire specimens, and combined vertical loading and fore-and-aft (longitudinal) loading of one tire specimen indicated the following conclusions:

1. The lateral spring constants for the tire specimens were generally found to decrease with increasing vertical tire deflection and to increase with increasing inflation pressure.

2. The lateral shift of the vertical-load center of pressure due to side load decreased slightly with increasing vertical tire deflection. This shift averaged approximately 75 percent of the side tire deflection for the tires tested.

3. The torsional spring constants, for the tires tested, increased with increasing vertical tire deflections. This variation appeared linear in the test range. Increasing the tire inflation pressure appeared to increase the torsional stiffness of the tire.

4. The fore-and-aft spring constant, like the torsional spring constant, increased with increasing vertical tire deflection and appeared to increase with increasing tire inflation pressure. The fore-and-aft spring constant appeared to have about three times the magnitude of the lateral spring constant at 50 percent of the maximum vertical tire deflection.

5. The fore-and-aft shift of the vertical-load center of pressure due to fore-and-aft loads appeared to be about 25 percent of the fore-and-aft tire deflection and was independent of vertical tire deflection over the range of the tests.

6. The pressure rises occurring at 50 percent of the maximum vertical tire deflection averaged approximately 8 percent of the initial inflation pressures for the tires tested.

Langley Aeronautical Laboratory,
National Advisory Committee for Aeronautics,
Langley Field, Va., December 17, 1952.

REFERENCES

1. Anon.: Military Specification Casings; Aircraft Pneumatic Tire. Military Specification, MIL-C-5041, Sept. 16, 1949; Amendment-2, Feb. 8, 1951.

Anon.: Army-Navy Aeronautical Specification Casings; Aircraft Landing, Nose, Tail and Beaching Tire. Army-Navy Aeronautical Specification, AN-C-55e, Dec. 20, 1946; Amendment-1, June 16, 1947.

2. Rotta, J.: Properties of the Aeroplane During Take-Off and Alighting. Reps. and Translations No. 969, British M.A.P. Völkenrode, Dec. 15, 1947.

TABLE I.- TIRE SPECIFICATIONS

[Obtained from reference 1 and by direct measurement]

Specification	Tire A	Tire B	Tire C	Tire D	Tire E-1
Tire:					
Type[a]	VII	VII	III	I	I
Ply rating	32	24	14	10	10
Static load, lb	60,000	45,000	20,000	13,000	5,500
Inflation pressure, lb/sq in.	240	178	85	60	70
Burst pressure, lb/sq in.	960	712	340	240	280
Moment of static unbalance, oz-in.	90	90	52	50	12
Diameter, deflated, in.	54.3	54.0	43.3	43.63	27.7
Diameter, inflated, in.	56.0	55.5	44.6	------	28.2
Maximum width, deflated, in.	14.2	15.1	14.6	14.9	9.3
Maximum width, inflated, in.	15.8	15.7	15.4	------	9.4
Bead width, in.	3.1	3.2	2.1	2.0	1.0
Minimum wall thickness, in.	1.1	0.9	0.58	0.57	0.4
Wall thickness at tread center line (including tread), in.	1.5	1.4	1.15	0.84	0.64
Depth of tread, deflated, in.	0.38	0.38	0.38	0.38	0.22
Casing weight, lb	281	250	138	100	29
Innertube:					
Thickness, in.	0.2	0.2	0.13	0.06	0.06
Weight, lb	26.7	26.7	20.5	15.2	4.5
Wheel:					
Rim diameter, in.	32.5	32.5	23.22	24.1	15.32
Weight, lb	217	217	80	46	23.5

[a]Type I is smooth contour.
Type III is low pressure.
Type VII is extra high pressure.

TABLE II.- INDEX OF PRINCIPAL DATA PLOTS

	Figure					
	Tire A	Tire B	Tire C	Tire D	Tire E-1	Tire E-2
Tire profiles	2	2	2	2	2	----------
Relative size and tread pattern	3	3	3	3	3	----------
Vertical-load—vertical-tire-deflection data	5	6	7	8	9(c), 9(d), 9(e),10	9(a), 9(b), 9(d), 9(e), 10
Tire pressure against vertical tire deflection	11(a)	12(a)	13(a)	14(a)	15(a)	15(a)
Tire pressure against vertical load	11(b)	12(b)	13(b)	14(b)	15(b)	15(b)
Footprint area against vertical tire deflection	16	16	16	16	16	16
Side load, lateral center-of-pressure shift, and increase in vertical tire deflection against side tire deflection	17	18	19	20	----------	21
Lateral spring constant against vertical tire deflection	22	22	22	22	----------	22
$\frac{\text{Lateral center-of-pressure shift}}{\text{Side tire deflection}}$ against vertical tire deflection	23	23	23	23	----------	23
$\frac{\text{Increase in vertical tire deflection}}{\text{Side tire deflection}}$ against vertical tire deflection	24	24	24	24	----------	24
Distortion of tire equatorial line under various side loads	25	------	------	------	----------	----------
Torsional moment and change in vertical tire deflection against torsion angle	26	27	28	29	----------	30
Torsional spring constant against vertical tire deflection	31	31	31	31	----------	31
Fore-and-aft load, fore-and-aft center-of-pressure shift, and increase in vertical tire deflection against fore-and-aft tire deflection	32	------	------	------	----------	----------
Fore-and-aft-load tire characteristics against vertical tire deflection	33	------	------	------	----------	----------

(a) Undeflected position. Inflation pressure, 35 pounds per square inch.

Figure 1.- Test setup and instrumentation for the 44-inch, 10-ply-rating tire specimen (tire D).

(a) Undeflected position. Inflation pressure, 35 pounds per square inch.

Figure 1.- Test setup and instrumentation for the 44-inch, 10-ply-rating tire specimen (tire D).

(c) Under 15,000 pounds vertical load and 1,600 pounds side load.

Figure 1.- Continued.

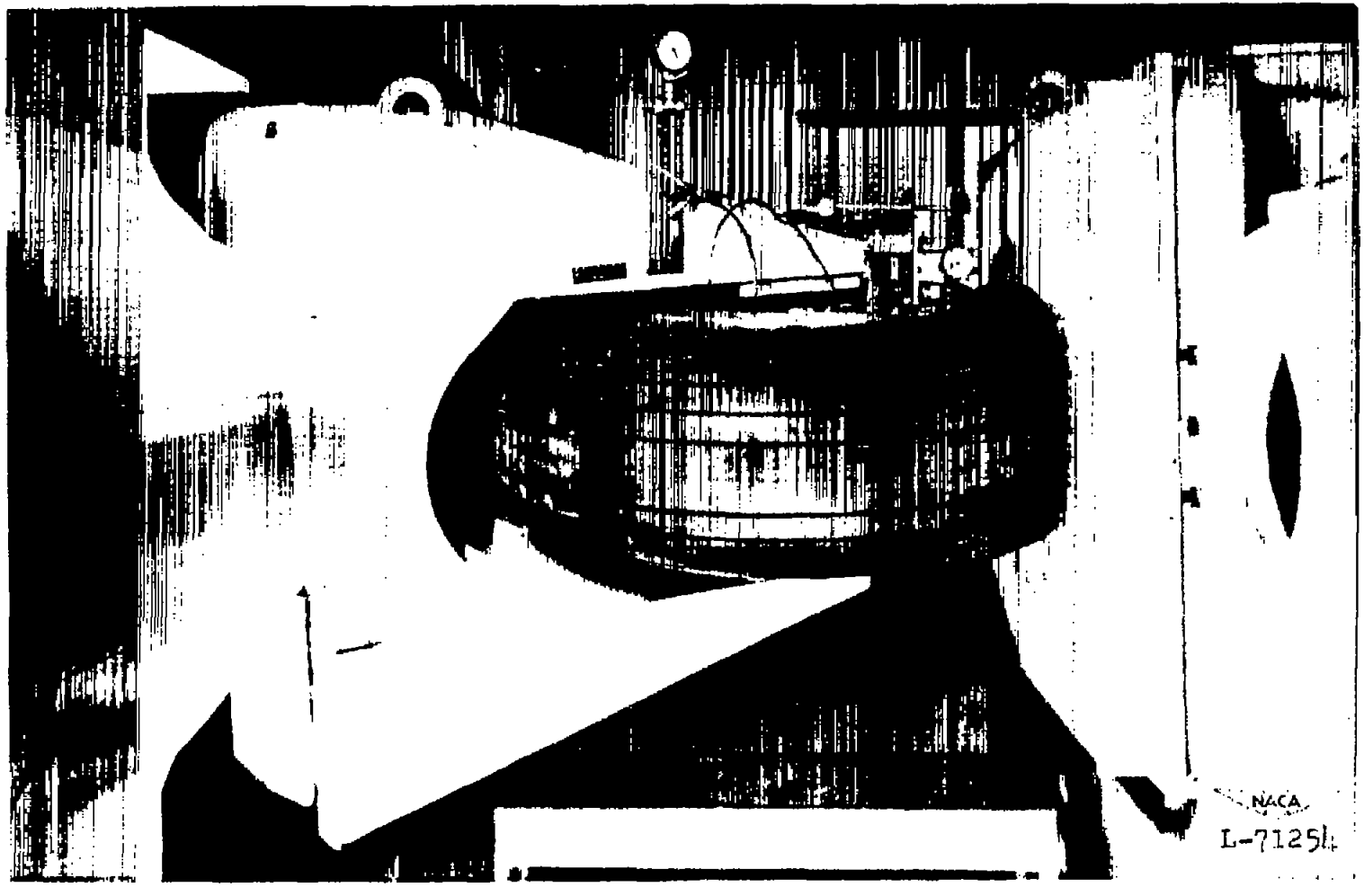

(d) Under 15,000 pounds vertical load and 64,000 pound-inches torsional moment.

Figure 1.- Concluded.

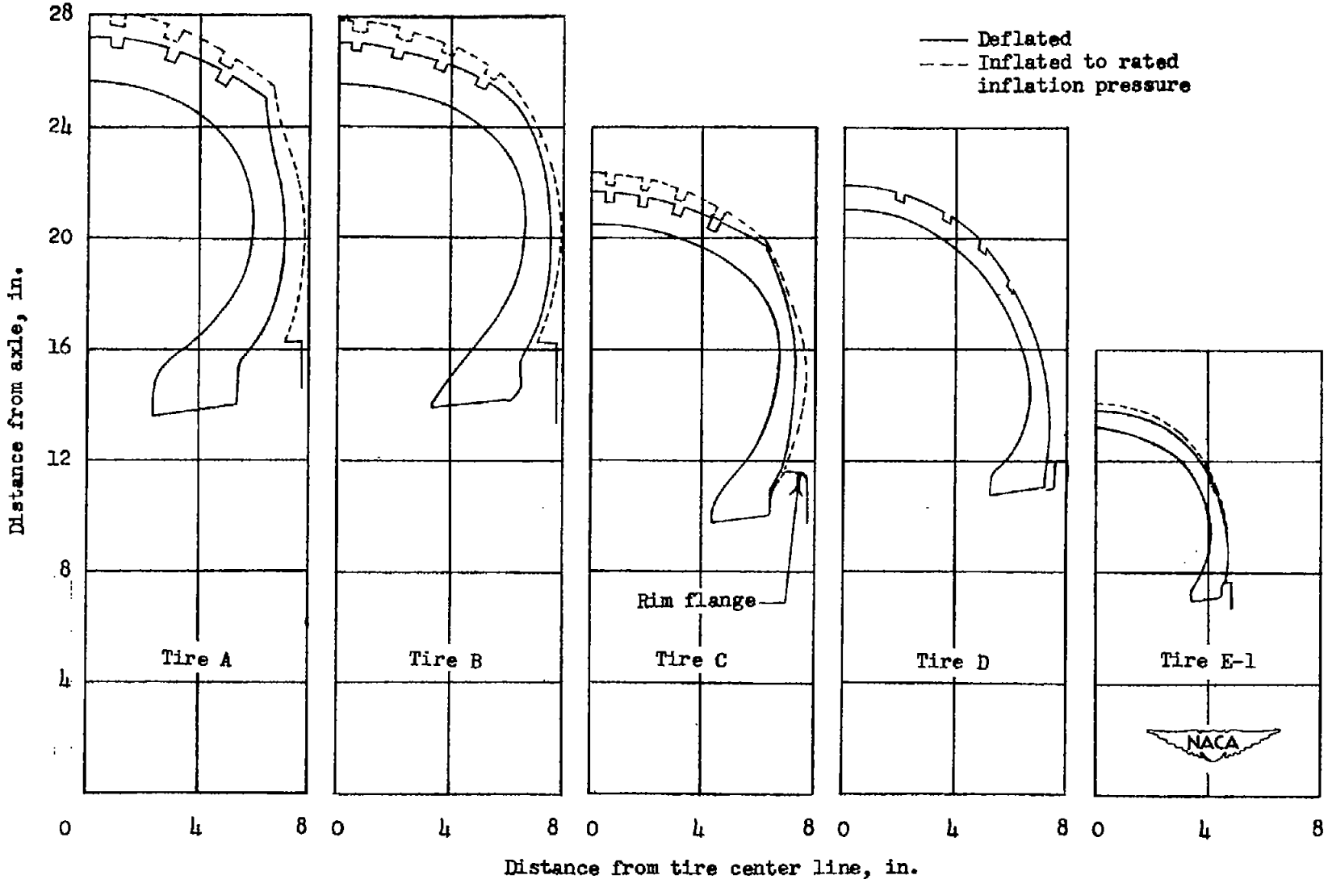

Figure 2.- Tire profiles.

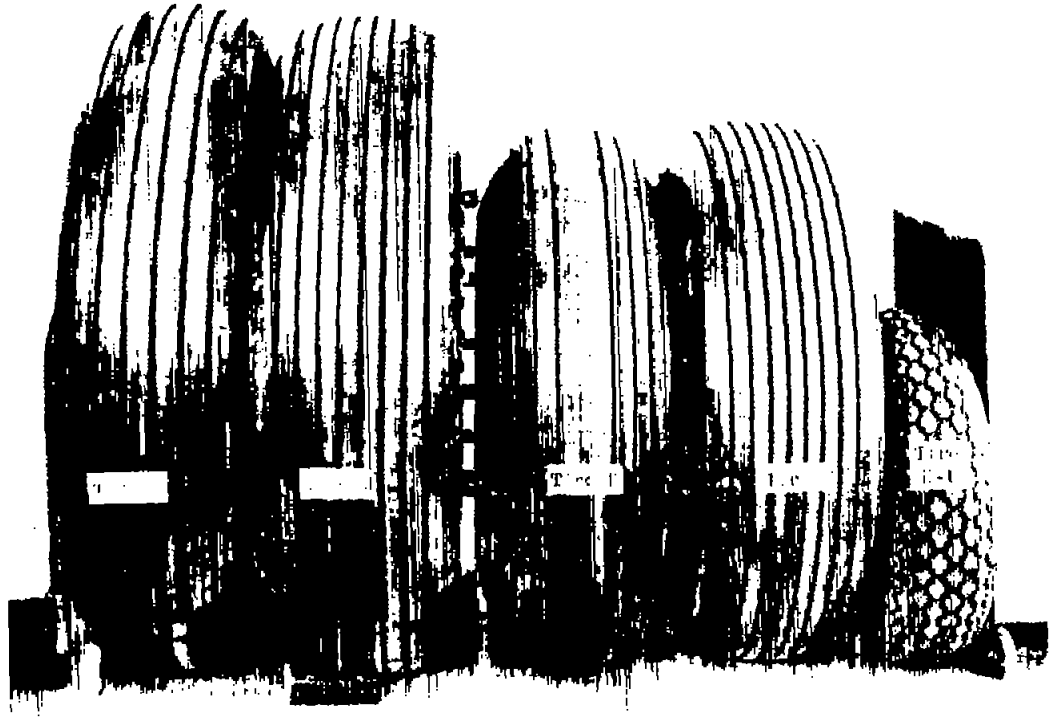

Tire A	56-inch (56 × 16), type VII (extra-high-pressure), 32-ply-rating
Tire B	56-inch (56 × 16), type VII (extra-high-pressure), 24-ply-rating
Tire C	45-inch (15.50-20), type III (low-pressure), 14-ply-rating
Tire D	44-inch, type I (smooth-contour), 10-ply-rating
Tire E-1	27-inch, type I (smooth-contour), 10-ply-rating

NACA
L-74867.1

Figure 3.- Relative size and tread pattern of tire specimens.

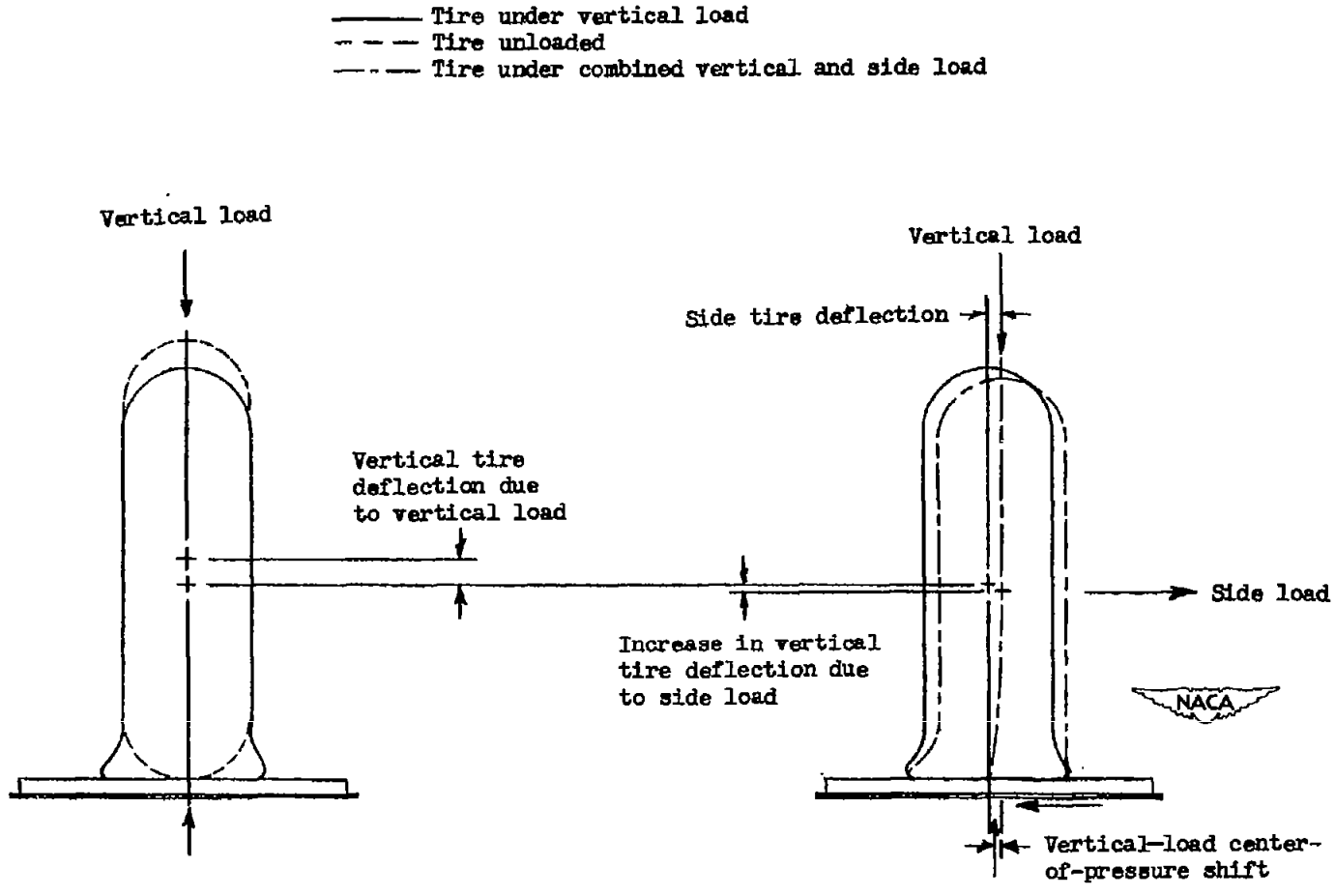

(a) Vertical and side loading.

Figure 4.- Forces acting on a tire specimen under vertical loading combined with side or fore-and-aft loading.

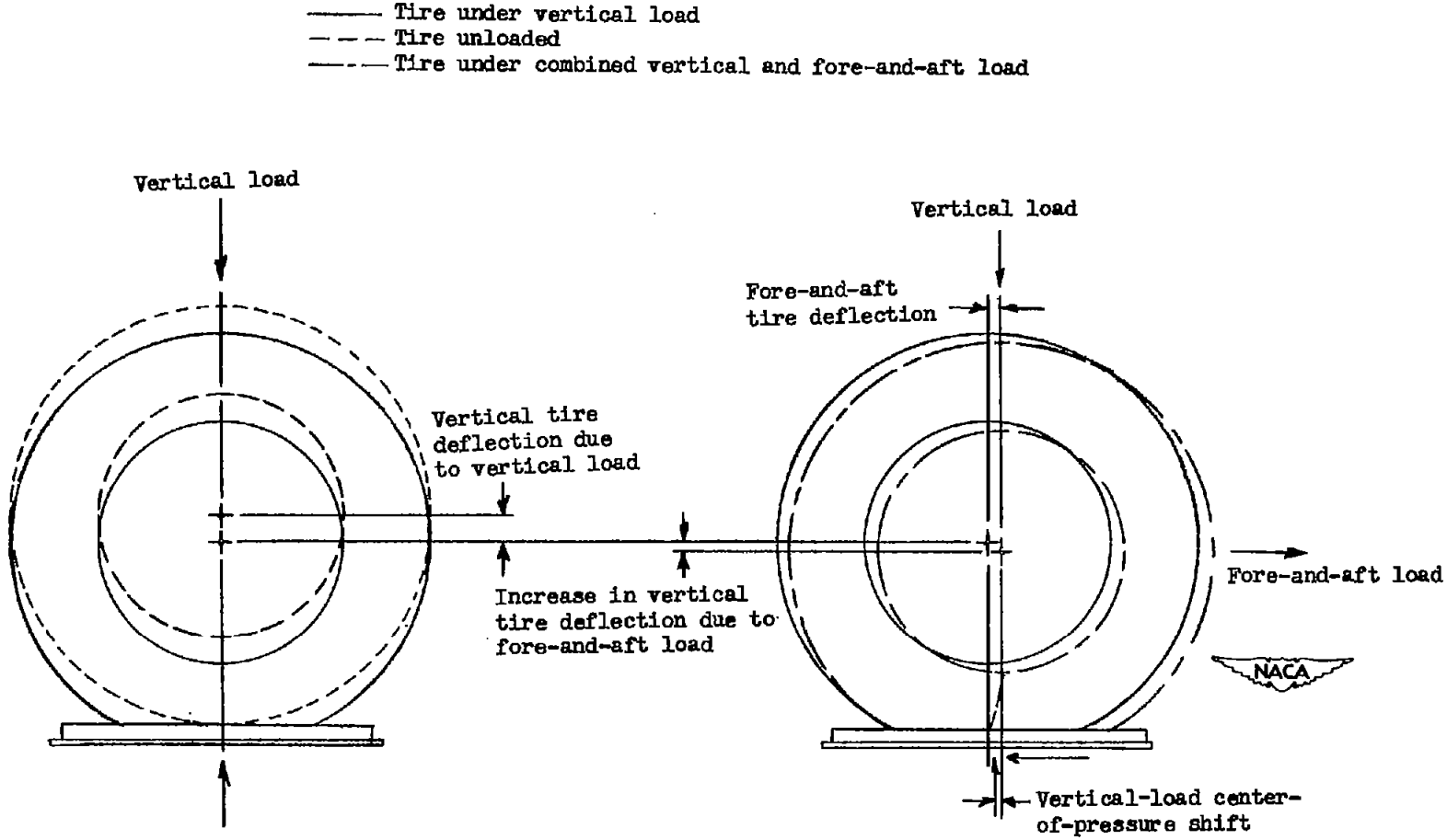

(b) Vertical and fore-and-aft loading.

Figure 4.- Concluded.

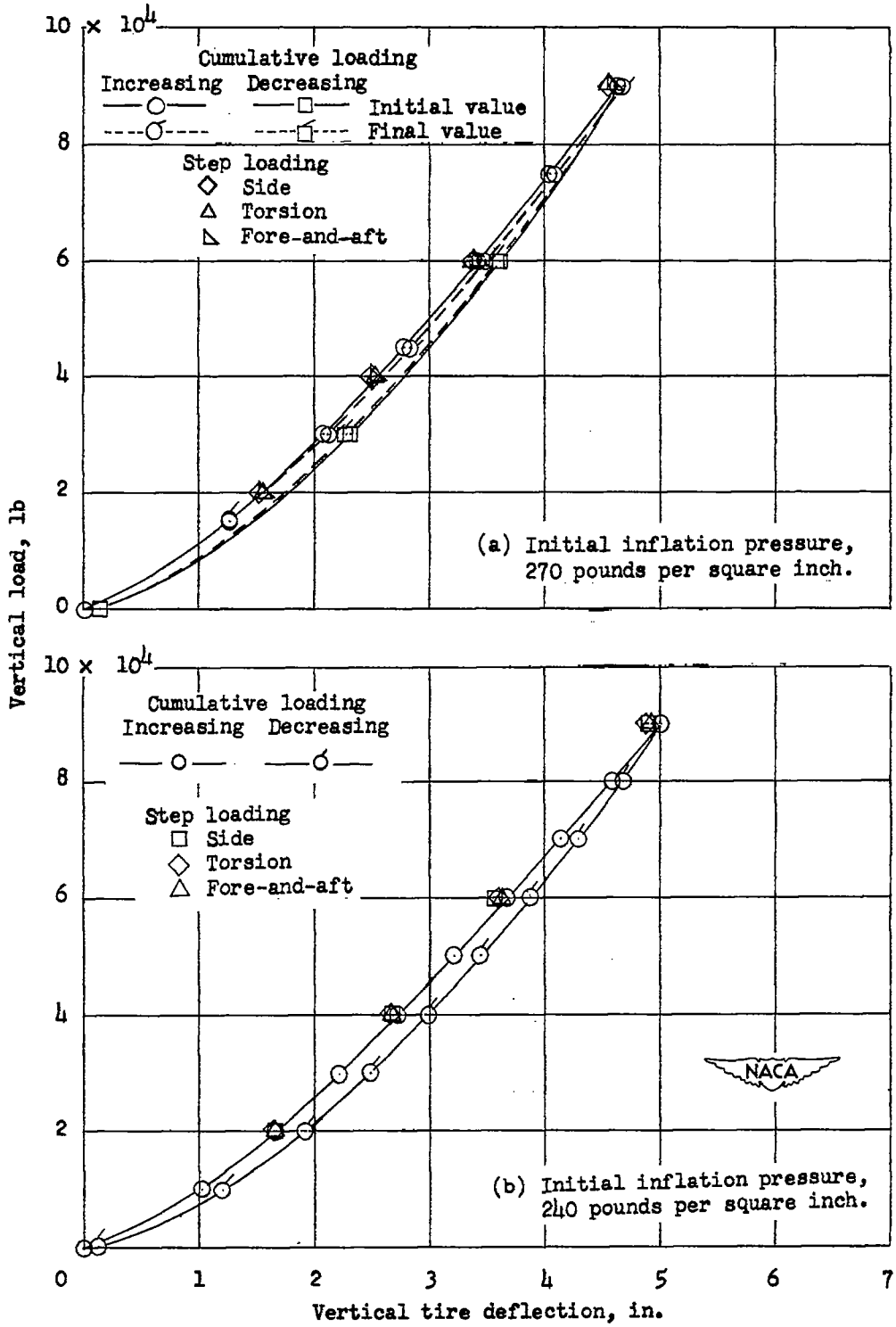

Figure 5.- Vertical-load—vertical-tire-deflection test data at initial inflation pressures of 270, 240, 200, 180, and 0 pounds per square inch for the 56-inch, 32-ply-rating tire (tire A).

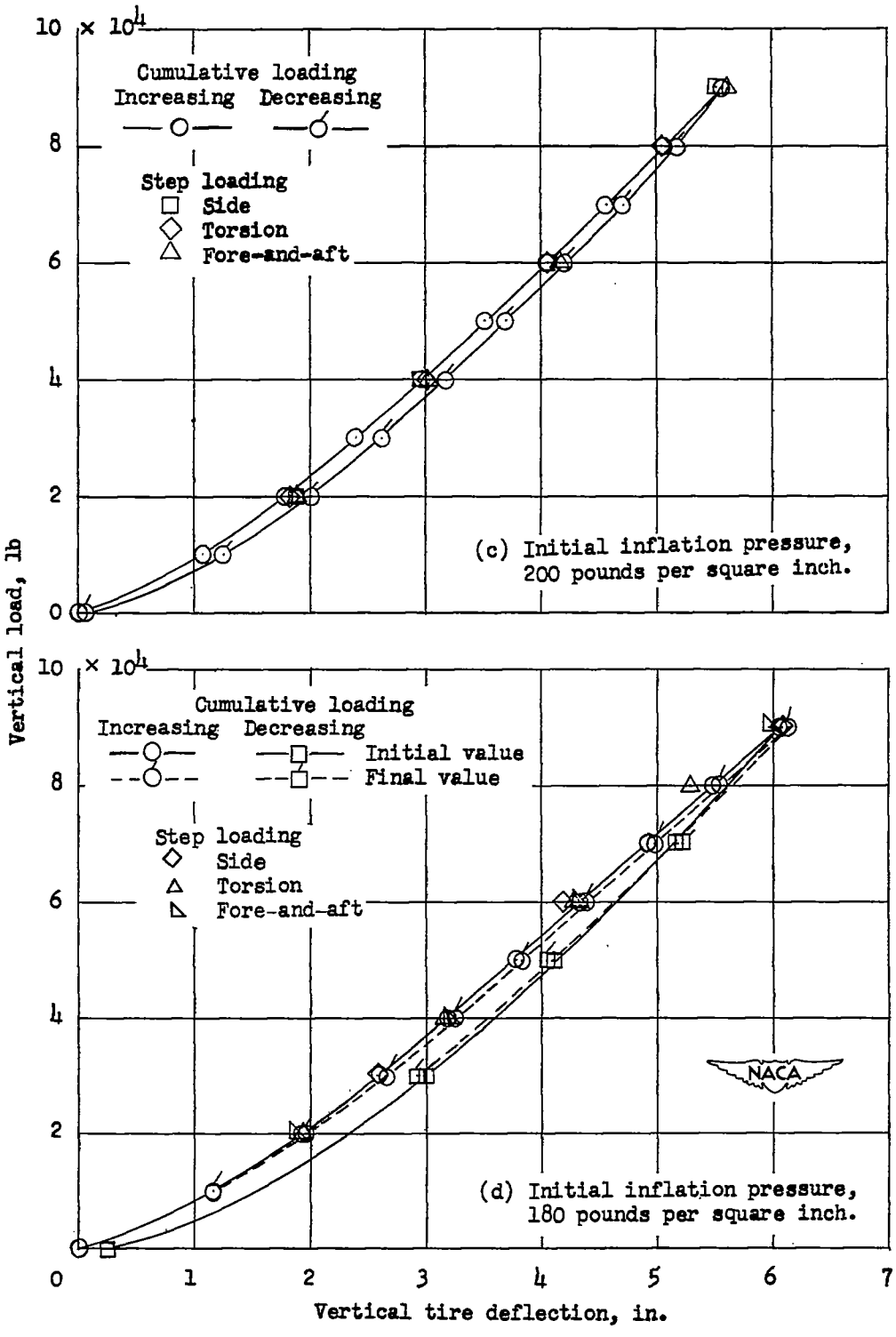

Figure 5.- Continued.

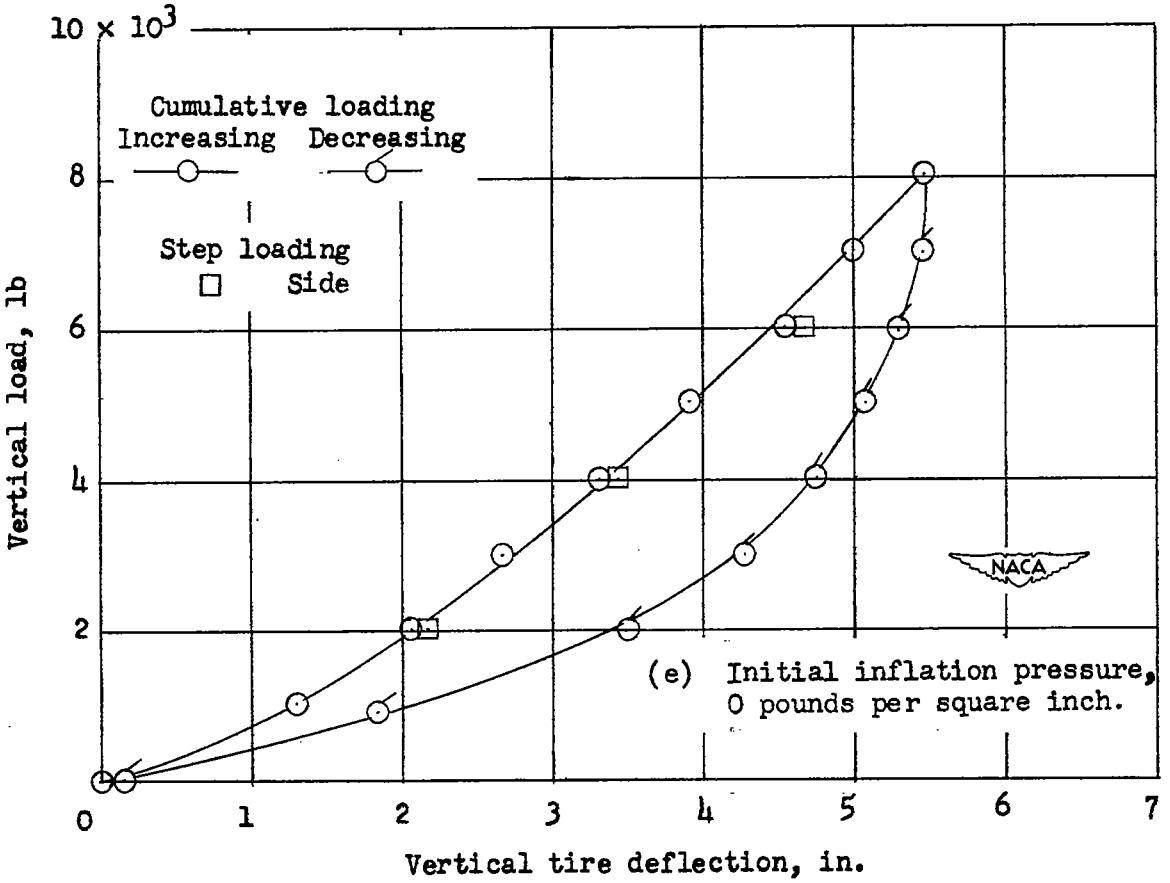

Figure 5.- Concluded.

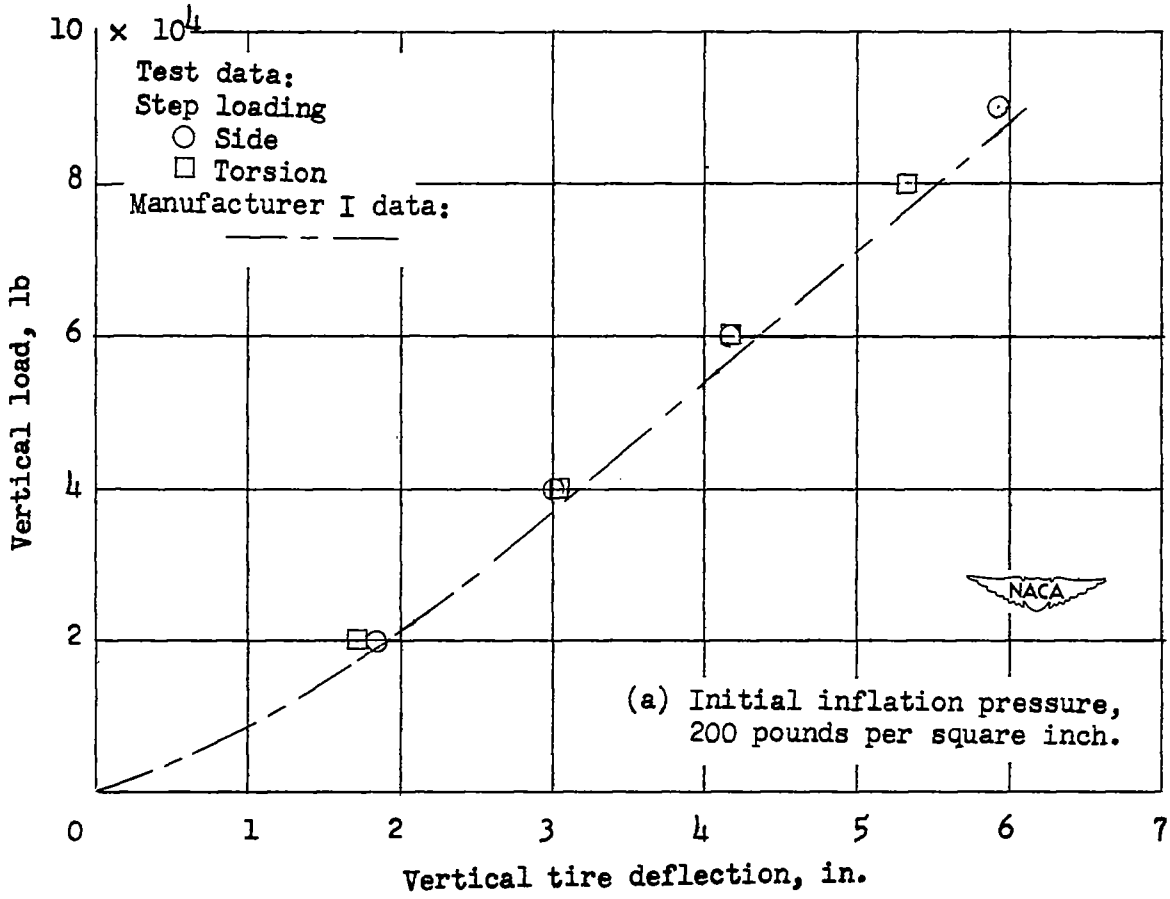

Figure 6.- Comparison of test and manufacturer I vertical-load—vertical-tire-deflection data at initial inflation pressures of 200, 180, and 160 pounds per square inch for the 56-inch, 24-ply-rating tire (tire B).

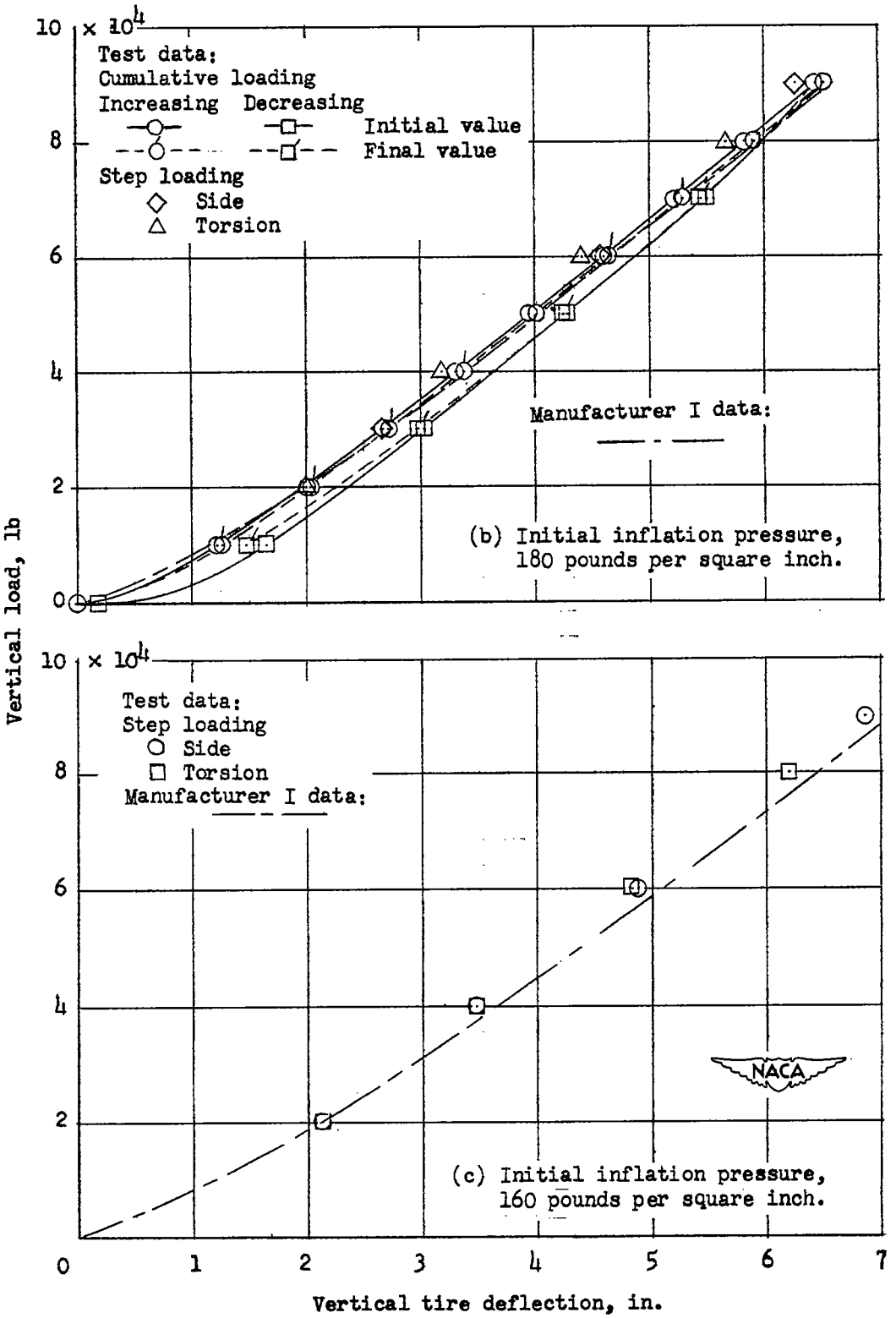

Figure 6.- Concluded.

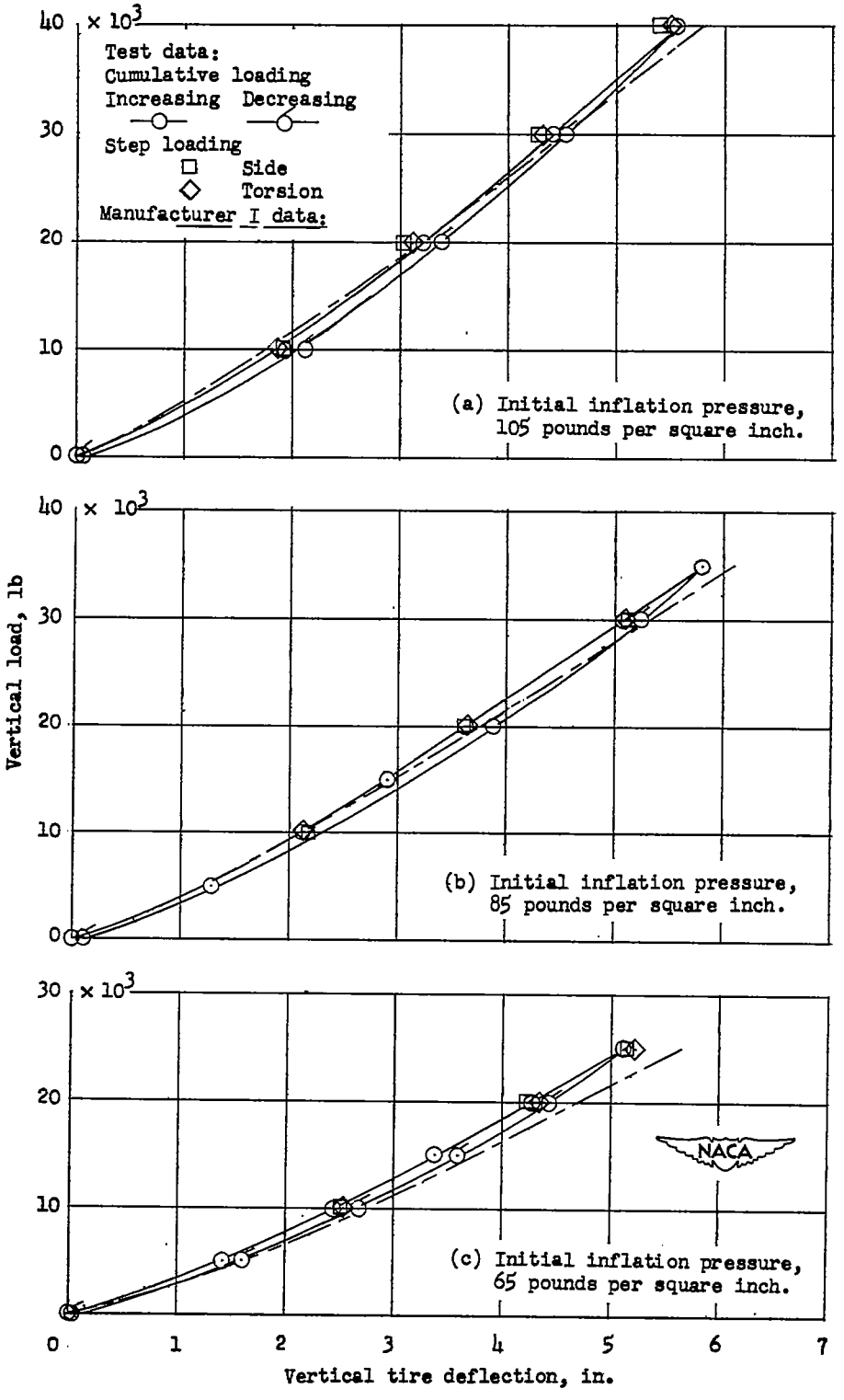

Figure 7.- Comparison of test and manufacturer I vertical-load—vertical-tire-deflection data at initial inflation pressures of 105, 85, and 65 pounds per square inch for the 45-inch, 14-ply-rating tire (tire C).

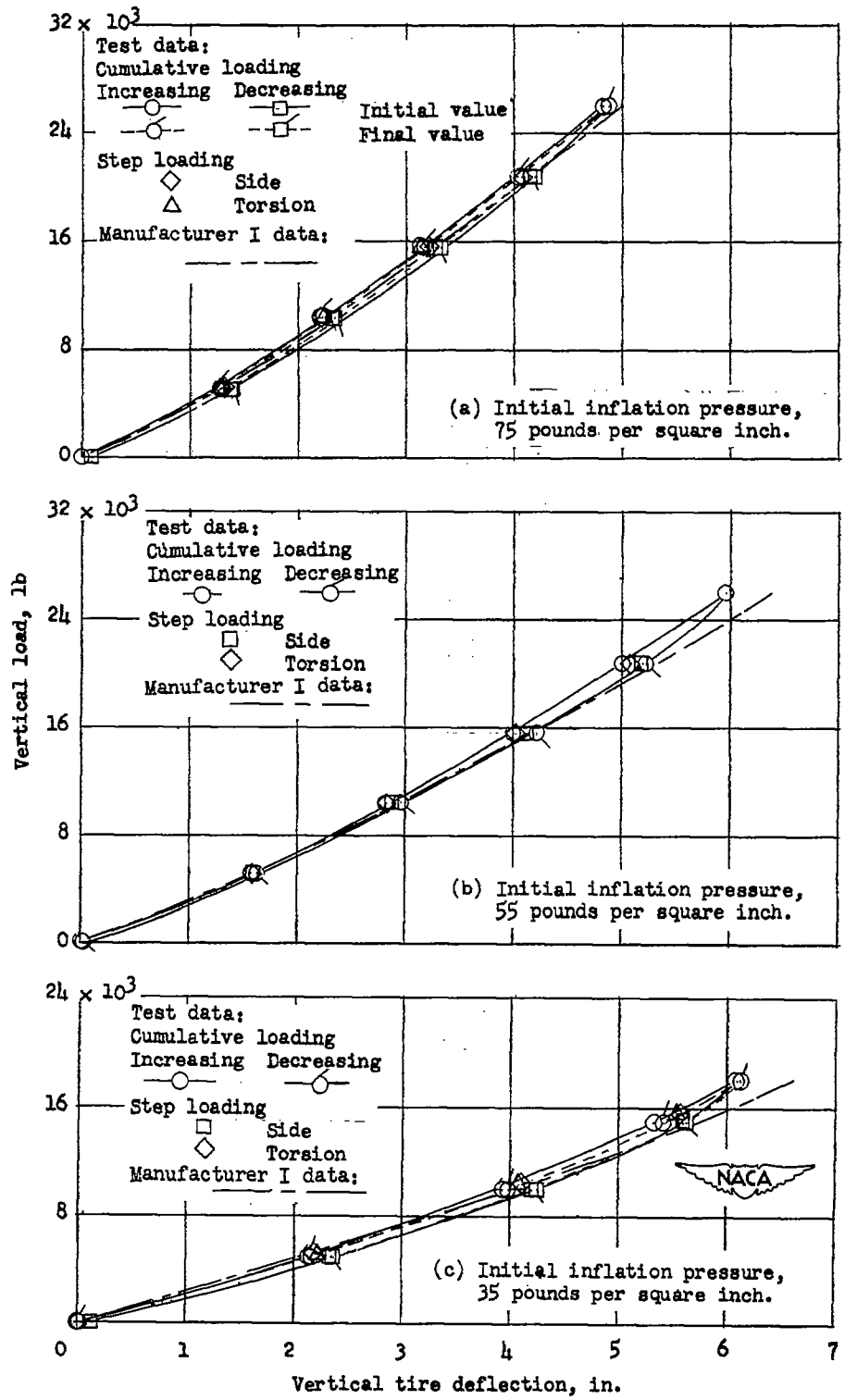

Figure 8.- Comparison of test and manufacturer I vertical-load—vertical-tire-deflection data at initial inflation pressures of 75, 55, and 35 pounds per square inch for the 44-inch, 10-ply-rating tire (tire D).

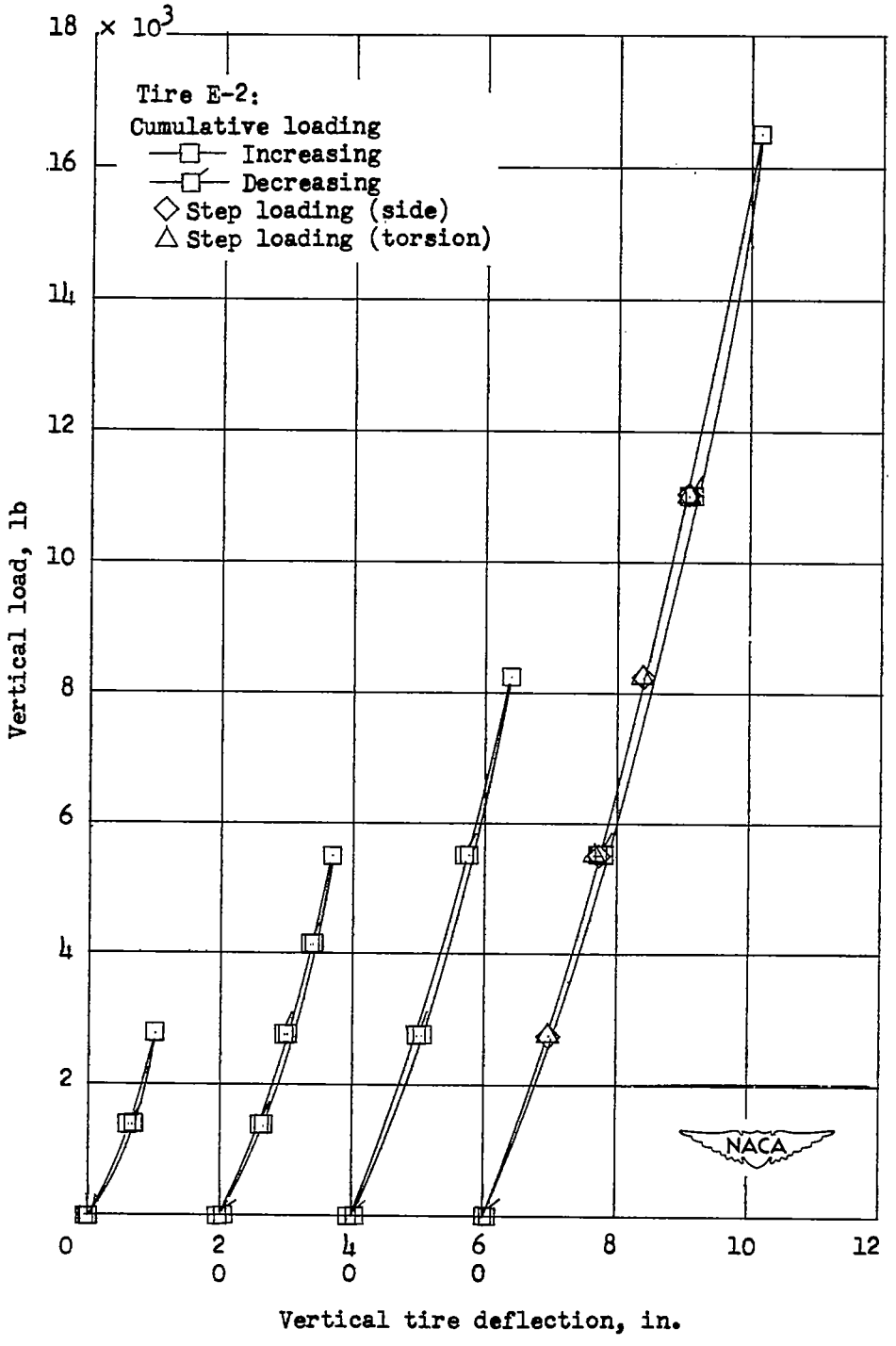

(a) Initial inflation pressure, 80 pounds per square inch; tire E-2.

Figure 9.- Vertical-load—vertical-tire-deflection test data at initial inflation pressures of 80, 40, 32, and 24 pounds per square inch for the 27-inch, 10-ply-rating tires (tires E-1 and E-2).

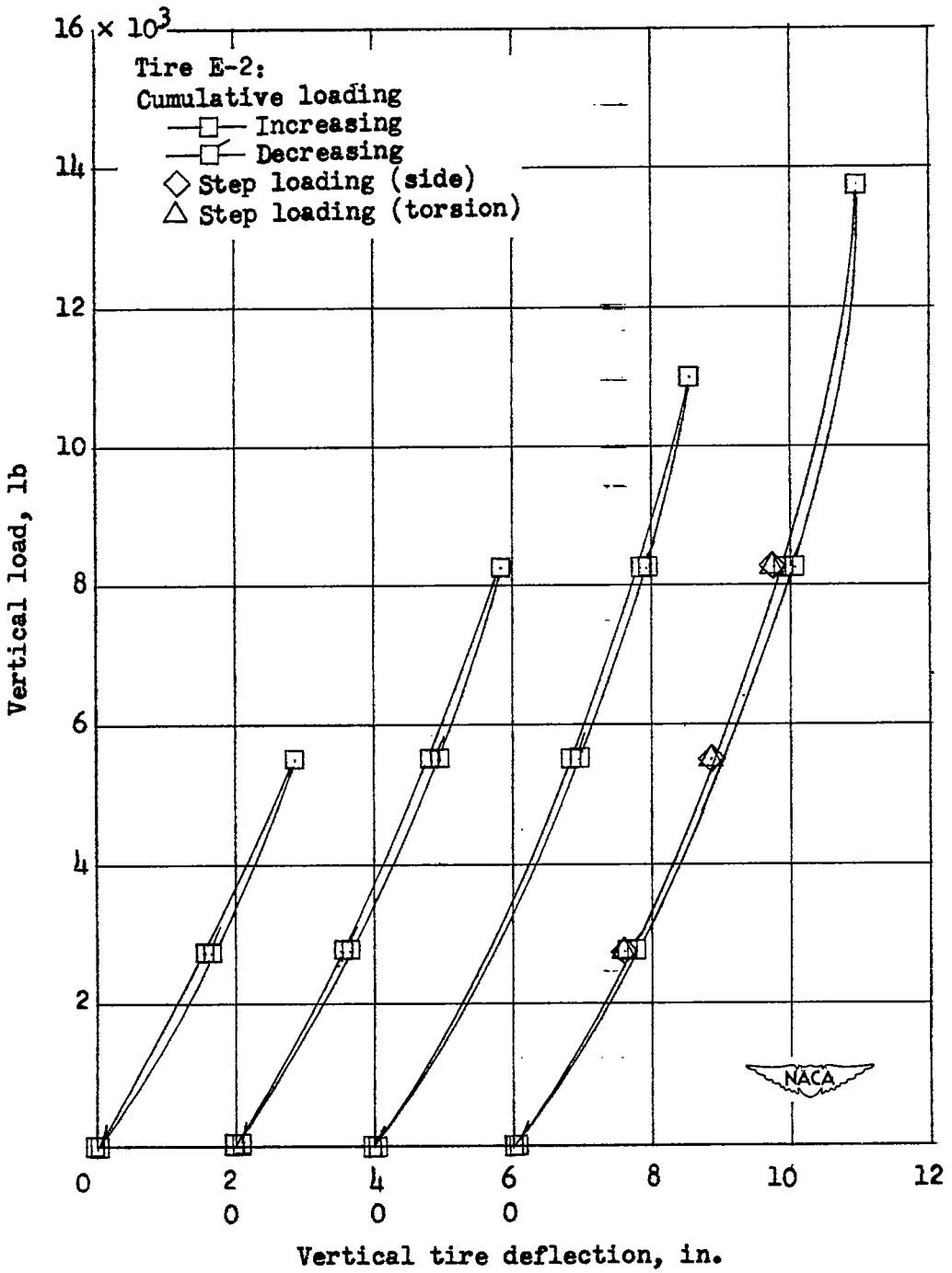

(b) Initial inflation pressure, 40 pounds per square inch; tire E-2.

Figure 9.- Continued.

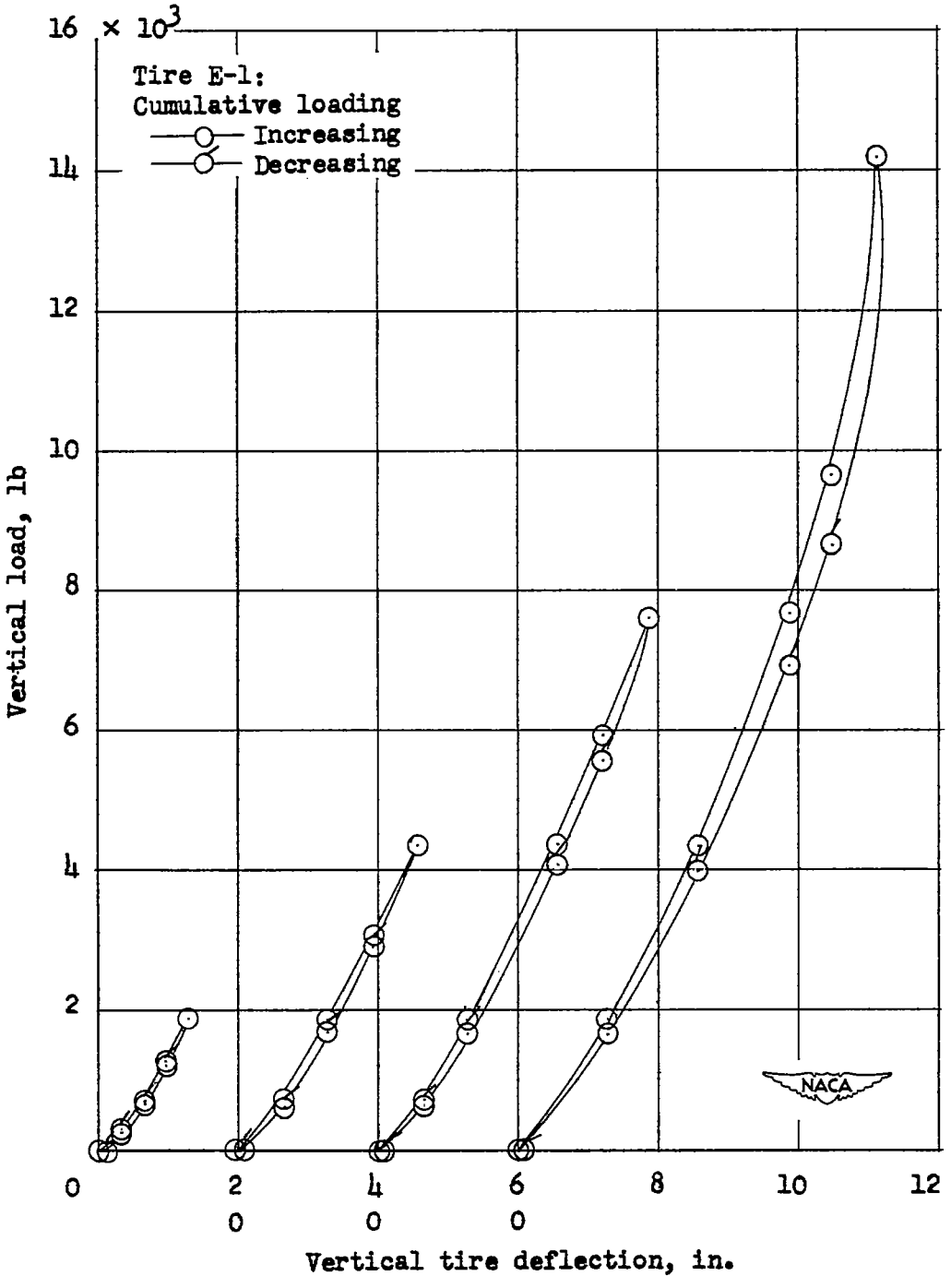

(c) Initial inflation pressure, 40 pounds per square inch; tire E-1.

Figure 9.- Continued.

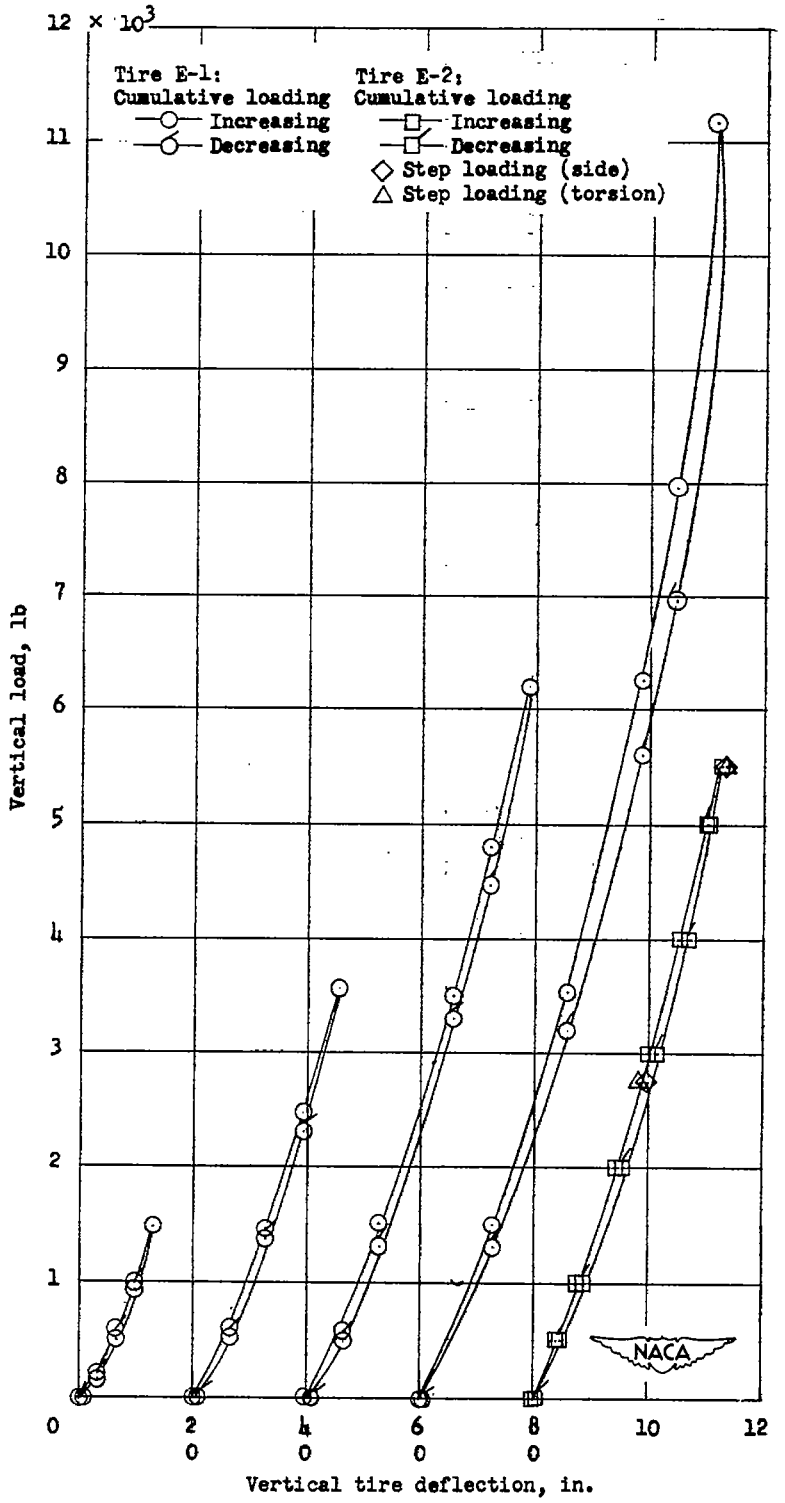

(d) Initial inflation pressure, 32 pounds per square inch; tires E-1 and E-2.

Figure 9.- Continued.

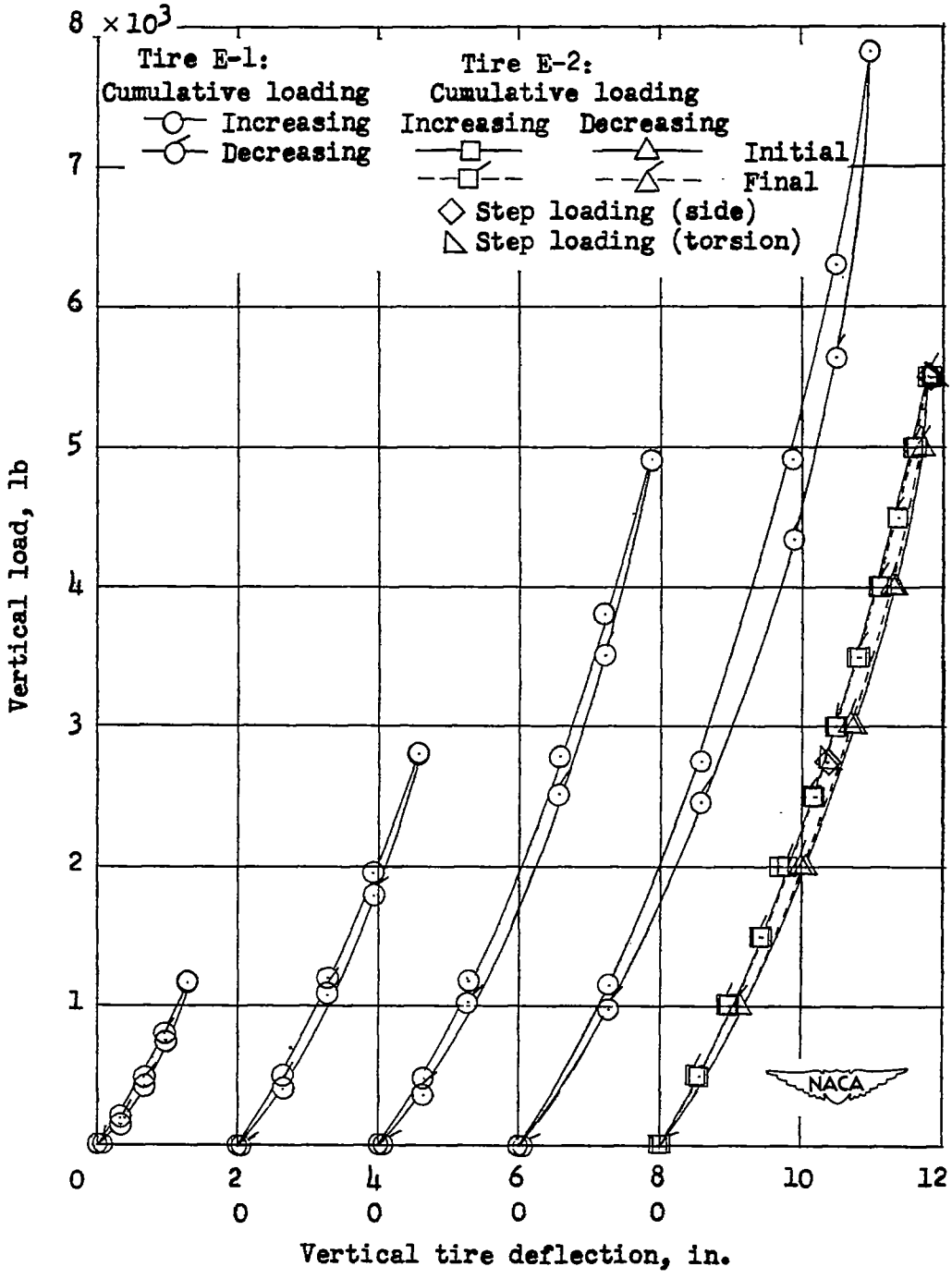

(e) Initial inflation pressure, 24 pounds per square inch; tires E-1 and E-2.

Figure 9.- Concluded.

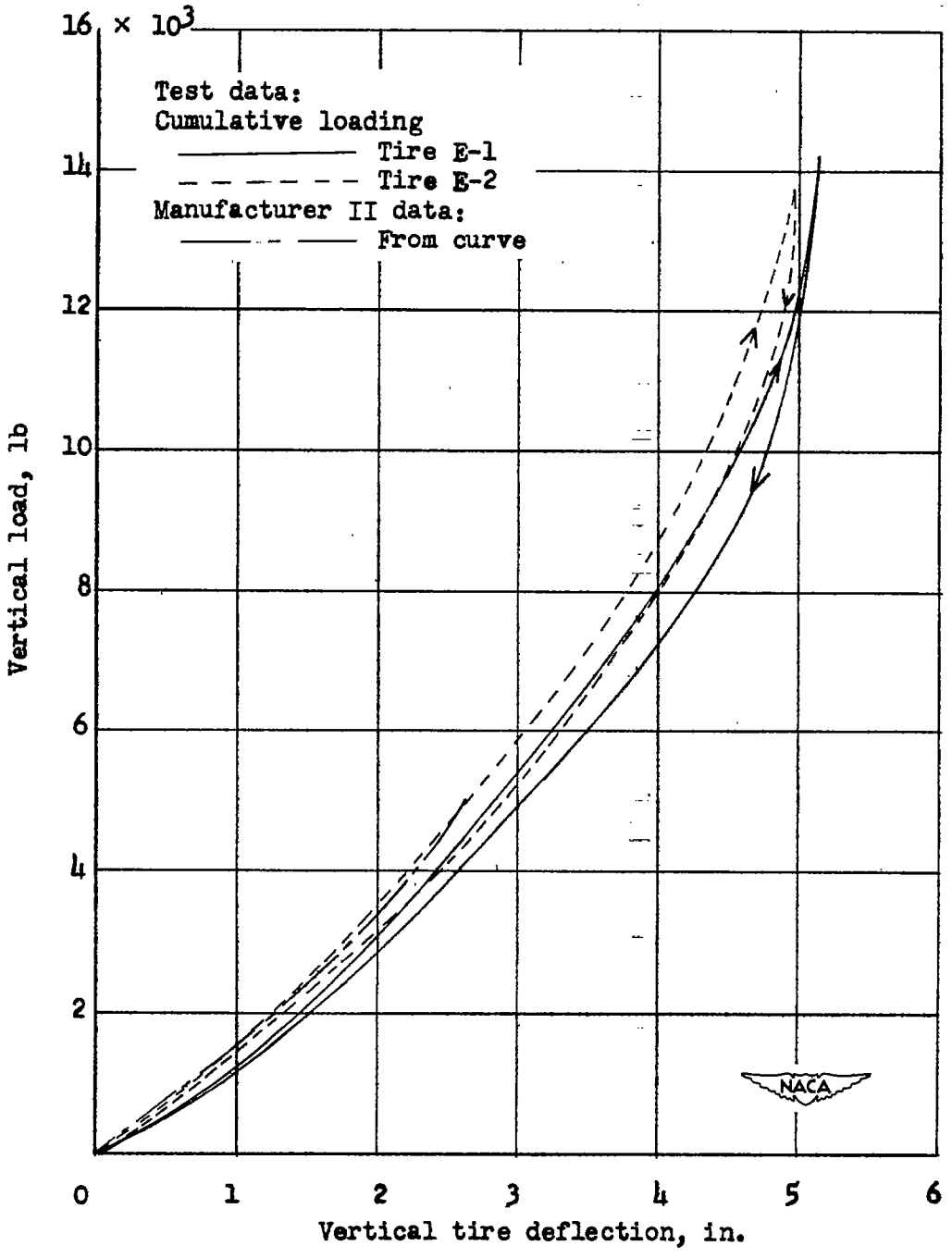

(a) Initial inflation pressure, 40 pounds per square inch.

Figure 10.- Comparison of test and manufacturer II (manufacturer of tire E-1) vertical-load—vertical-tire-deflection data at inflation pressures of 40, 32, and 24 pounds per square inch for the 27-inch, 10-ply-rating tires (tires E-1 and E-2).

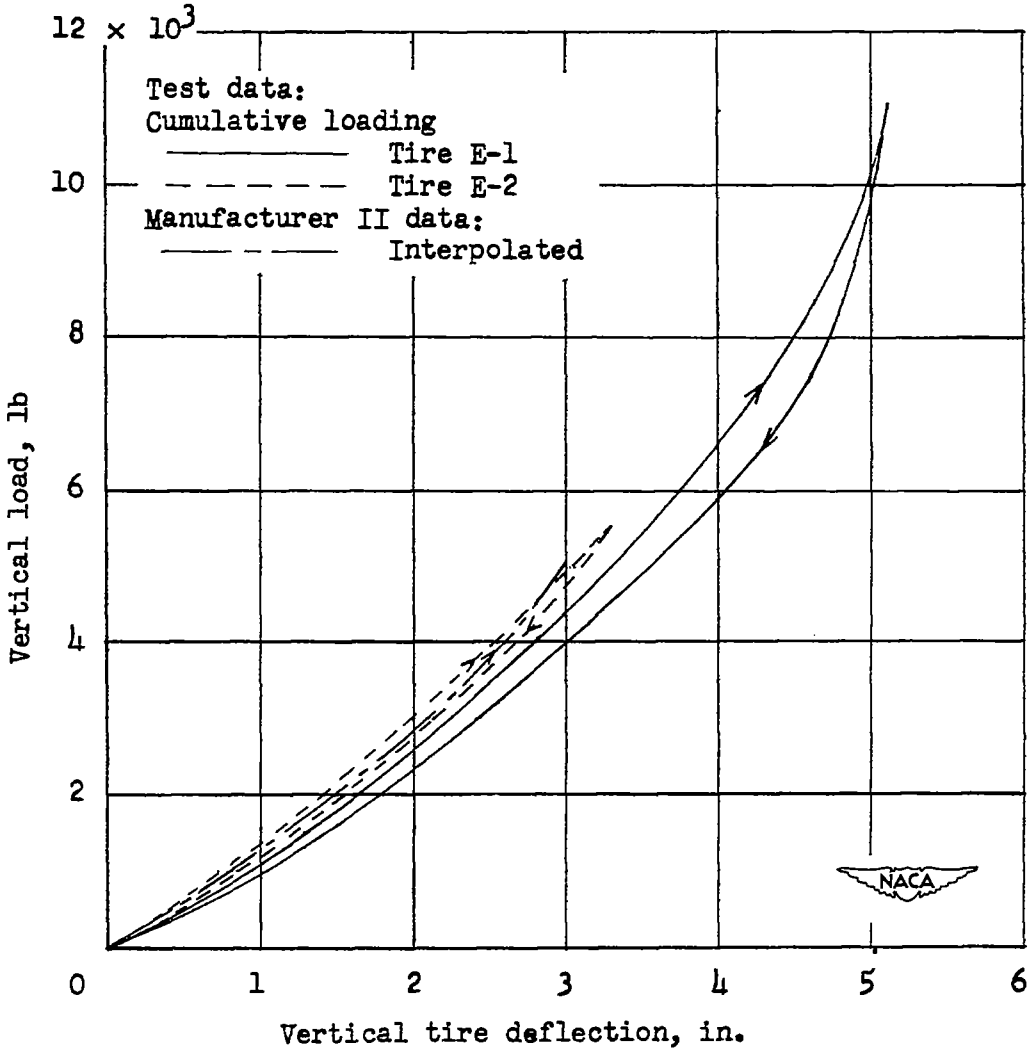

(b) Initial inflation pressure, 32 pounds per square inch.

Figure 10.- Continued.

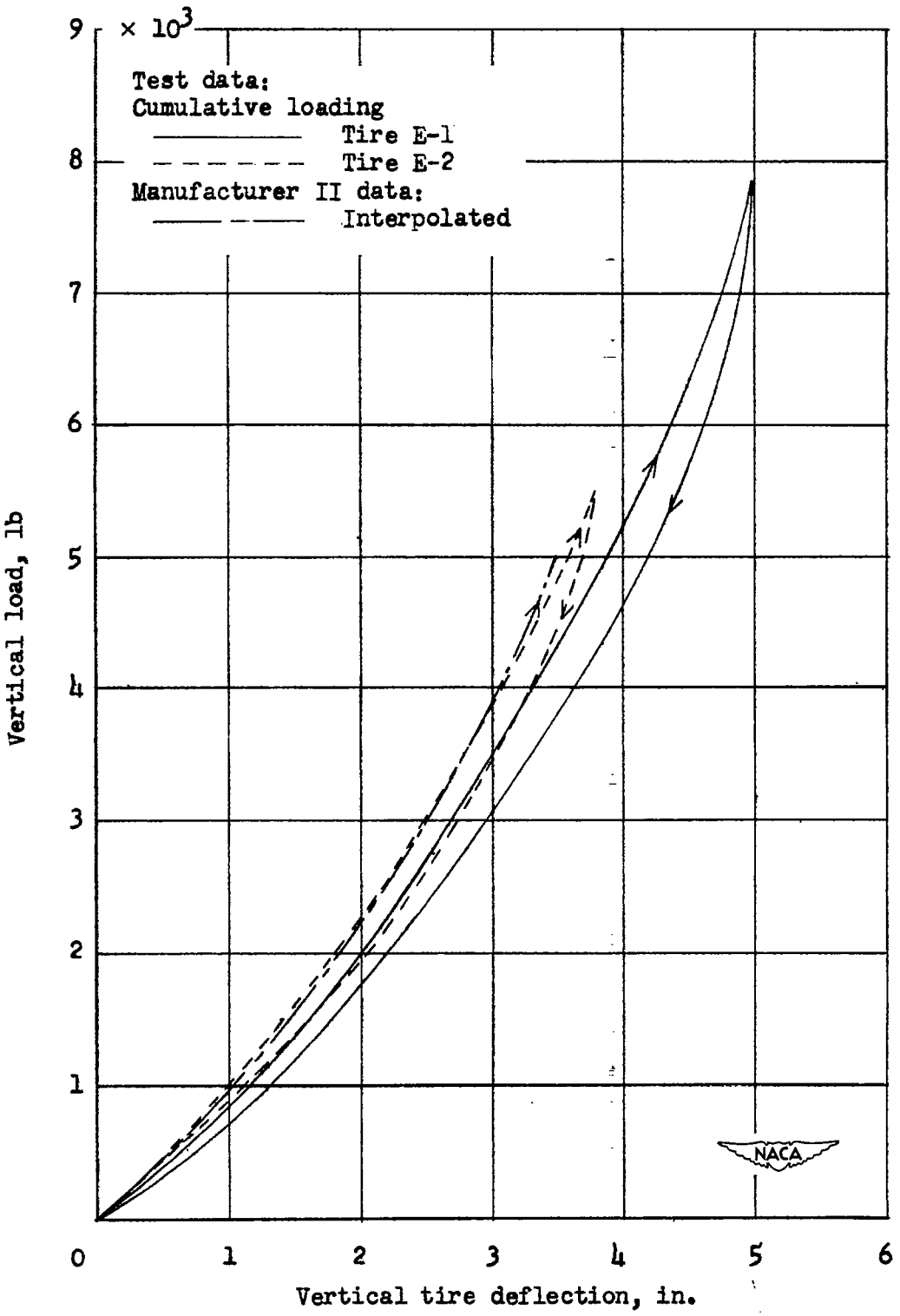

(c) Initial inflation pressure, 24 pounds per square inch.

Figure 10.- Concluded.

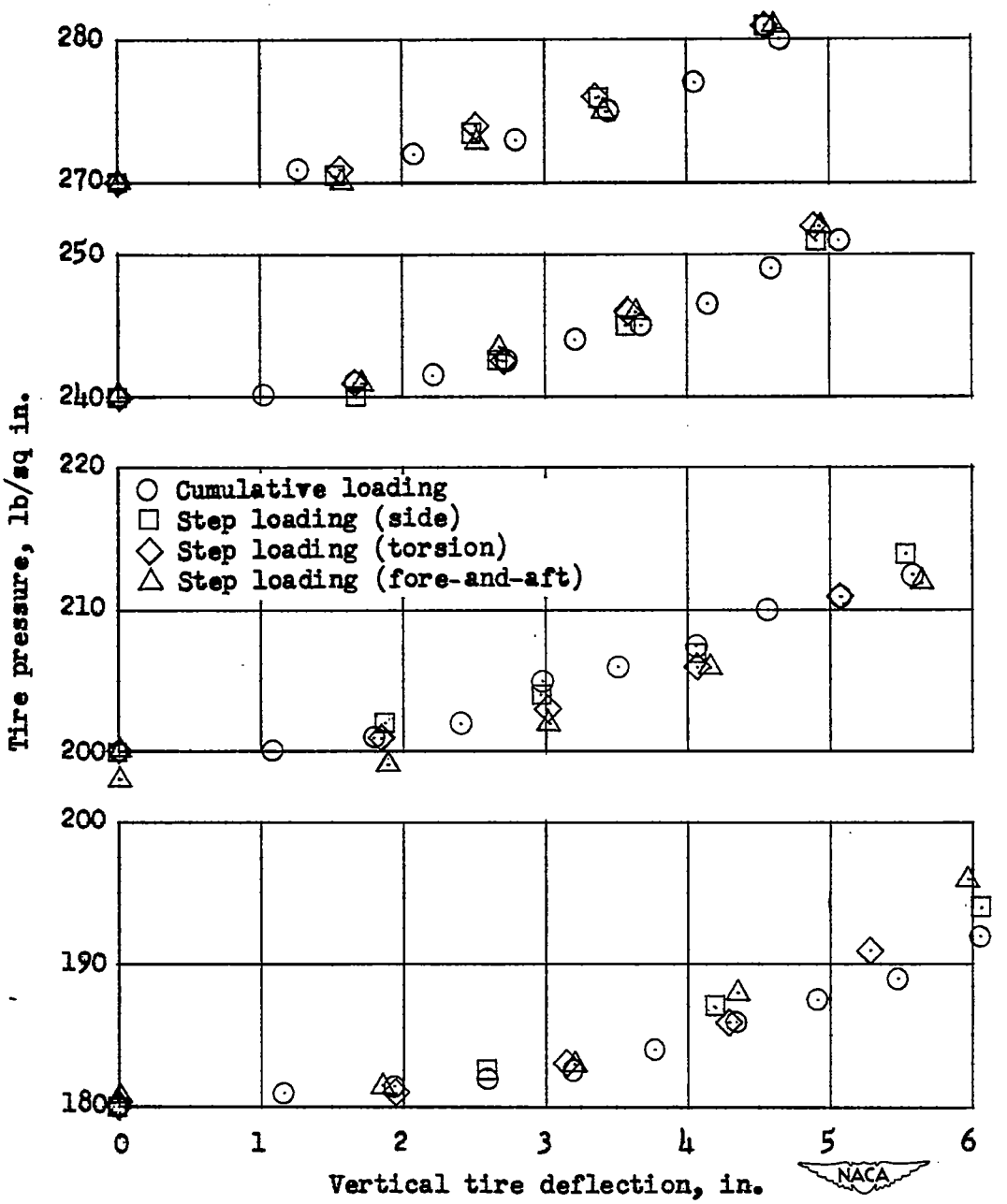

(a) Tire pressure against vertical tire deflection.

Figure 11.- Variation of tire pressure with vertical tire deflection and with vertical load for cumulative loading and step loading procedures for the 56-inch, 32-ply-rating tire (tire A).

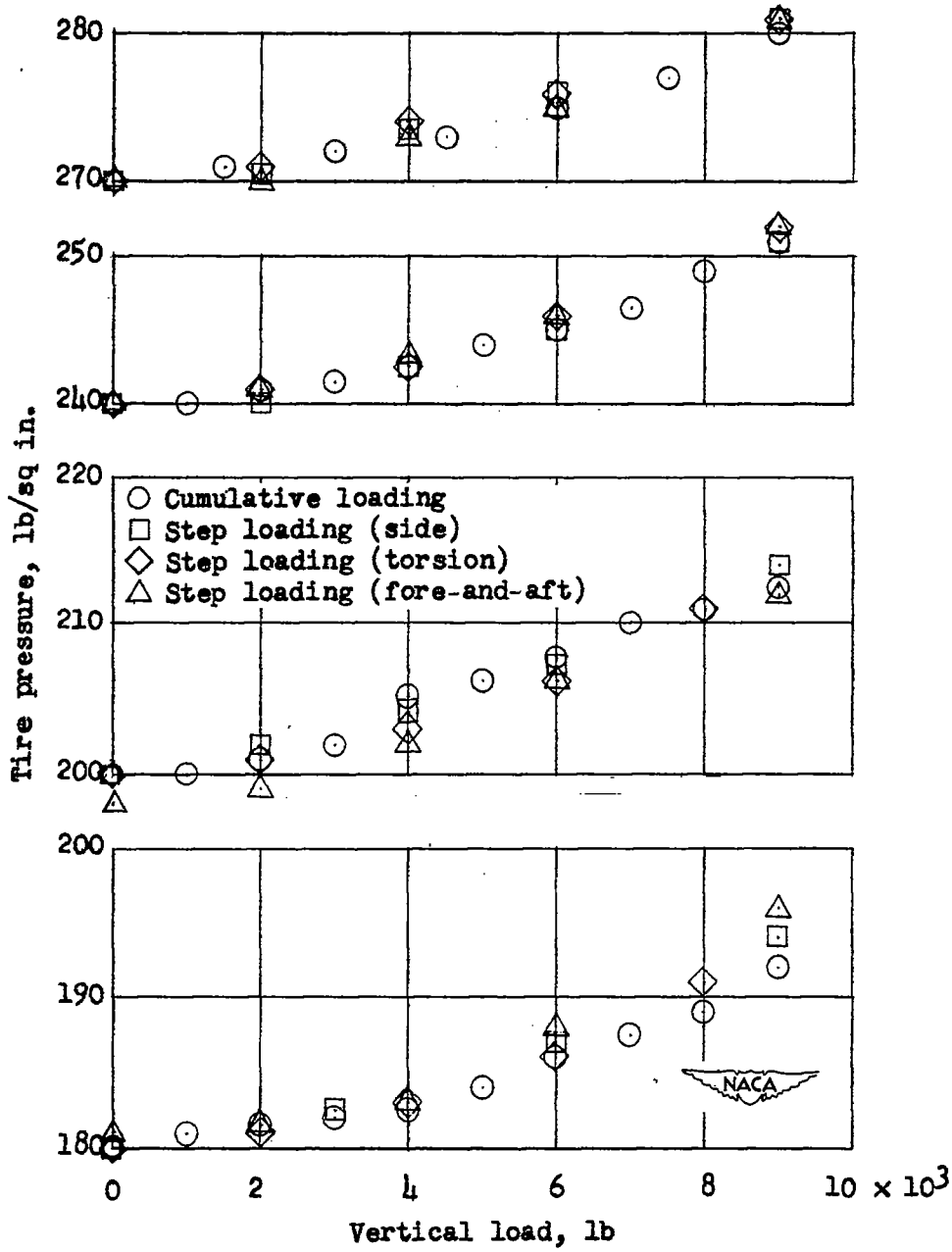

(b) Tire pressure against vertical load.

Figure 11.- Concluded.

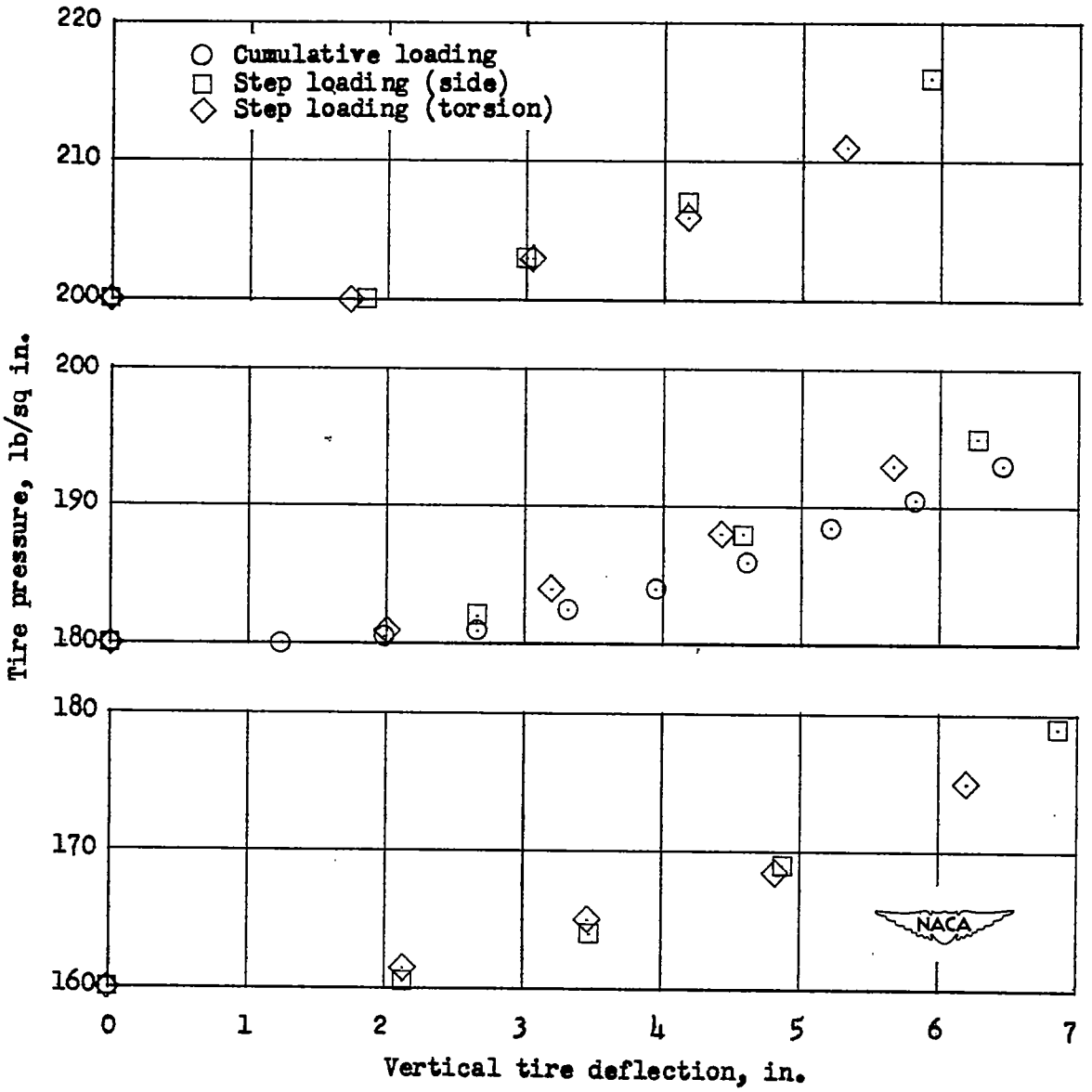

(a) Tire pressure against vertical tire deflection.

Figure 12.- Variation of tire pressure with vertical tire deflection and with vertical load for cumulative loading and step loading procedures for the 56-inch, 24-ply-rating tire (tire B).

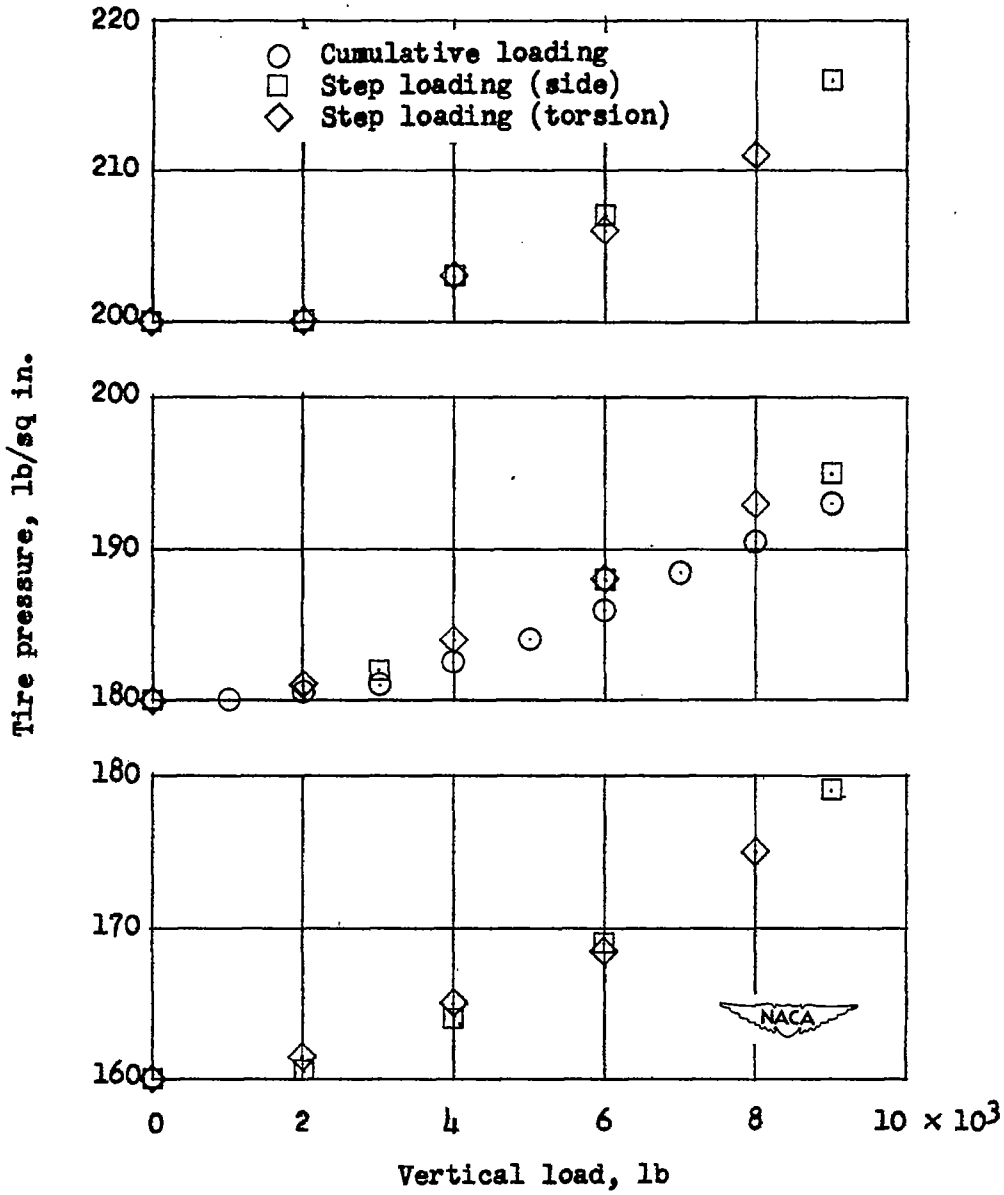

(b) Tire pressure against vertical load.

Figure 12.- Concluded.

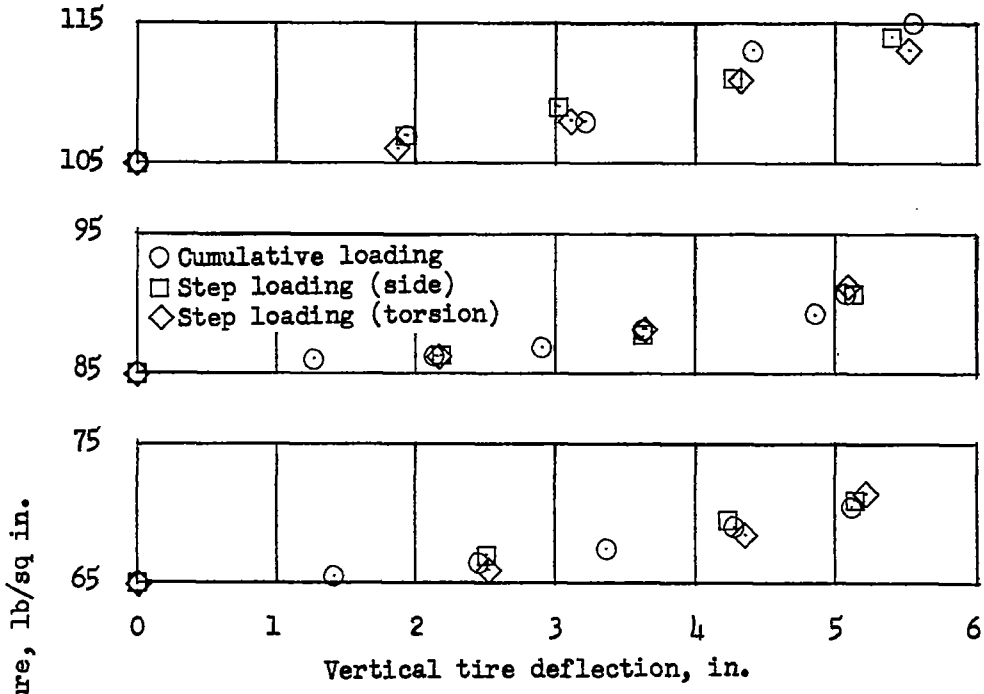

(a) Tire pressure against vertical tire deflection.

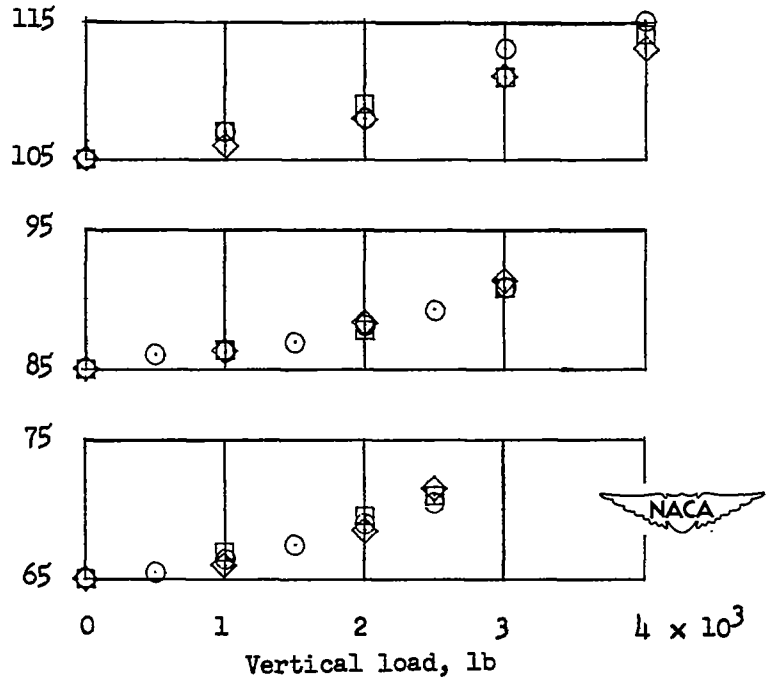

(b) Tire pressure against vertical load.

Figure 13.- Variation of tire pressure with vertical tire deflection and with vertical load for cumulative loading and step loading procedures for the 45-inch, 14-ply-rating tire (tire C).

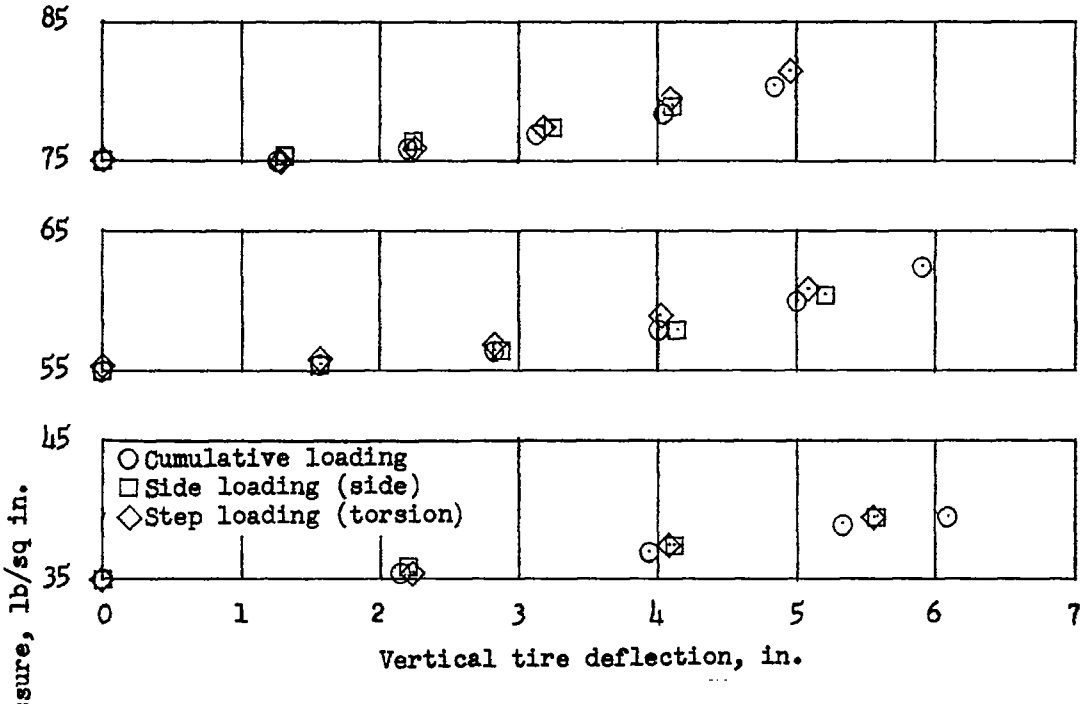

(a) Tire pressure against vertical tire deflection.

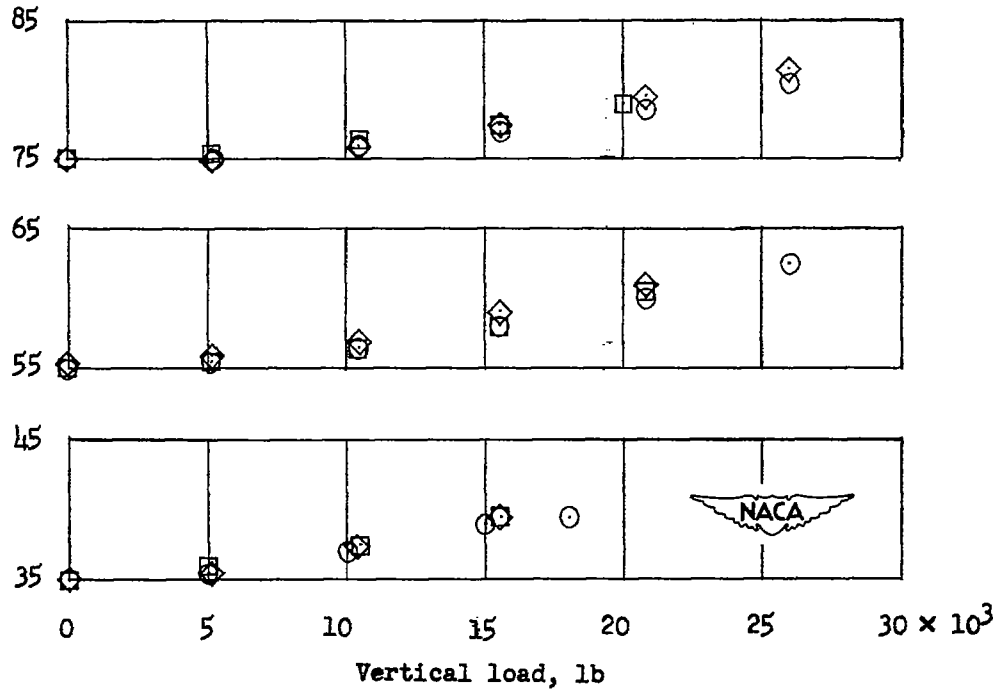

(b) Tire pressure against vertical load.

Figure 14.- Variation of tire pressure with vertical tire deflection and with vertical load for cumulative loading and step loading procedures for the 44-inch, 10-ply-rating tire (tire D).

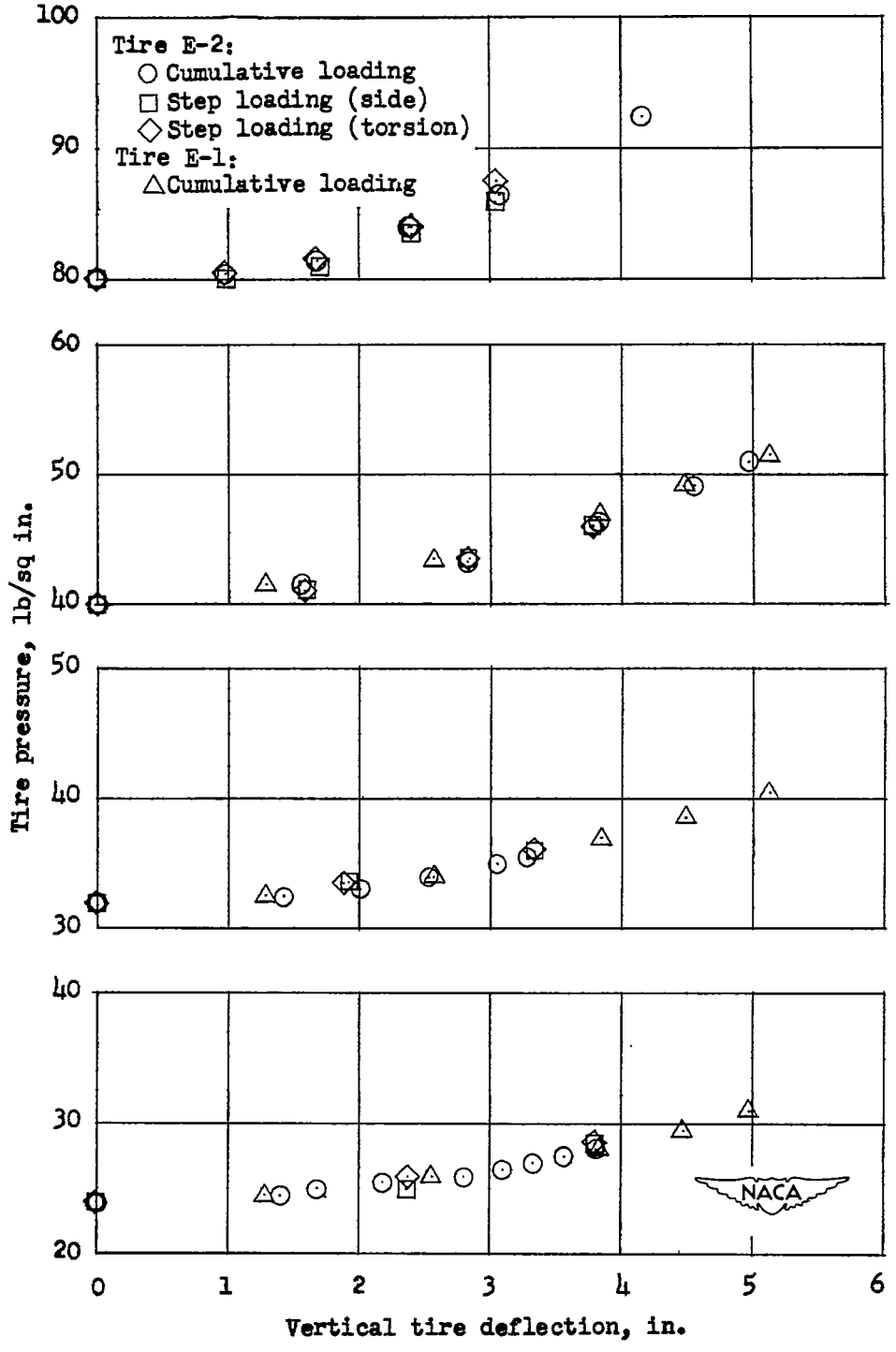

(a) Tire pressure against vertical tire deflection.

Figure 15.- Variation of tire pressure with vertical tire deflection and with vertical load for cumulative loading and step loading procedures for the 27-inch, 10-ply-rating tires (tires E-1 and E-2).

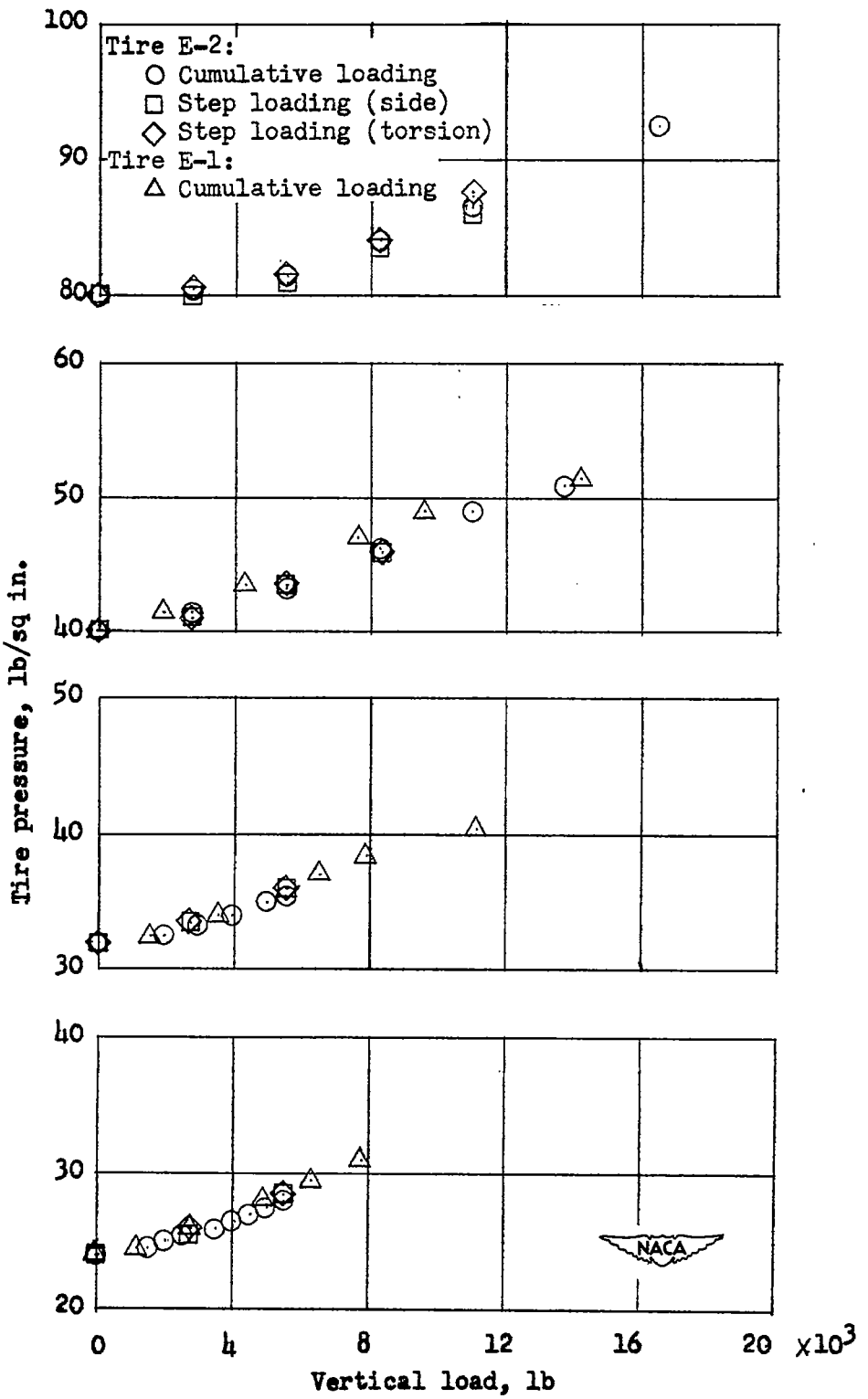

(b) Tire pressure against vertical load.

Figure 15.- Concluded.

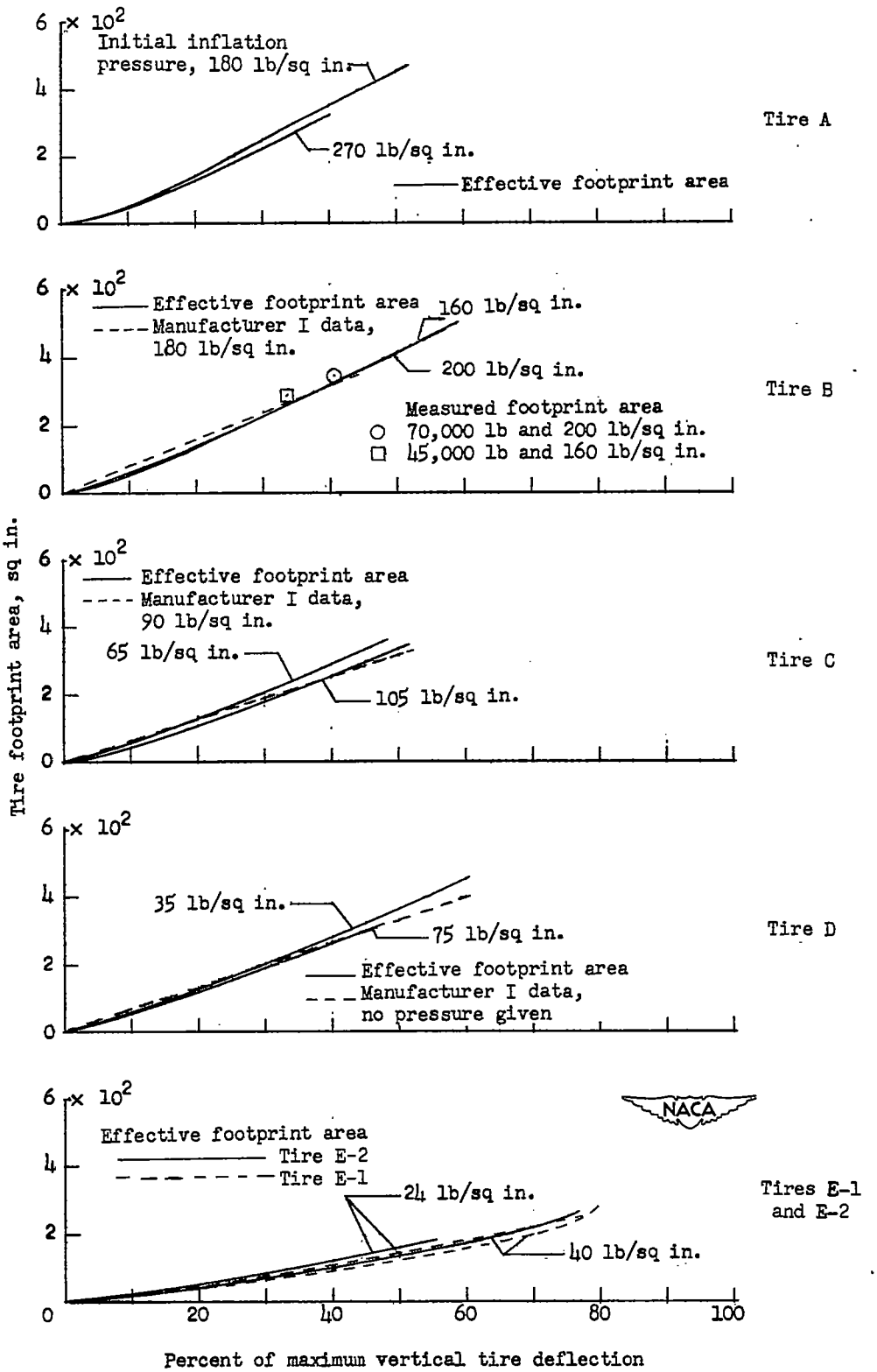

Figure 16.- Comparison of effective footprint area (Vertical load/Tire pressure) with data on footprint area obtained from manufacturer I and from tests.

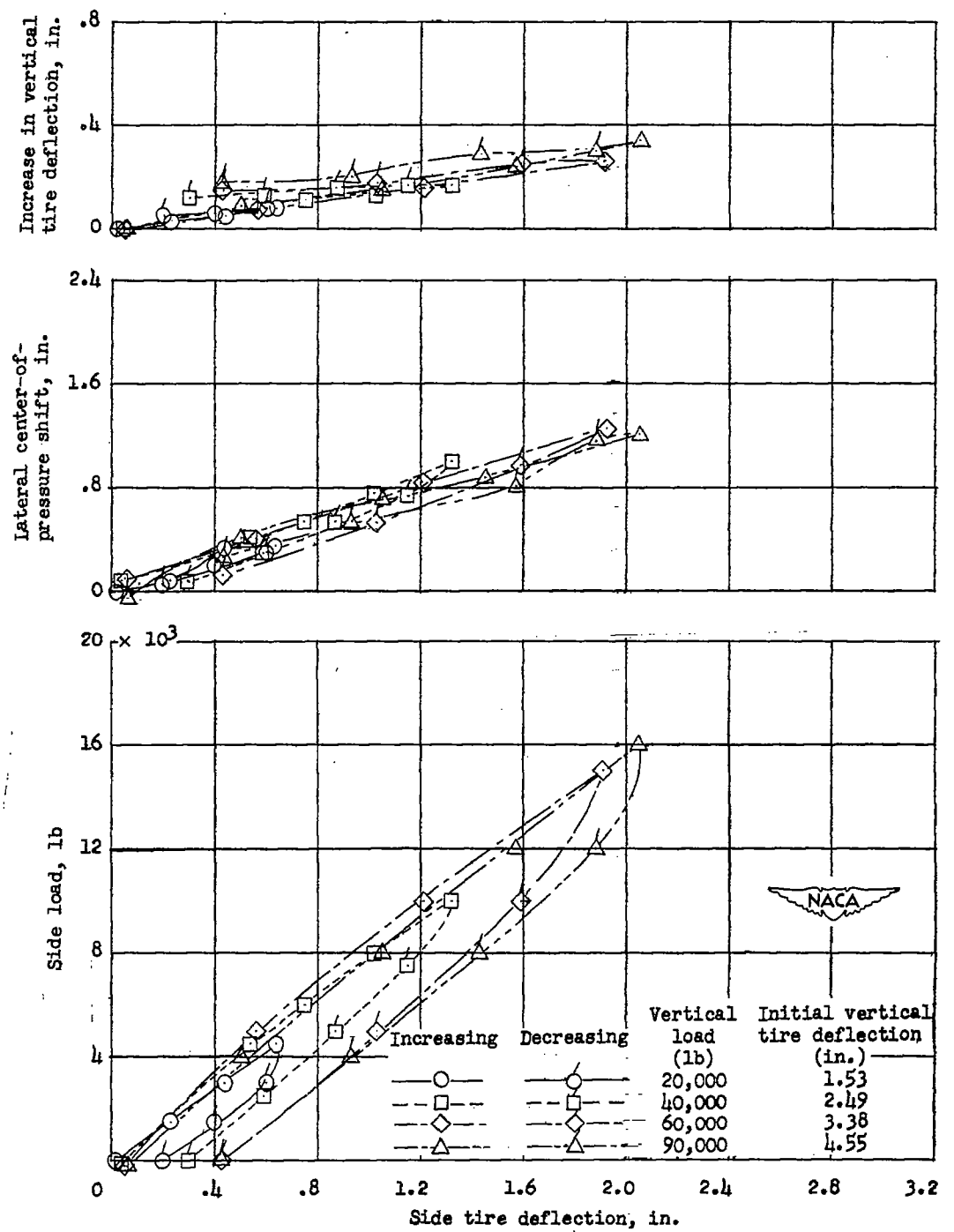

(a) Initial inflation pressure, 270 pounds per square inch.

Figure 17.- Variation with side tire deflection of side load, lateral center-of-pressure shift, and increase in vertical tire deflection for different vertical loads and inflation pressures for the 56-inch, 32-ply-rating tire (tire A).

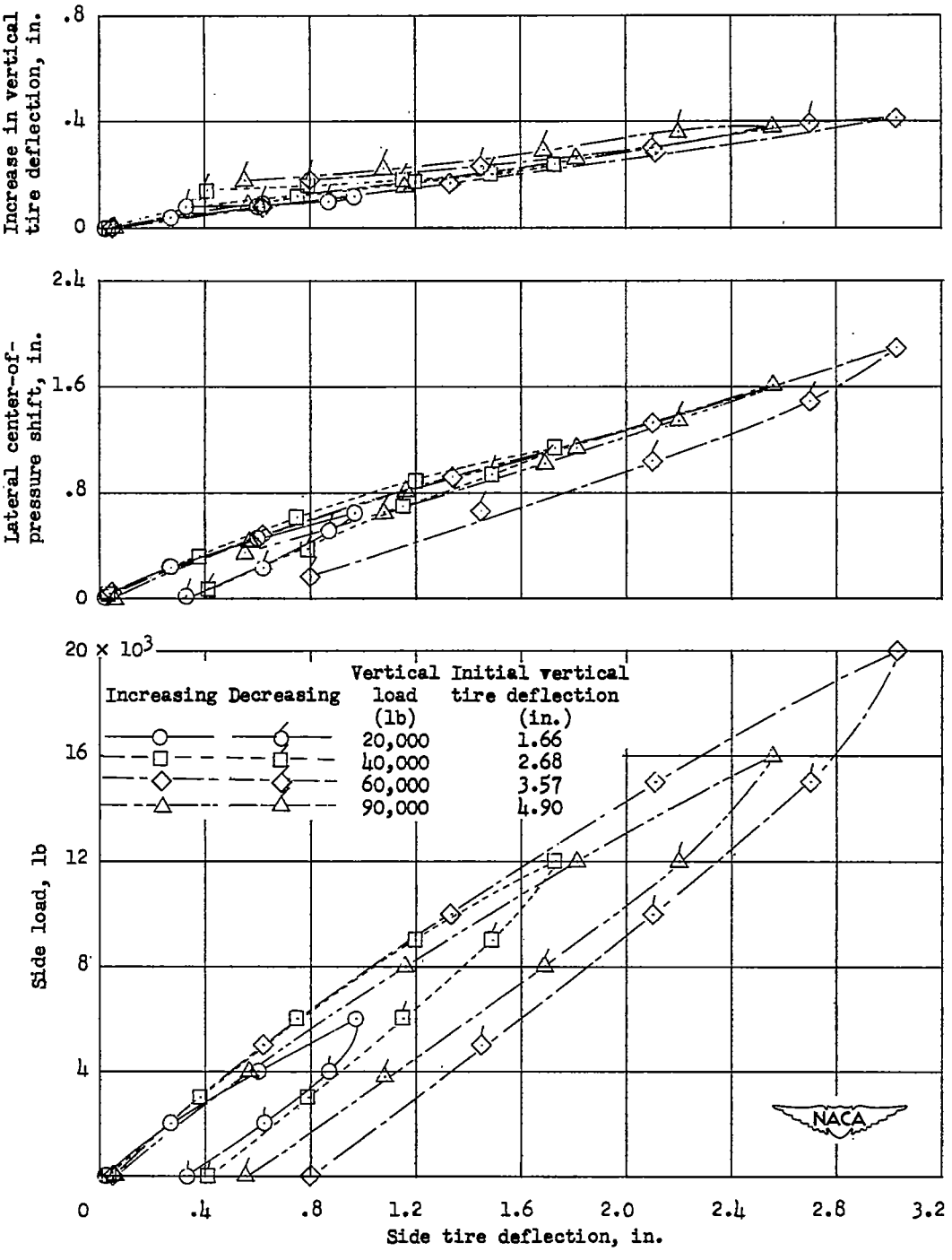

(b) Initial inflation pressure, 240 pounds per square inch.

Figure 17.- Continued.

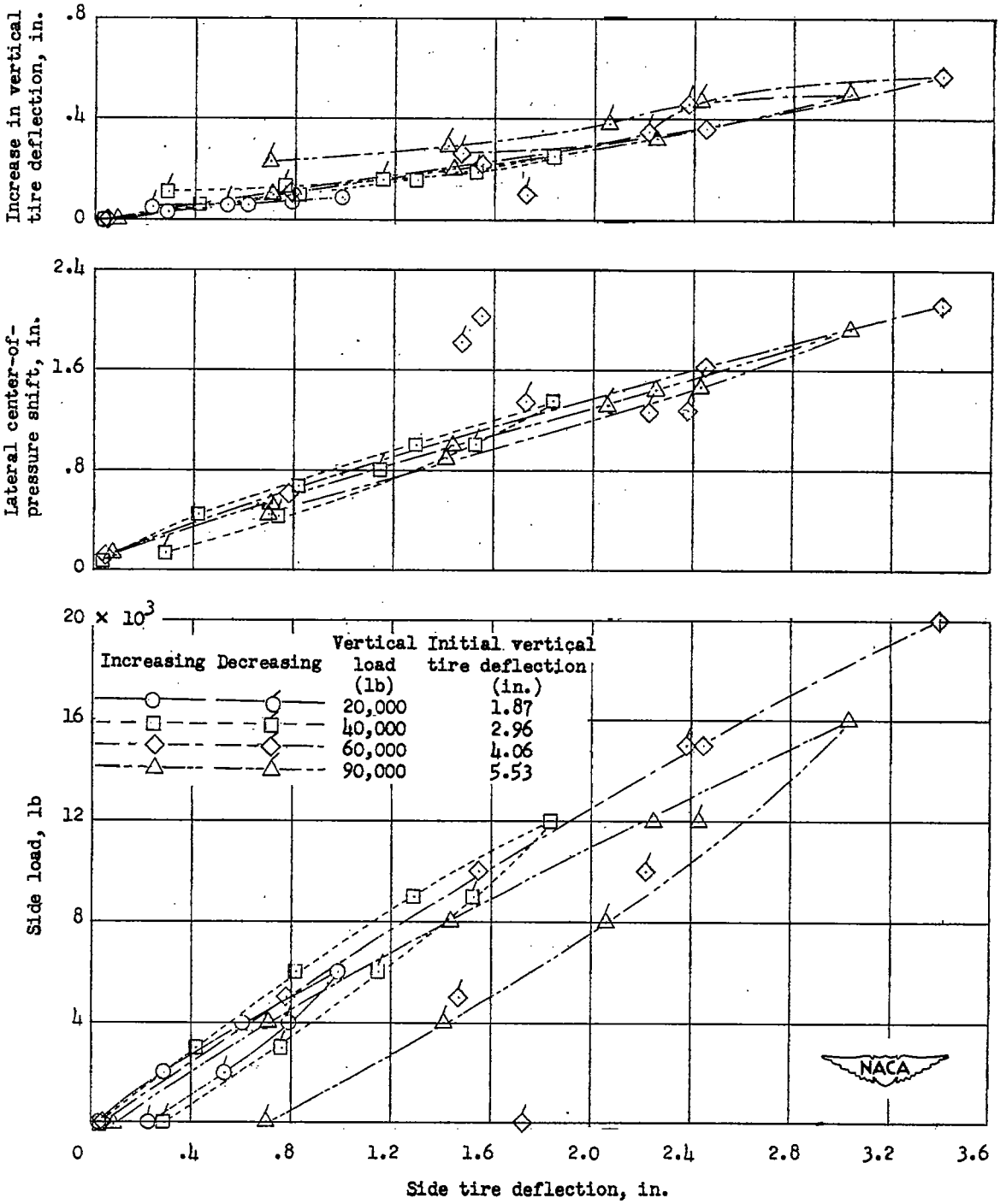

(c) Initial inflation pressure, 200 pounds per square inch.

Figure 17.- Continued.

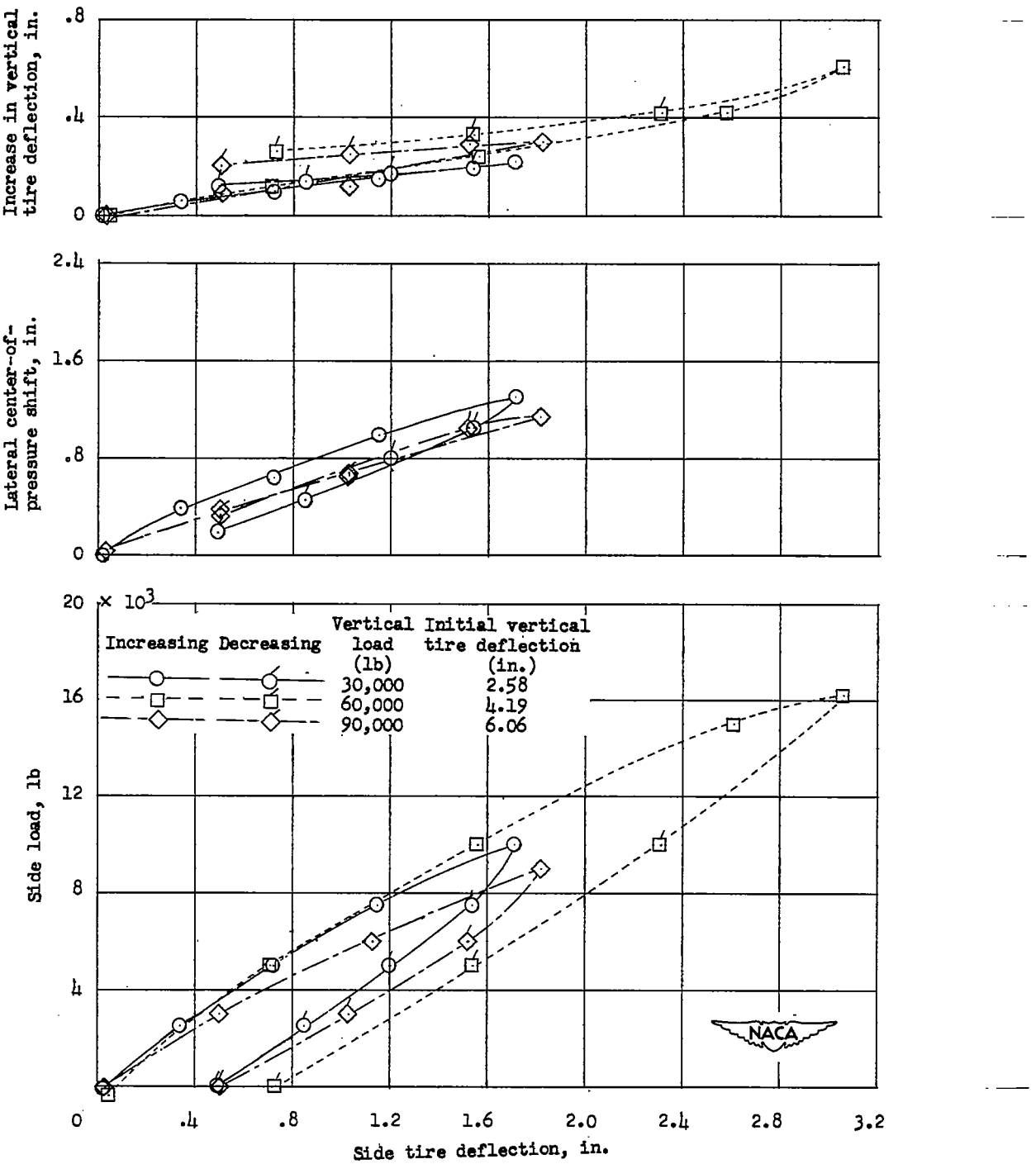

(d) Initial inflation pressure, 180 pounds per square inch.

Figure 17.- Continued.

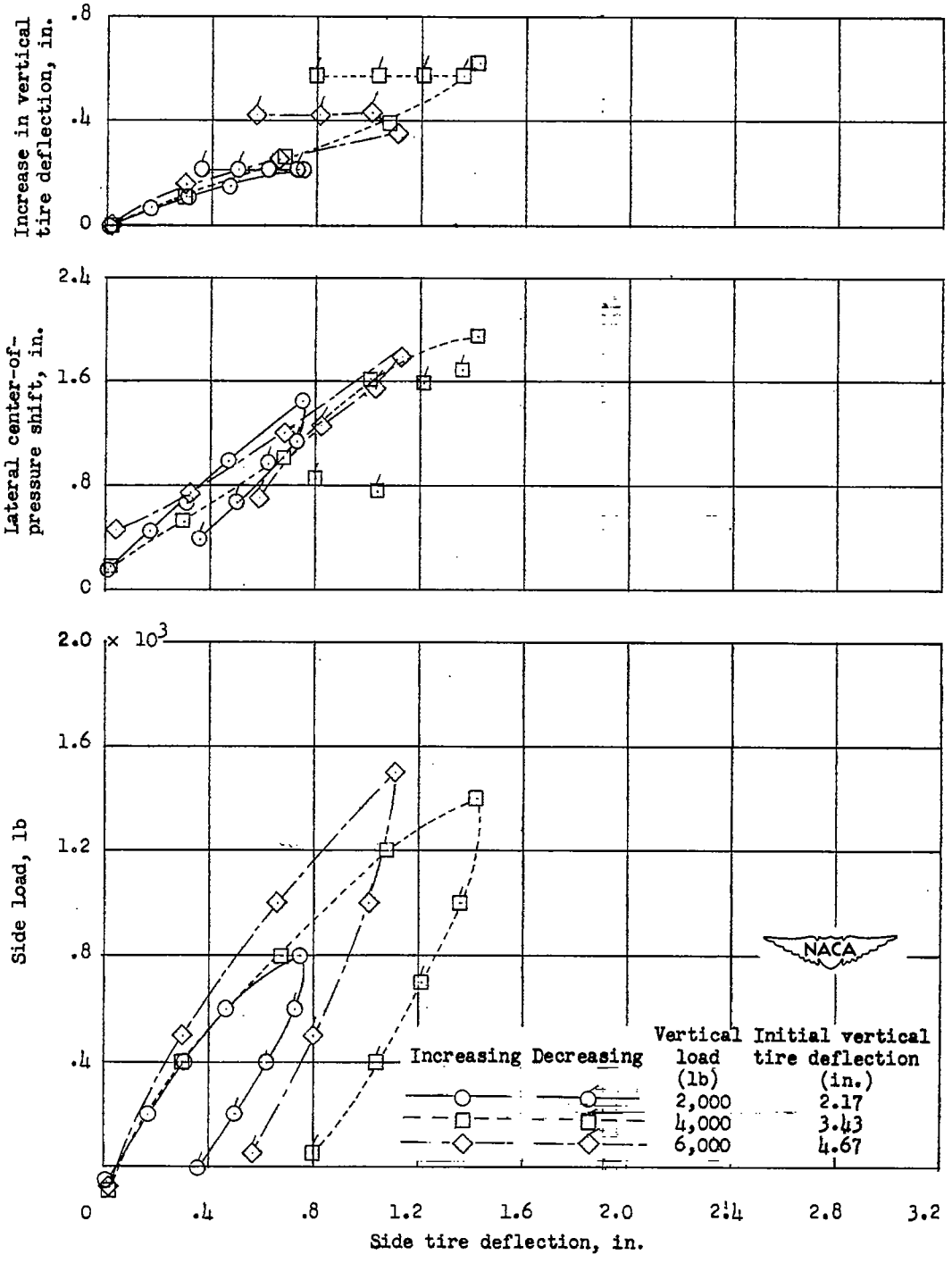

(e) Initial inflation pressure, 0 pounds per square inch.

Figure 17.- Concluded.

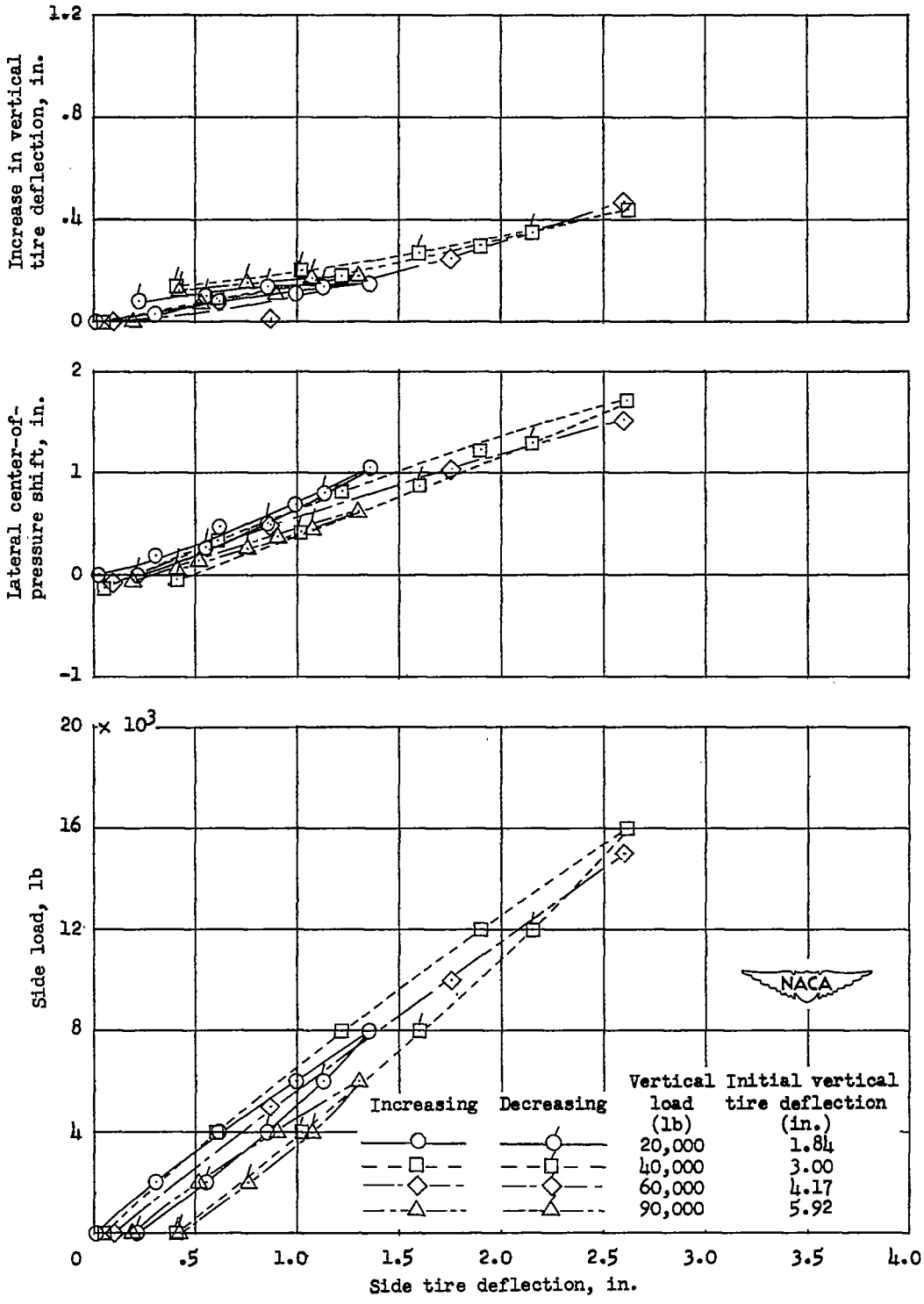

(a) Initial inflation pressure, 200 pounds per square inch.

Figure 18.- Variation with side tire deflection of side load, lateral center-of-pressure shift, and increase in vertical tire deflection for different vertical loads and inflation pressures for the 56-inch, 24-ply-rating tire (tire B).

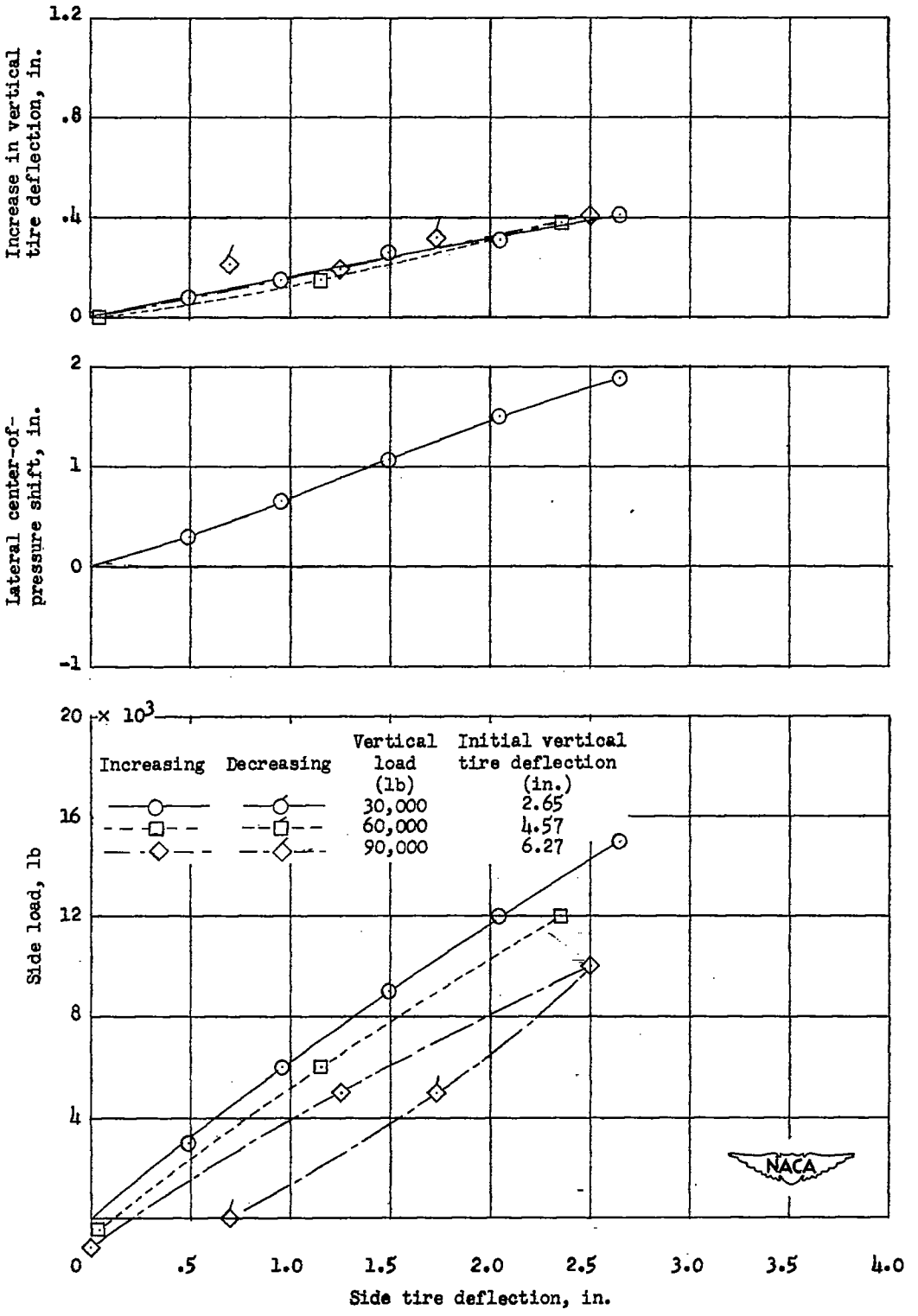

(b) Initial inflation pressure, 180 pounds per square inch.

Figure 18.- Continued.

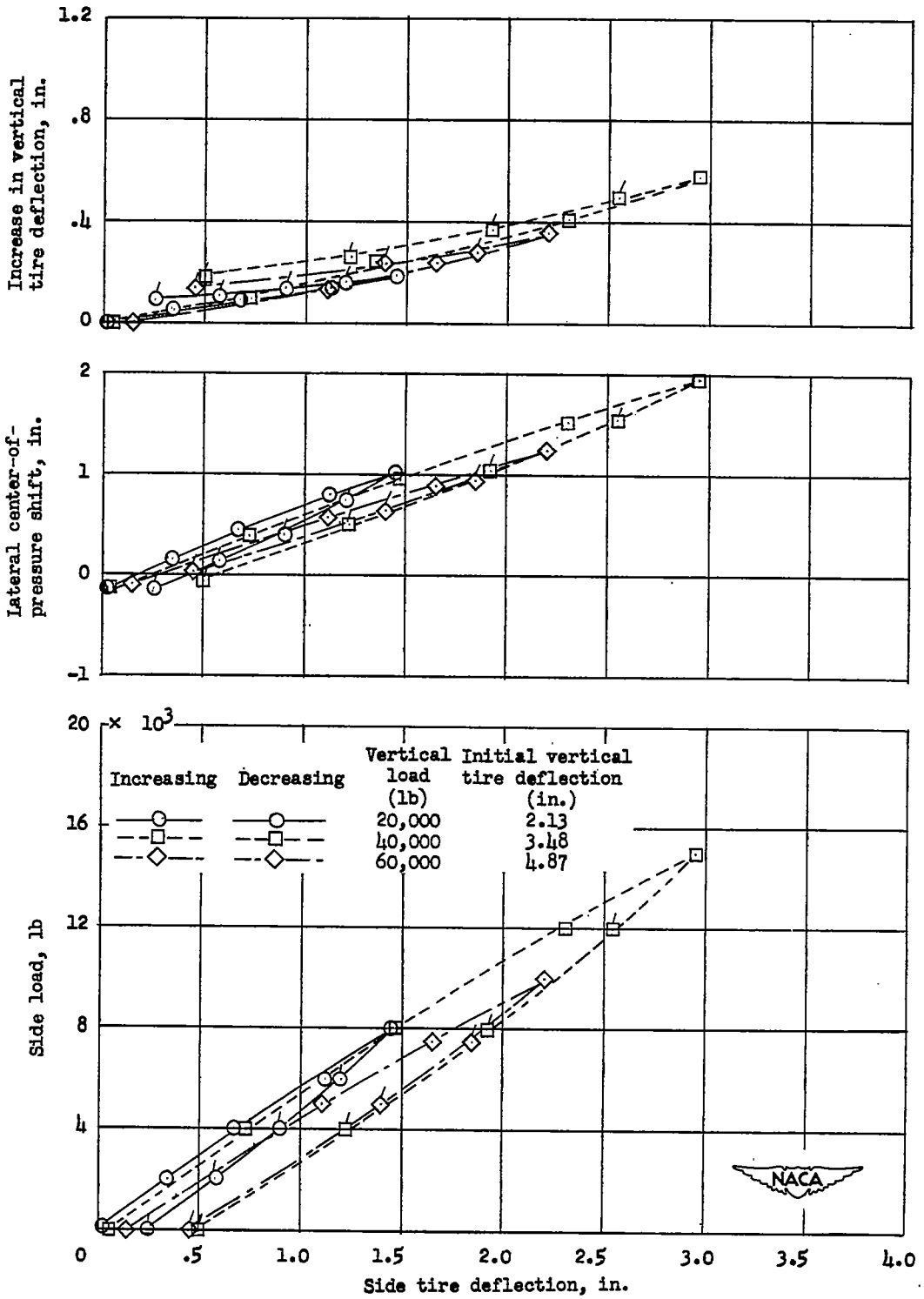

(c) Initial inflation pressure, 160 pounds per square inch.

Figure 18.- Concluded.

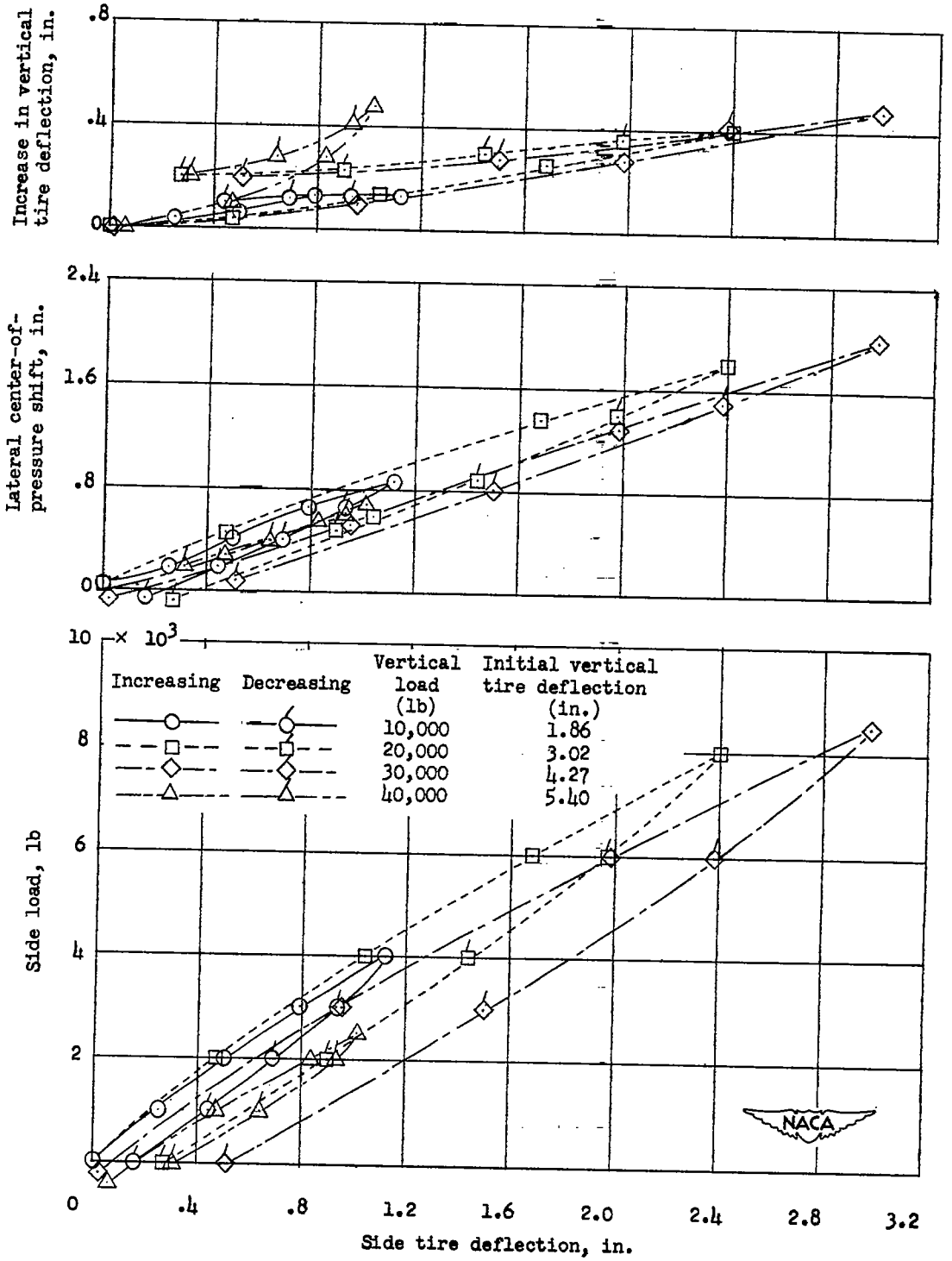

(a) Initial inflation pressure, 105 pounds per square inch.

Figure 19.- Variation with side tire deflection of side load, lateral center-of-pressure shift, and increase in vertical tire deflection for different vertical loads and inflation pressures for the 45-inch, 14-ply-rating tire (tire C).

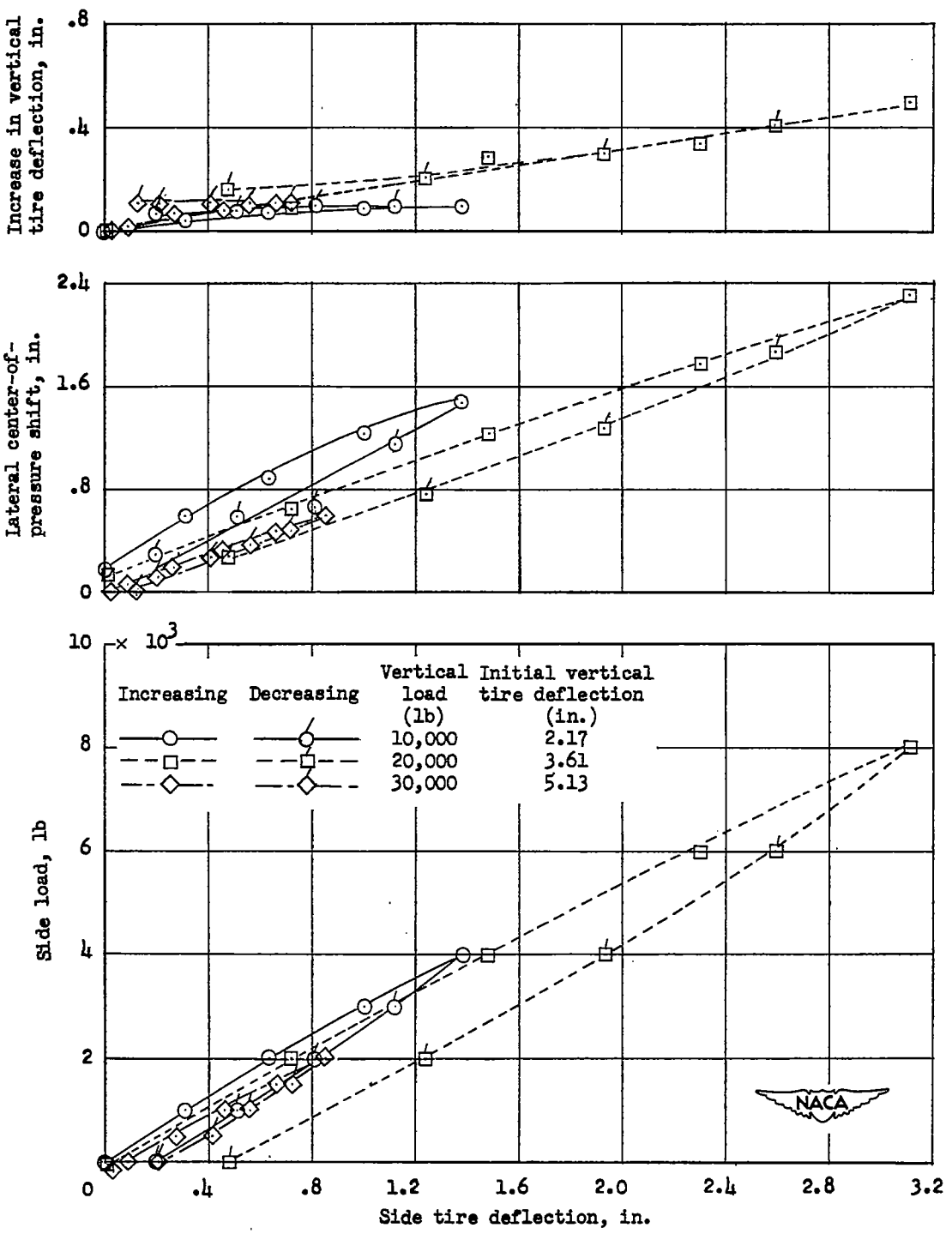

(b) Initial inflation pressure, 85 pounds per square inch.

Figure 19.- Continued.

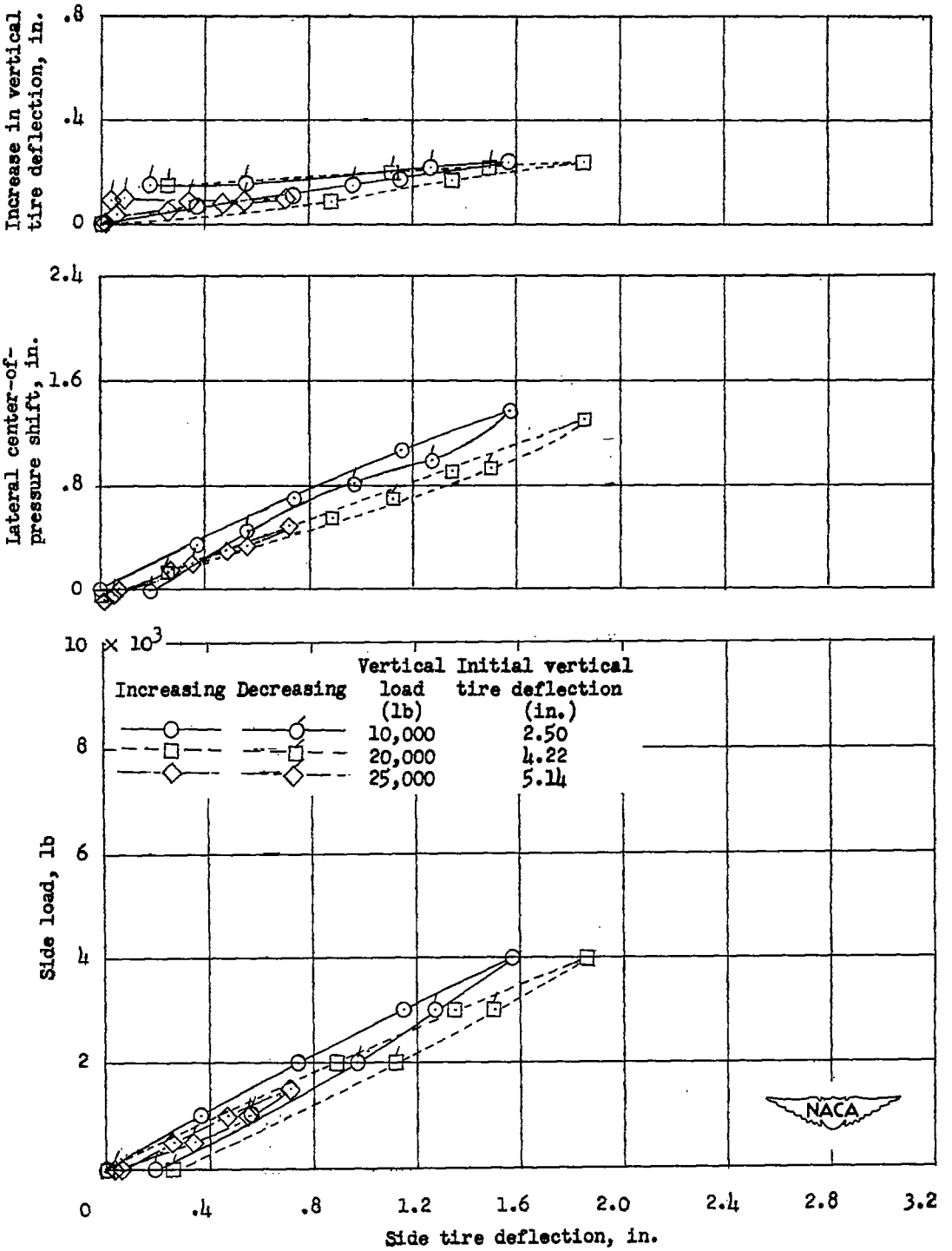

(c) Initial inflation pressure, 65 pound per square inch.

Figure 19.- Concluded.

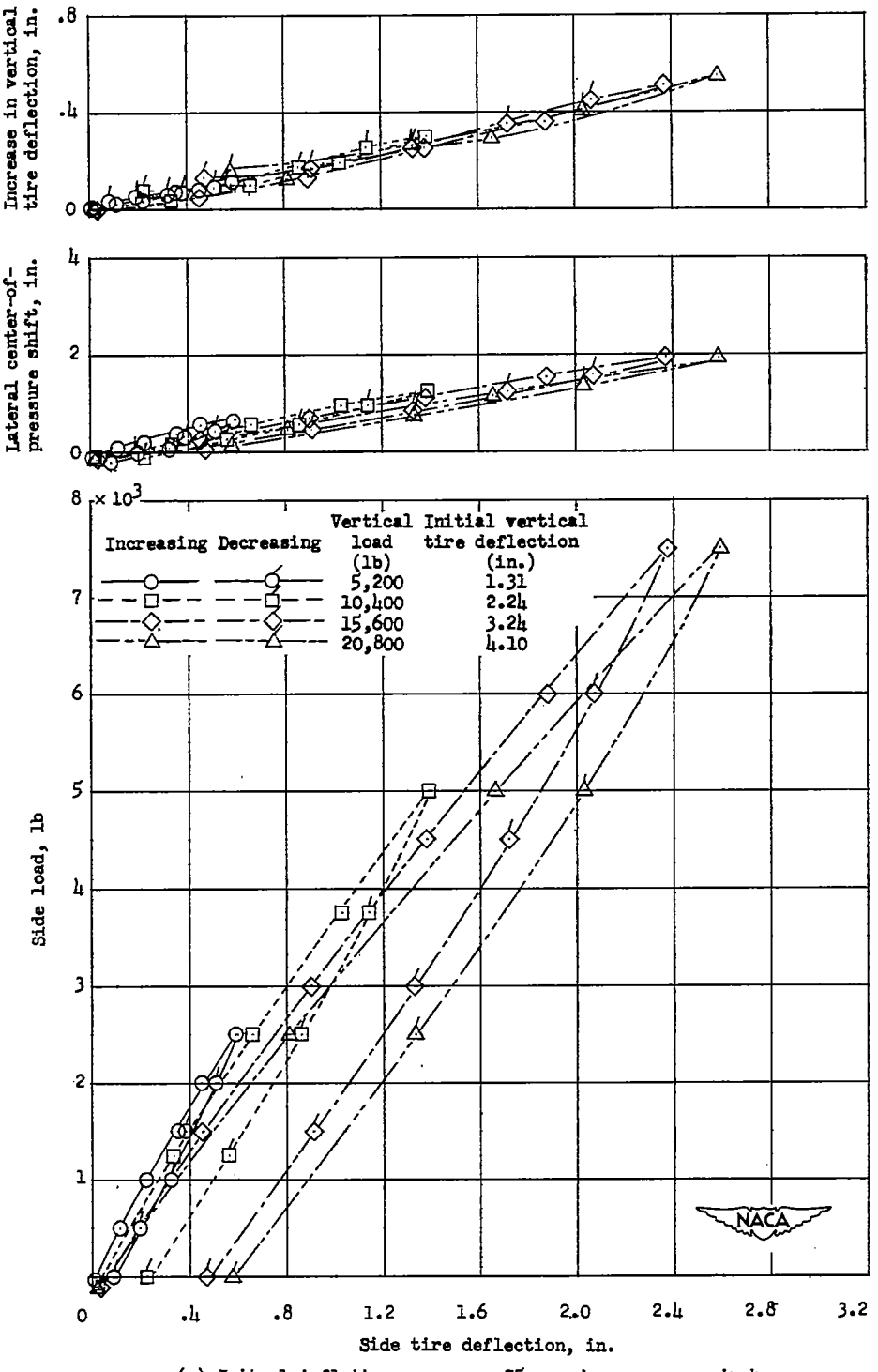

(a) Initial inflation pressure, 75 pounds per square inch.

Figure 20.- Variation with side tire deflection of side load, lateral center-of-pressure shift, and increase in vertical tire deflection for different vertical loads and inflation pressures for the 44-inch, 10-ply-rating tire (tire D).

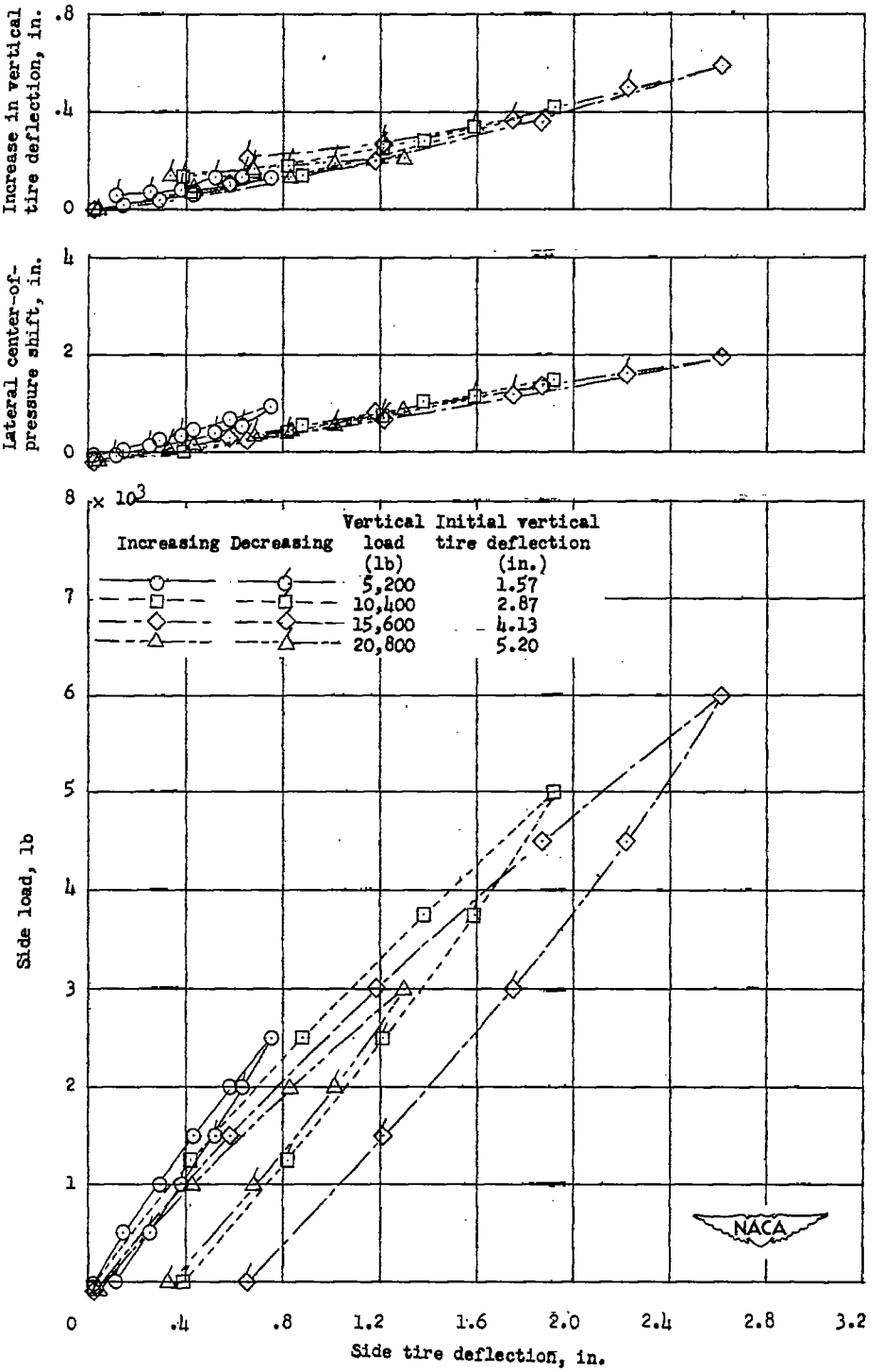

(b) Initial inflation pressure, 55 pounds per square inch.

Figure 20.- Continued.

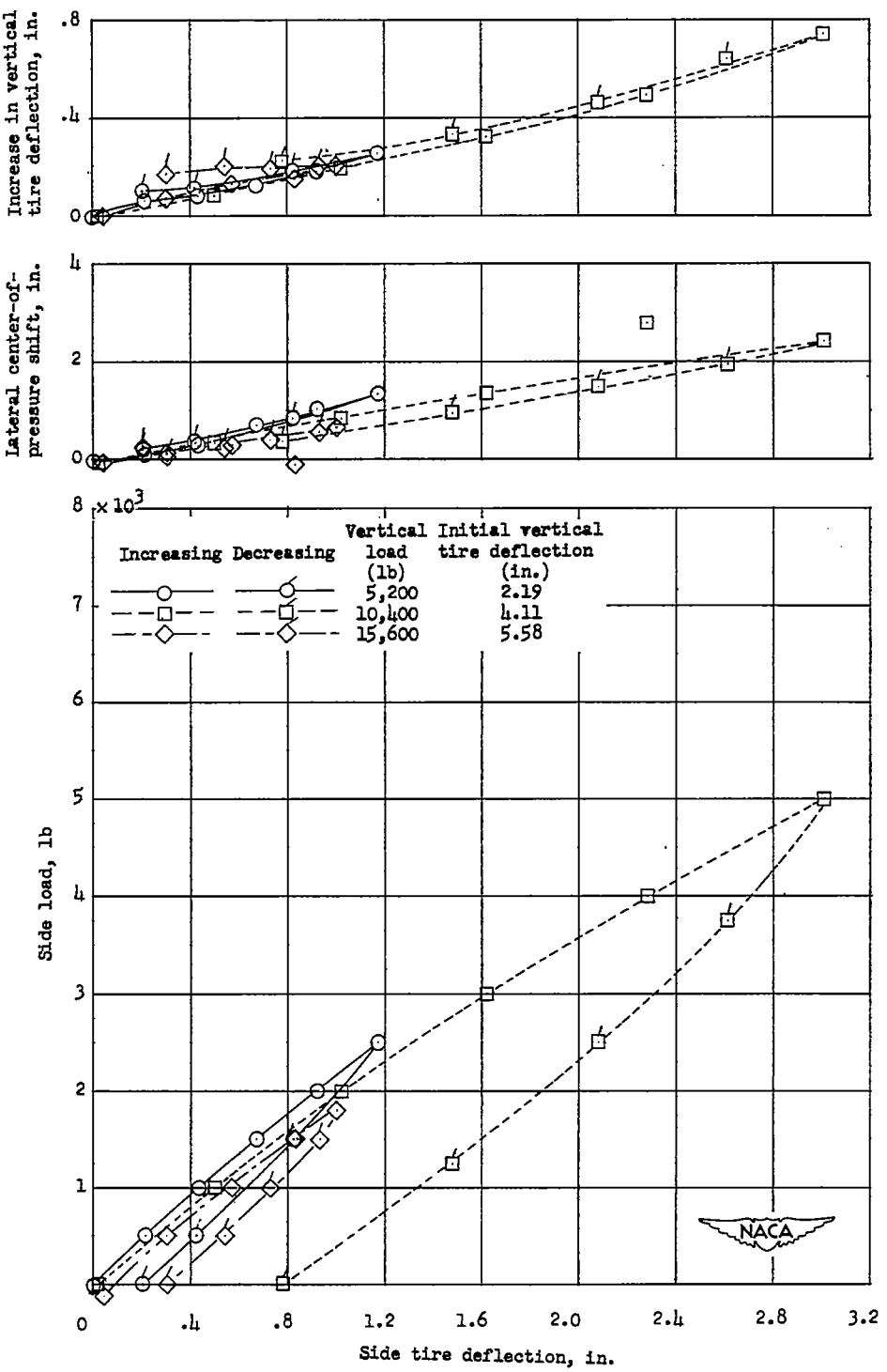

(c) Initial inflation pressure, 35 pounds per square inch.

Figure 20.- Concluded.

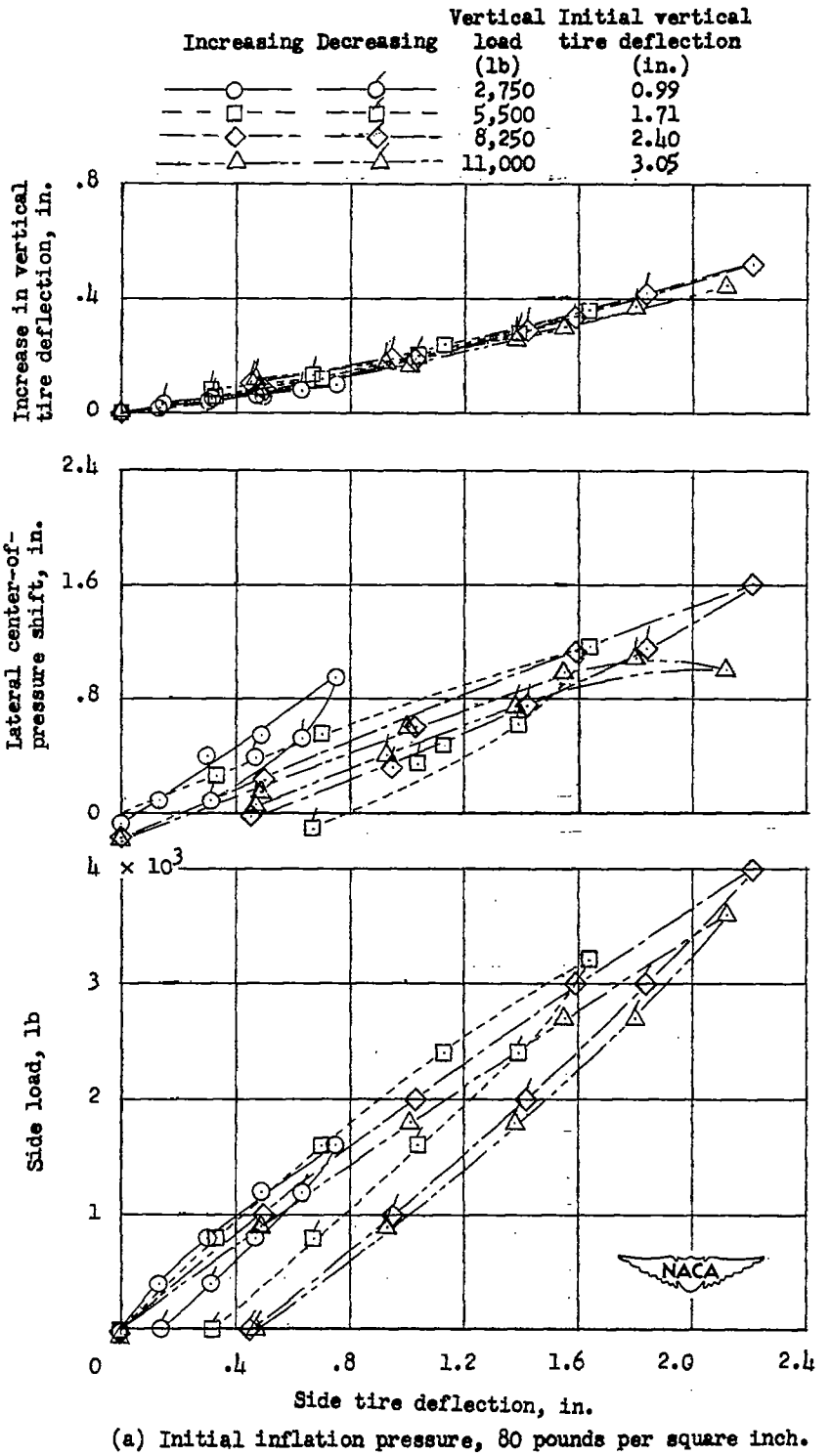

(a) Initial inflation pressure, 80 pounds per square inch.

Figure 21.- Variation with side tire deflection of side load, lateral center-of-pressure shift, and increase in vertical tire deflection for different vertical loads and inflation pressures for the 27-inch, 10-ply-rating tire (tire E-2).

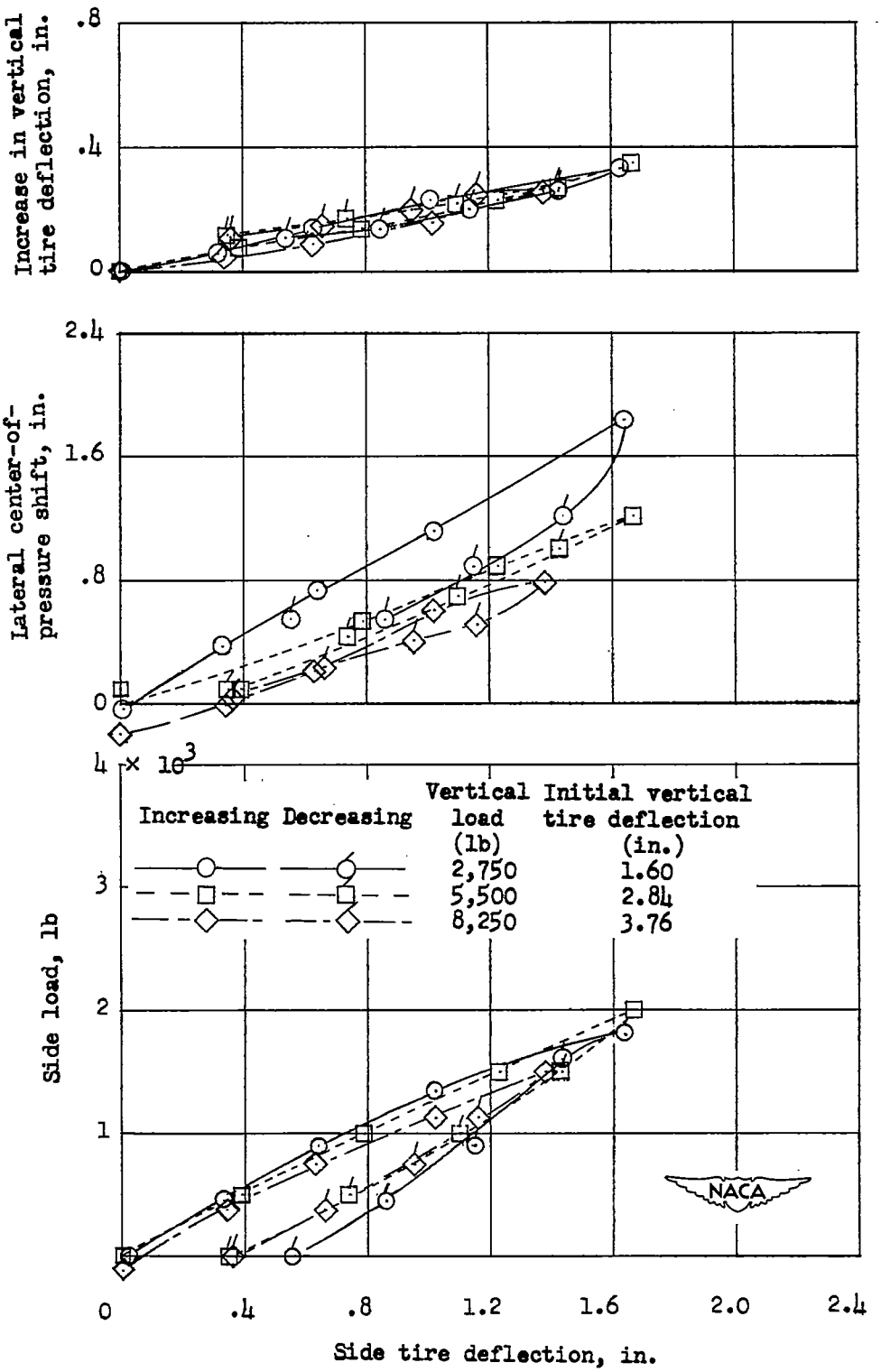

(b) Initial inflation pressure, 40 pounds per square inch.

Figure 21.- Continued.

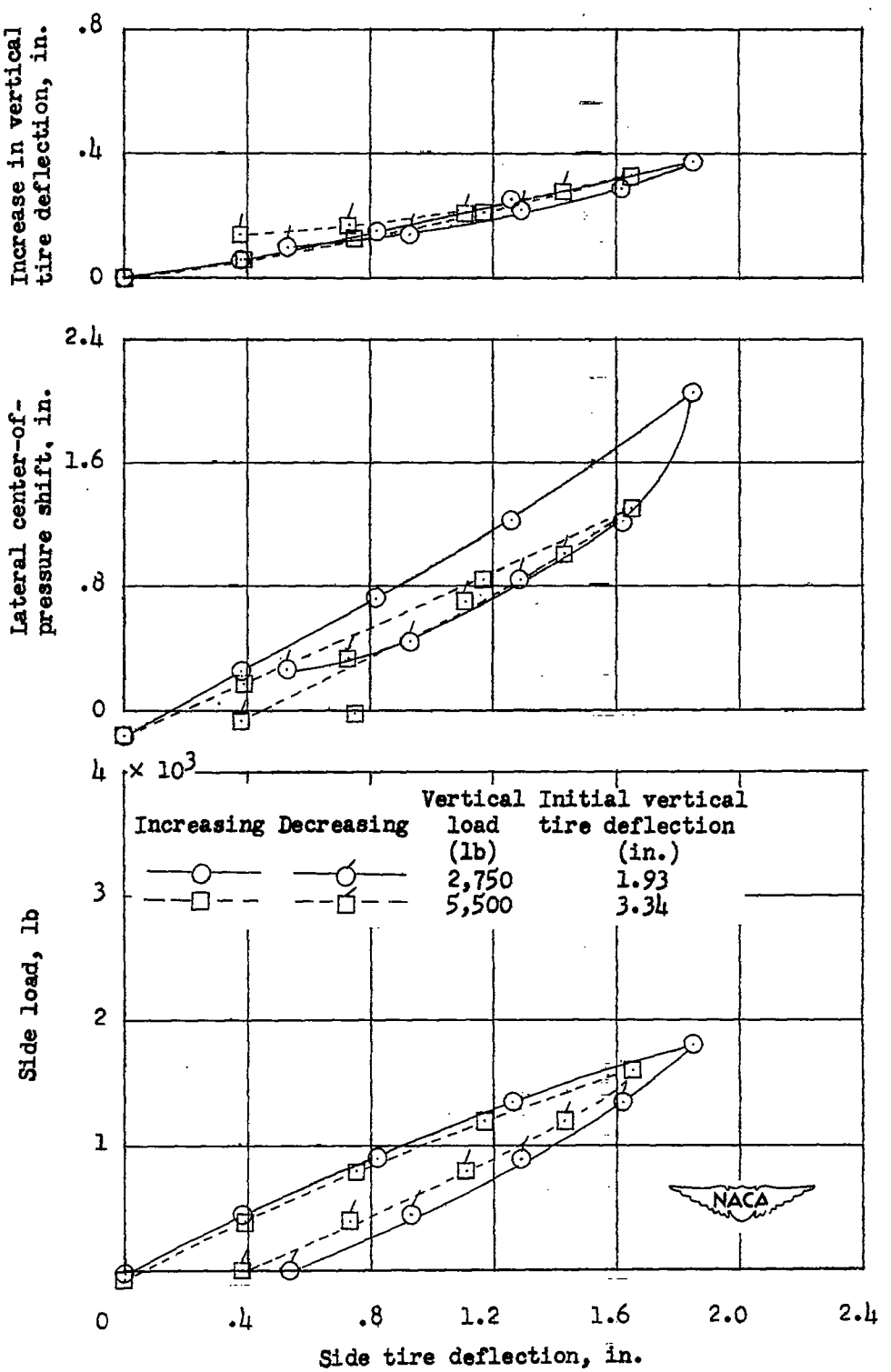

(c) Initial inflation pressure, 32 pounds per square inch.

Figure 21.- Continued.

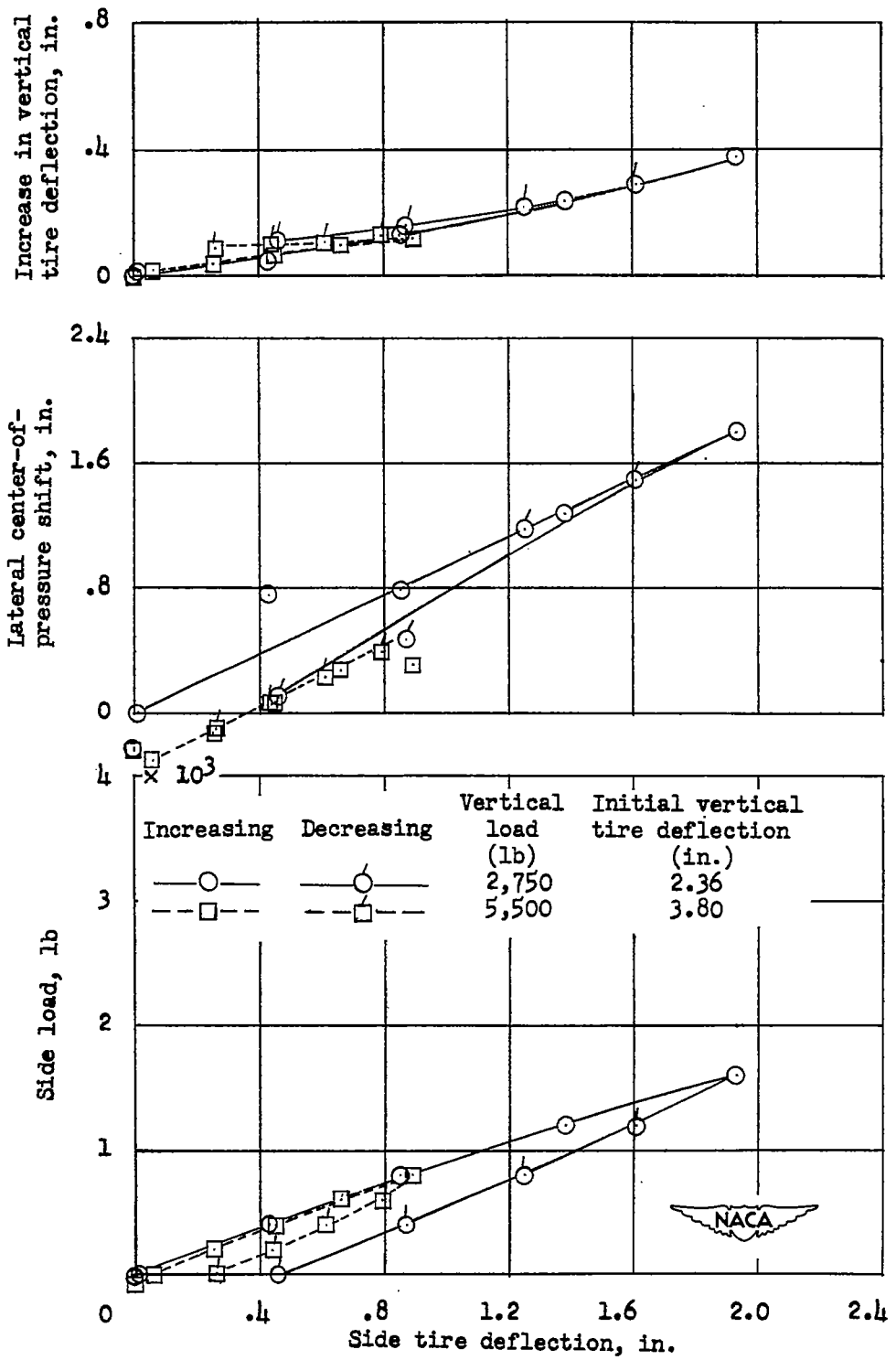

(d) Initial inflation pressure, 24 pounds per square inch.

Figure 21.- Concluded.

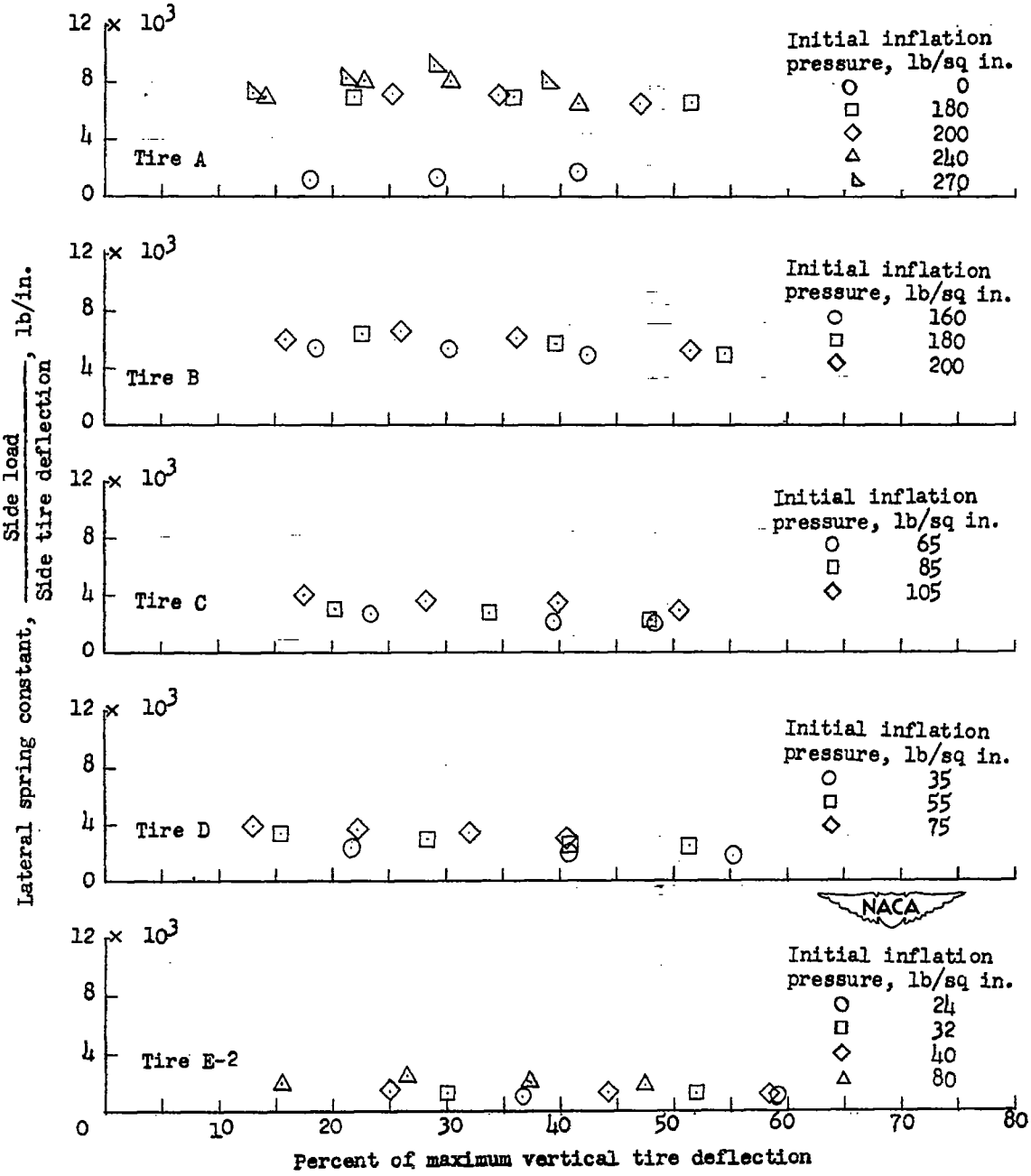

Figure 22.- Variation of lateral spring constants with vertical tire deflection and initial inflation pressure. Spring constant measured at side tire deflection of 0.5 inch.

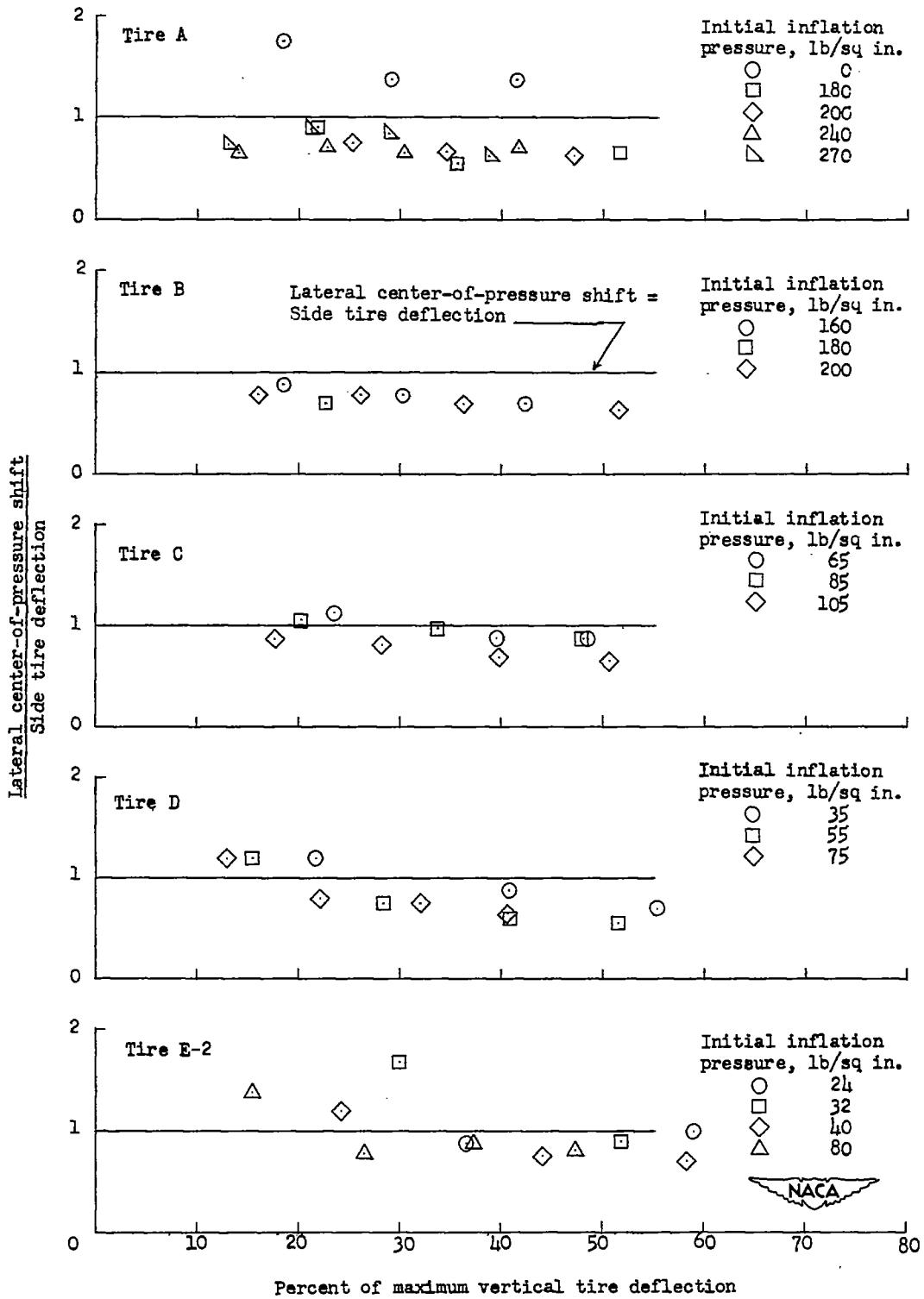

Figure 23.- Effects of vertical tire deflection and initial inflation pressure on ratio of lateral center-of-pressure shift to side tire deflection. Ratio measured at side tire deflection of 0.5 inch.

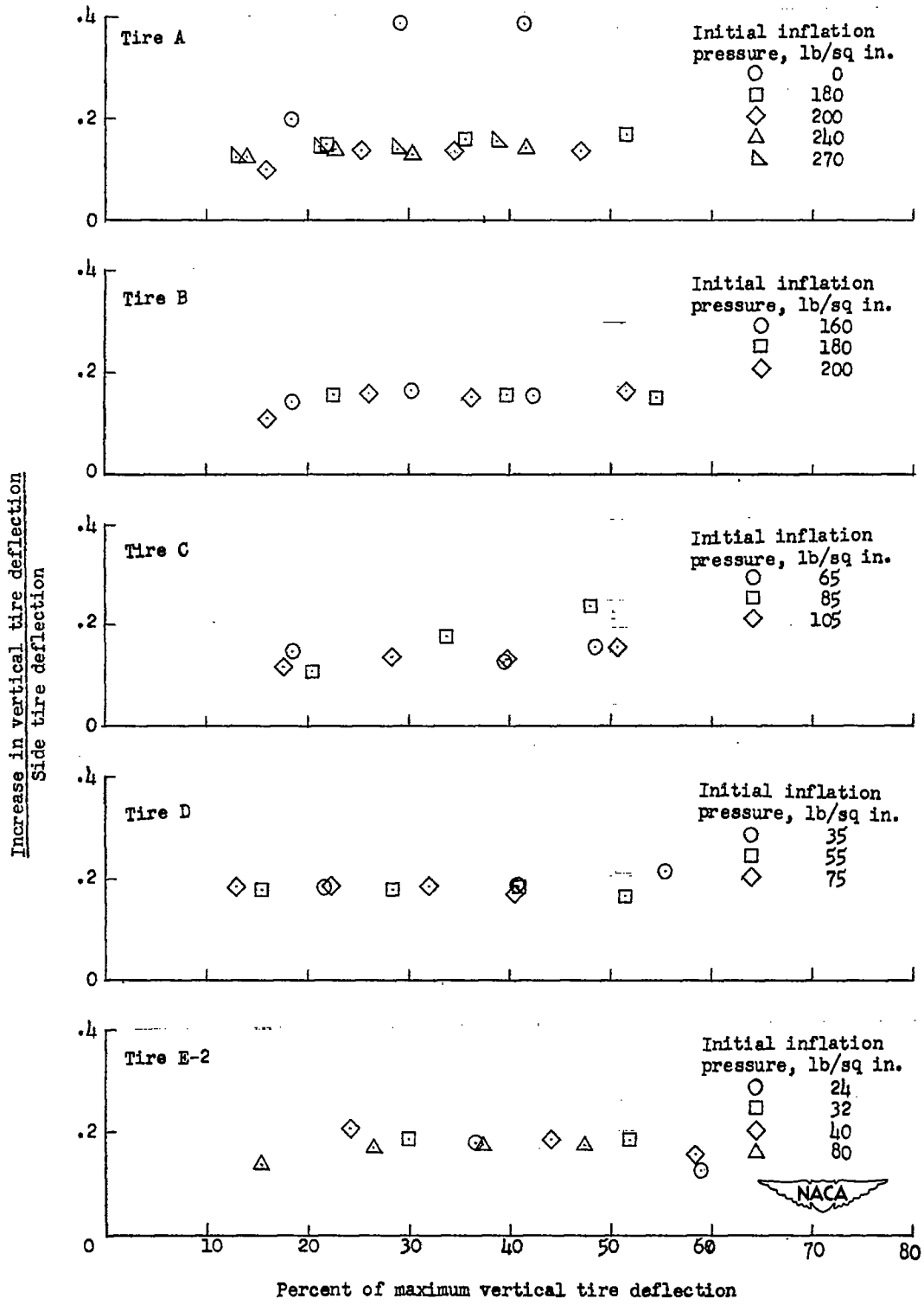

Figure 24.- Effects of vertical tire deflection and initial inflation pressure on ratio of increase in vertical tire deflection resulting from side load to side tire deflection. Ratio measured at side tire deflection of 0.5 inch.

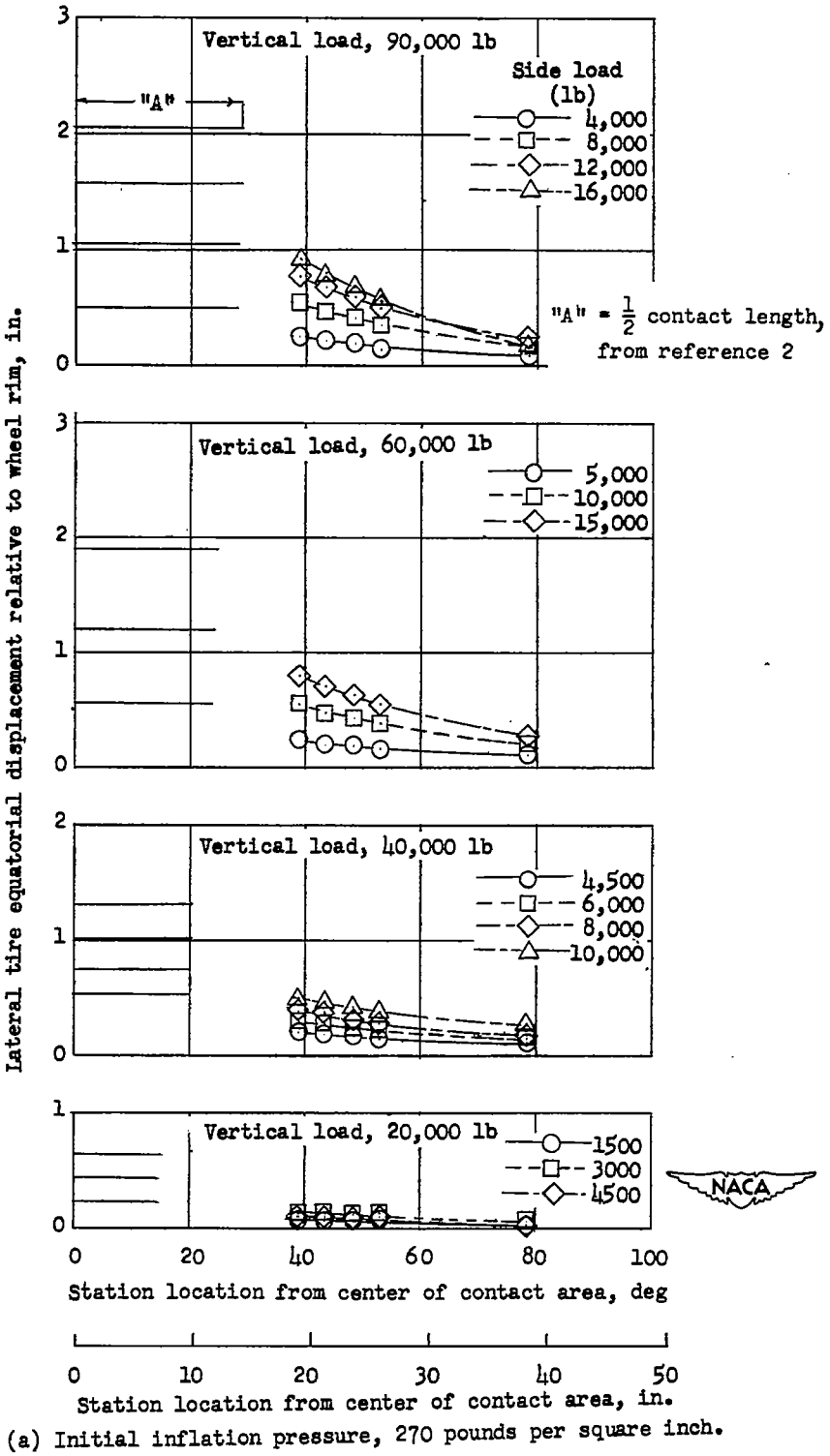

(a) Initial inflation pressure, 270 pounds per square inch.

Figure 25.- Distortion of tire equatorial line under various side loads for different vertical loads and initial inflation pressures for the 56-inch, 32-ply-rating tire (tire A).

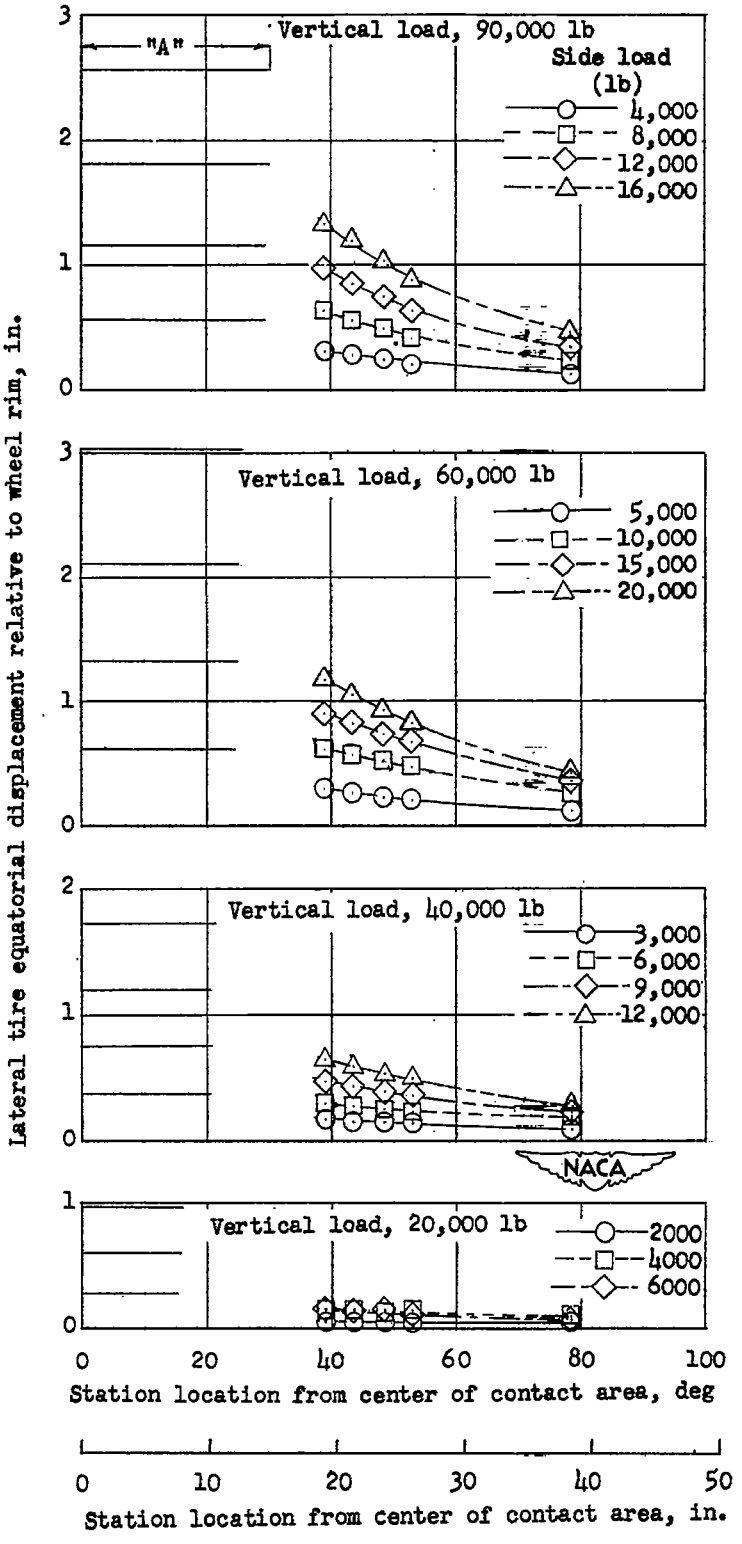

(b) Initial inflation pressure, 240 pounds per square inch.

Figure 25.- Continued.

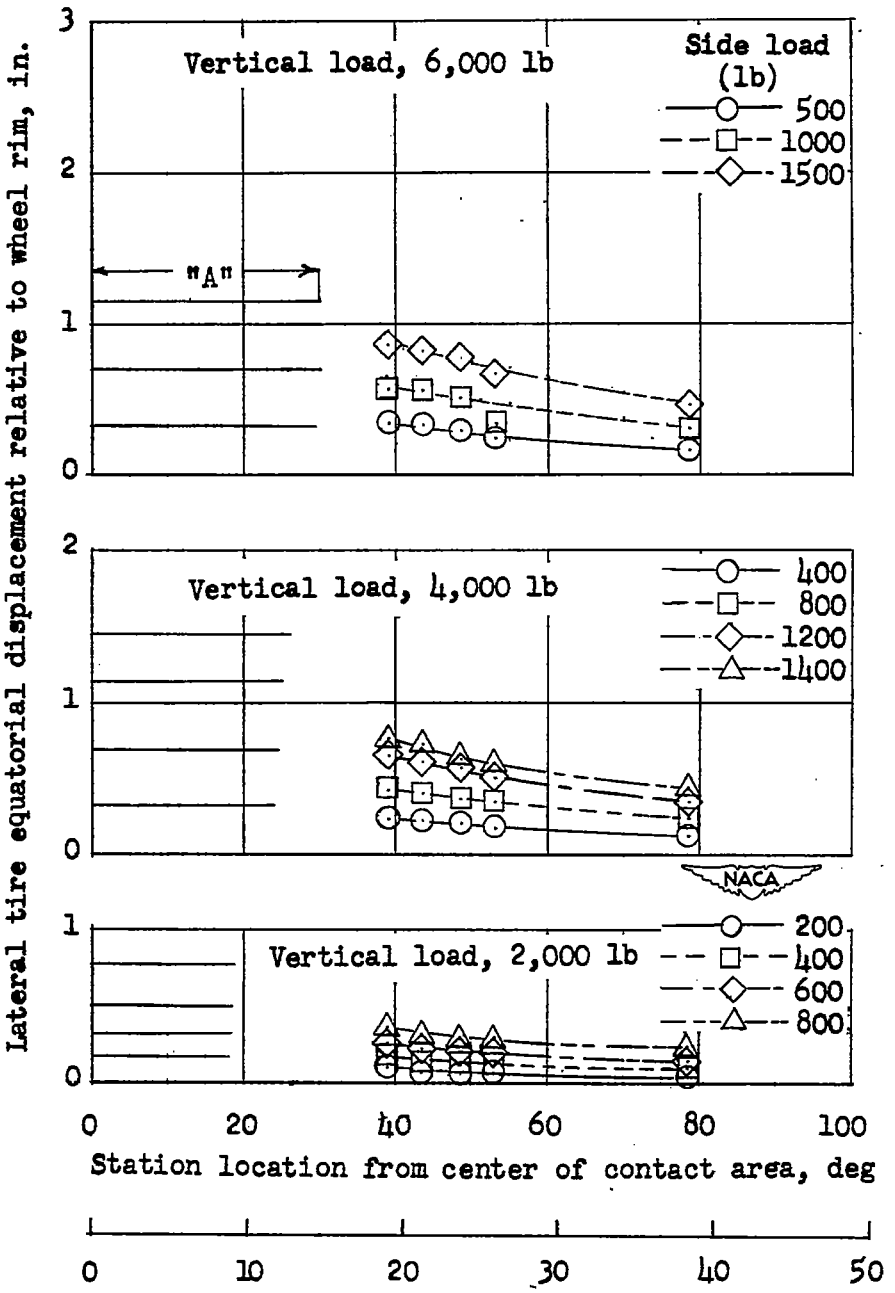

(c) Initial inflation pressure, 0 pounds per square inch.

Figure 25.- Concluded.

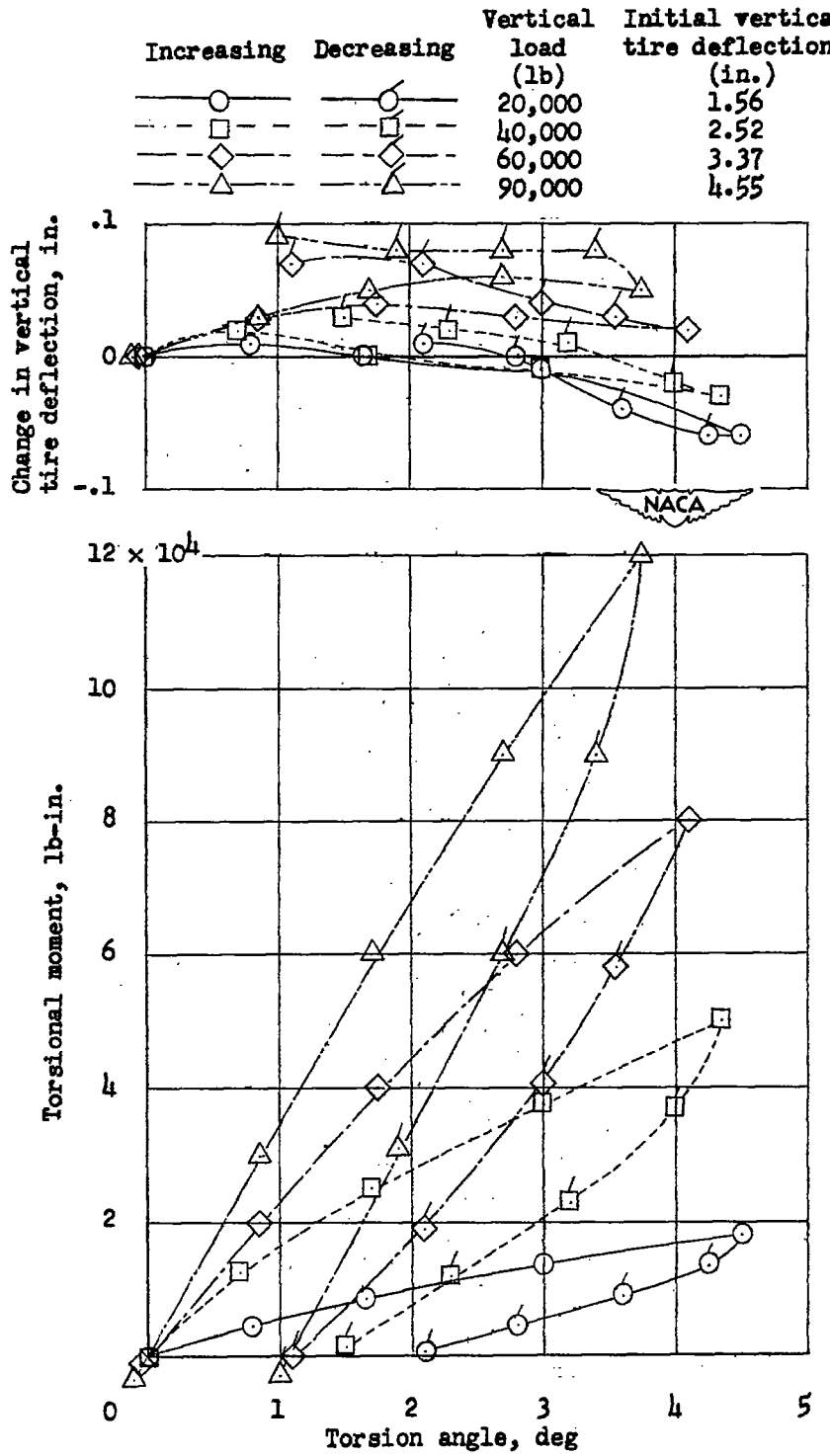

(a) Initial inflation pressure, 270 pounds per square inch.

Figure 26.- Variation with torsion angle of torsional moment and the change in vertical tire deflection for different vertical loads and inflation pressures for the 56-inch, 32-ply-rating tire (tire A).

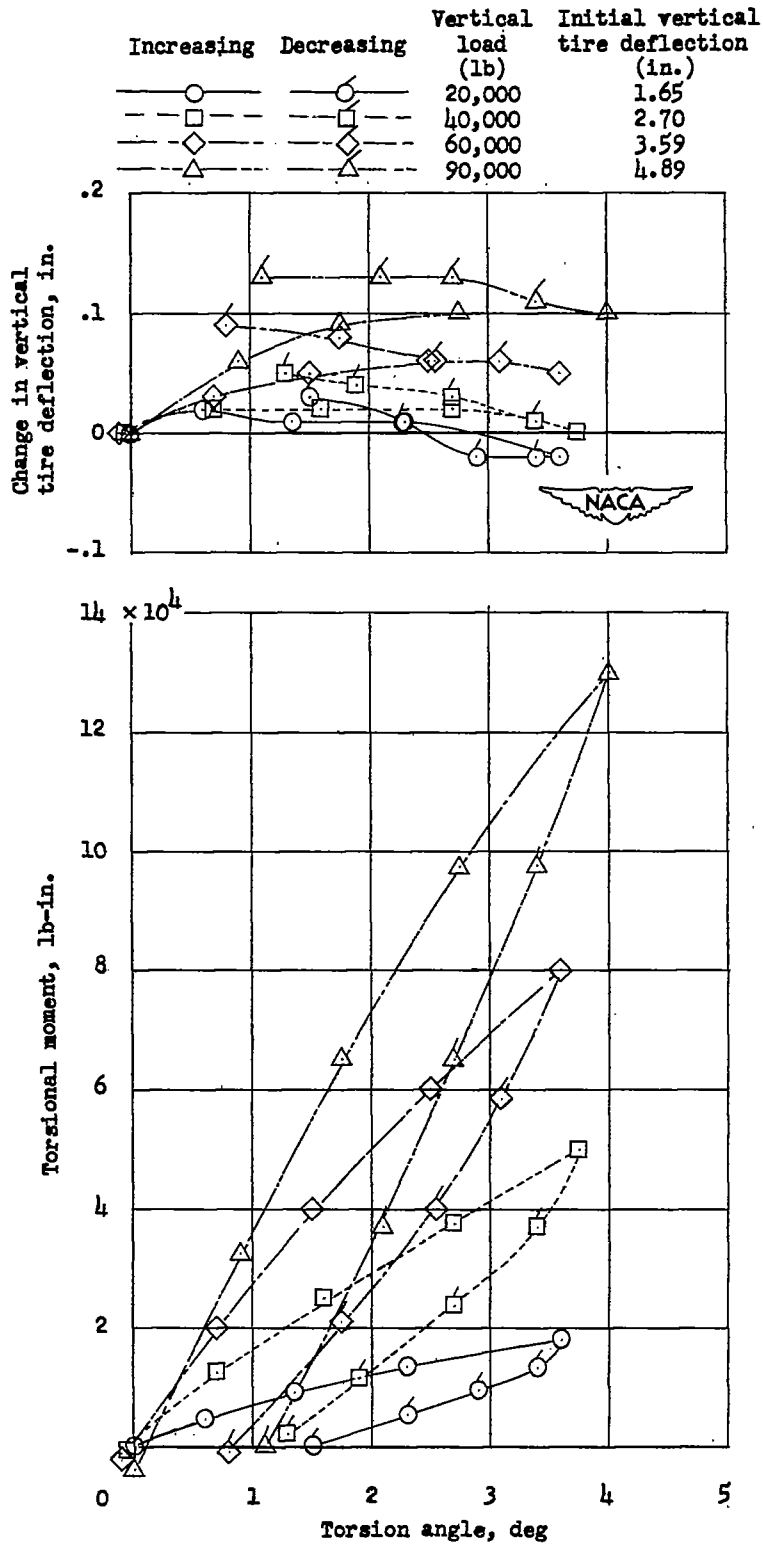

(b) Initial inflation pressure, 240 pounds per square inch.

Figure 26.- Continued.

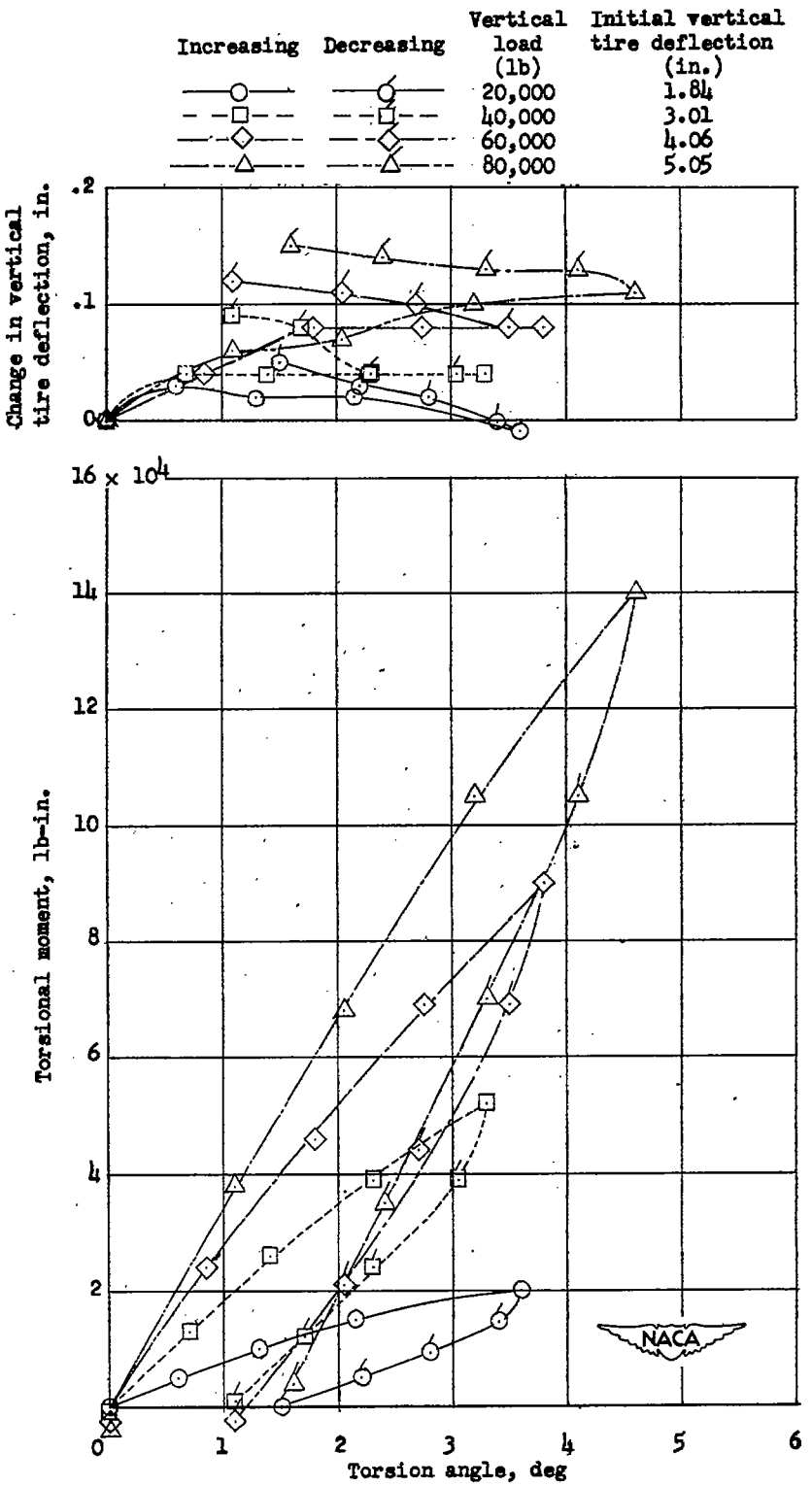

(c) Initial inflation pressure, 200 pounds per square inch.

Figure 26.- Continued.

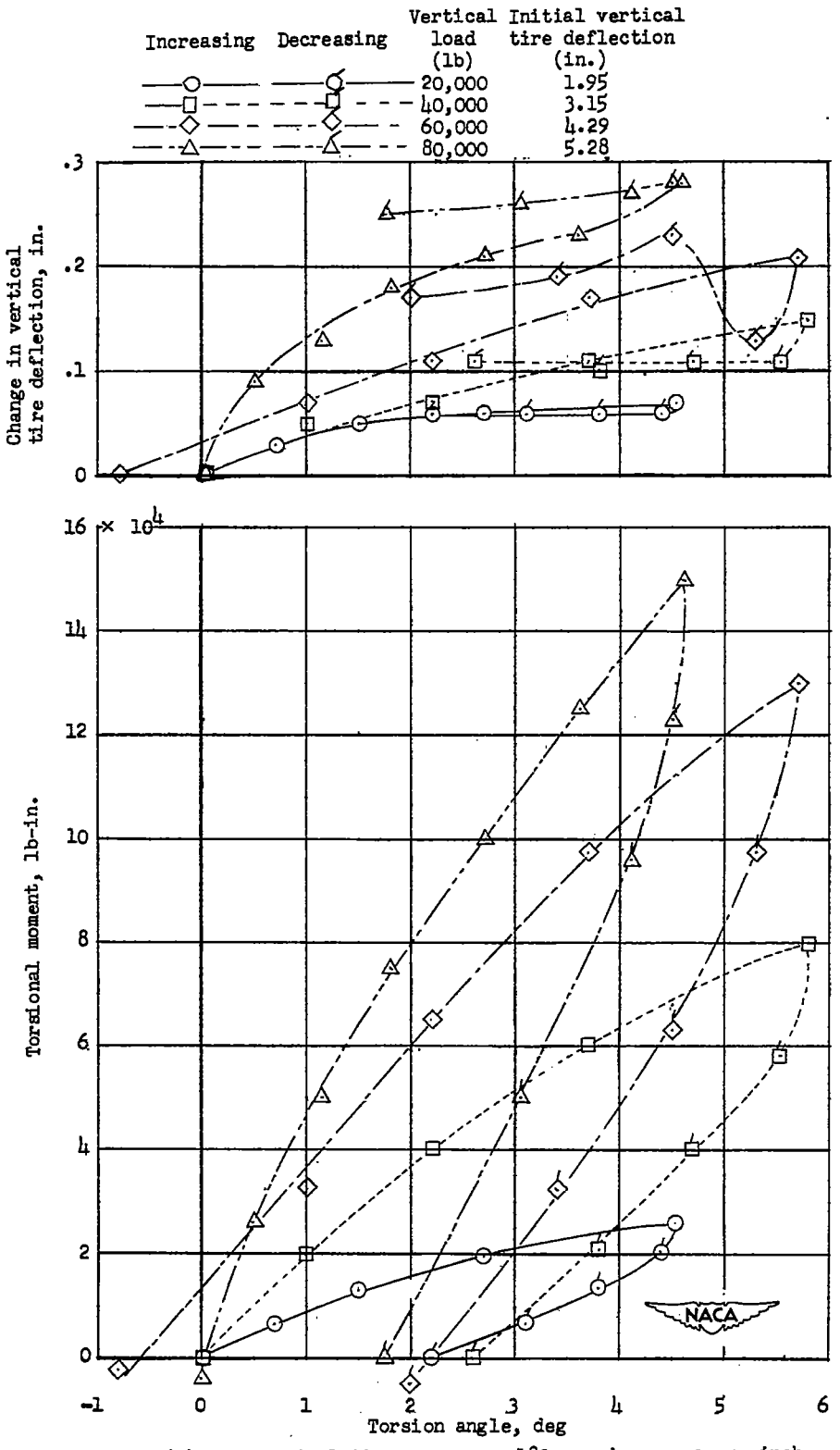

(d) Initial inflation pressure, 180 pounds per square inch.

Figure 26.- Concluded.

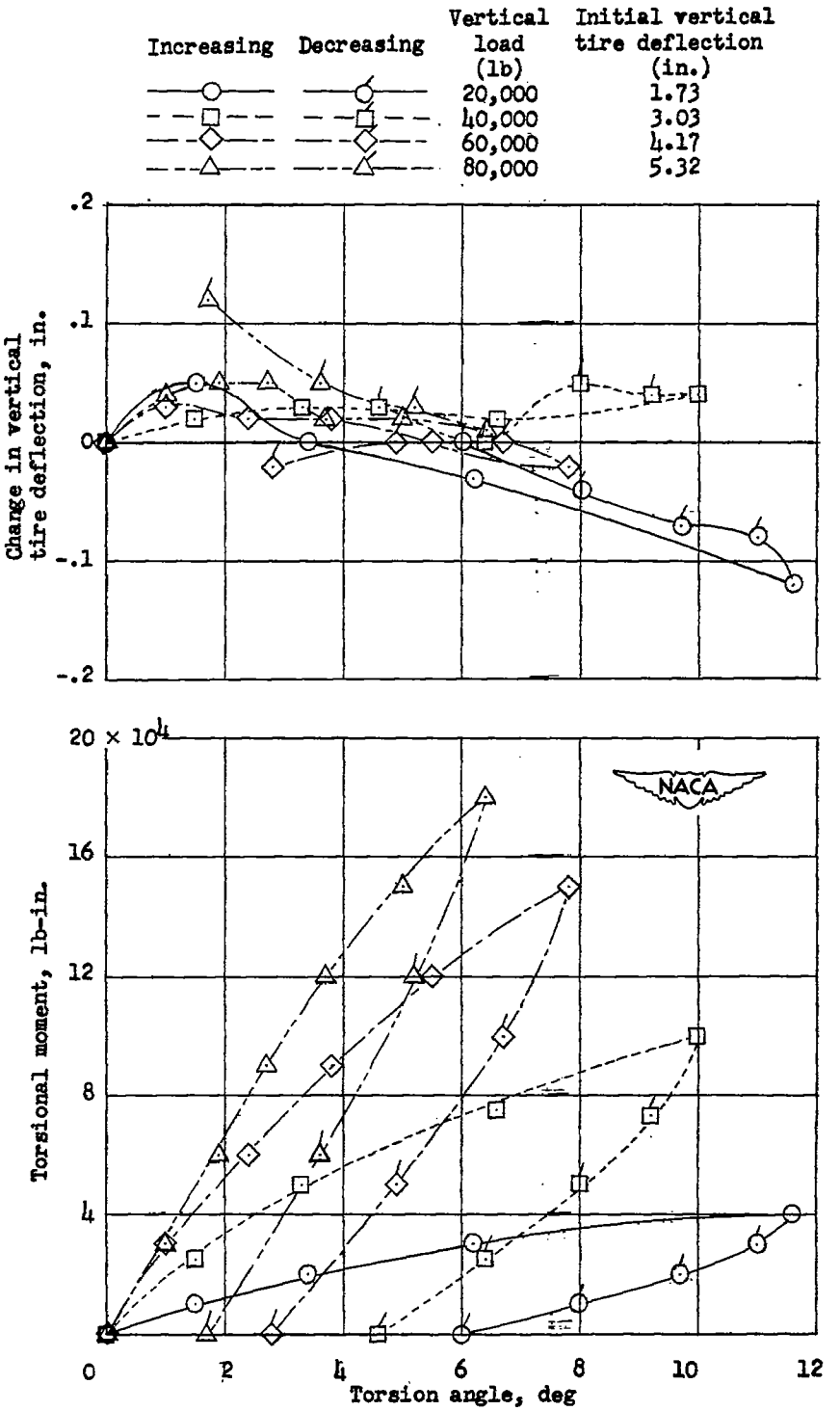

(a) Initial inflation pressure, 200 pounds per square inch.

Figure 27.- Variation with torsion angle of torsional moment and change in vertical tire deflection for different vertical loads and inflation pressures for the 56-inch, 24-ply-rating tire (tire B).

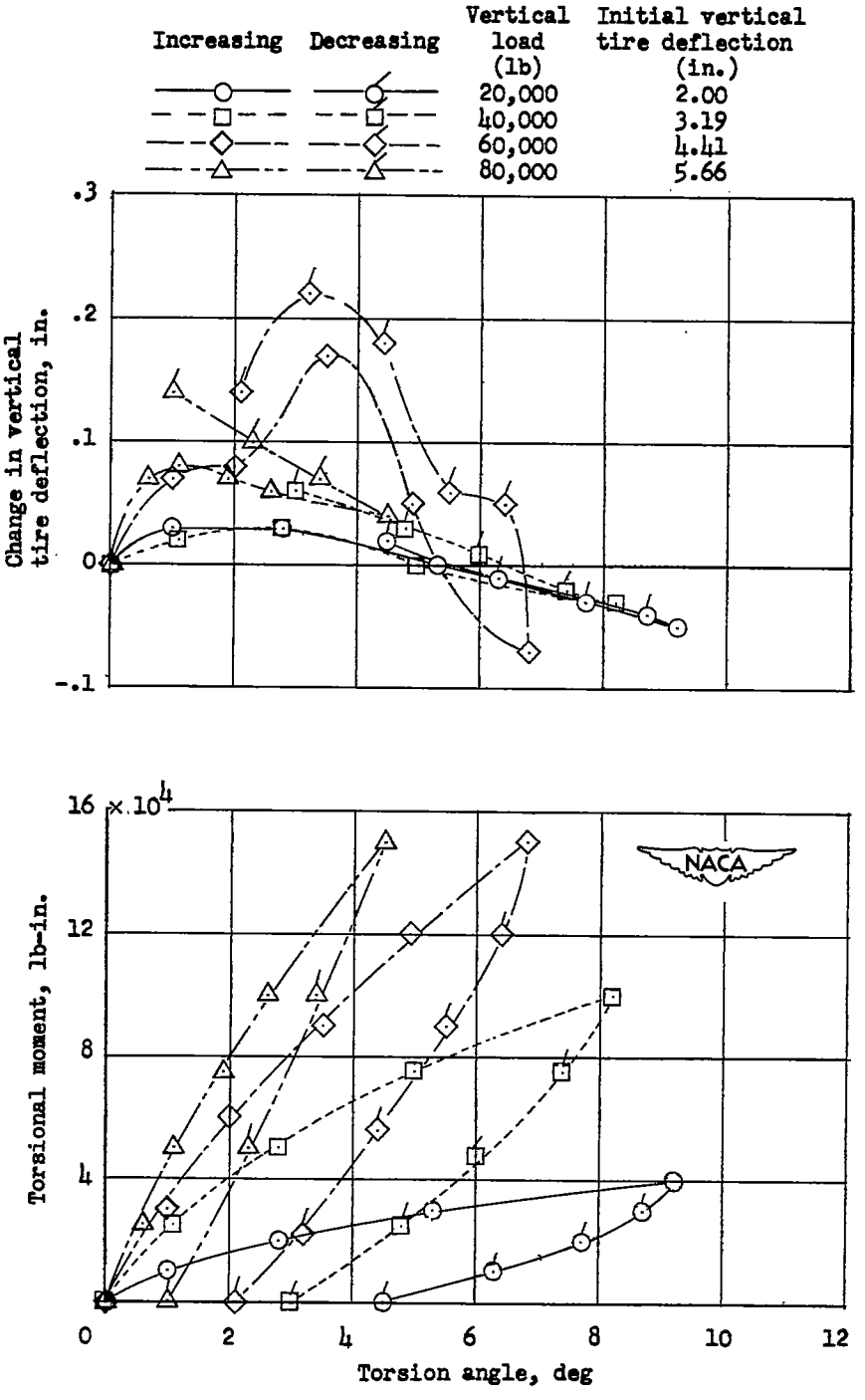

(b) Initial inflation pressure, 180 pounds per square inch.

Figure 27.- Continued.

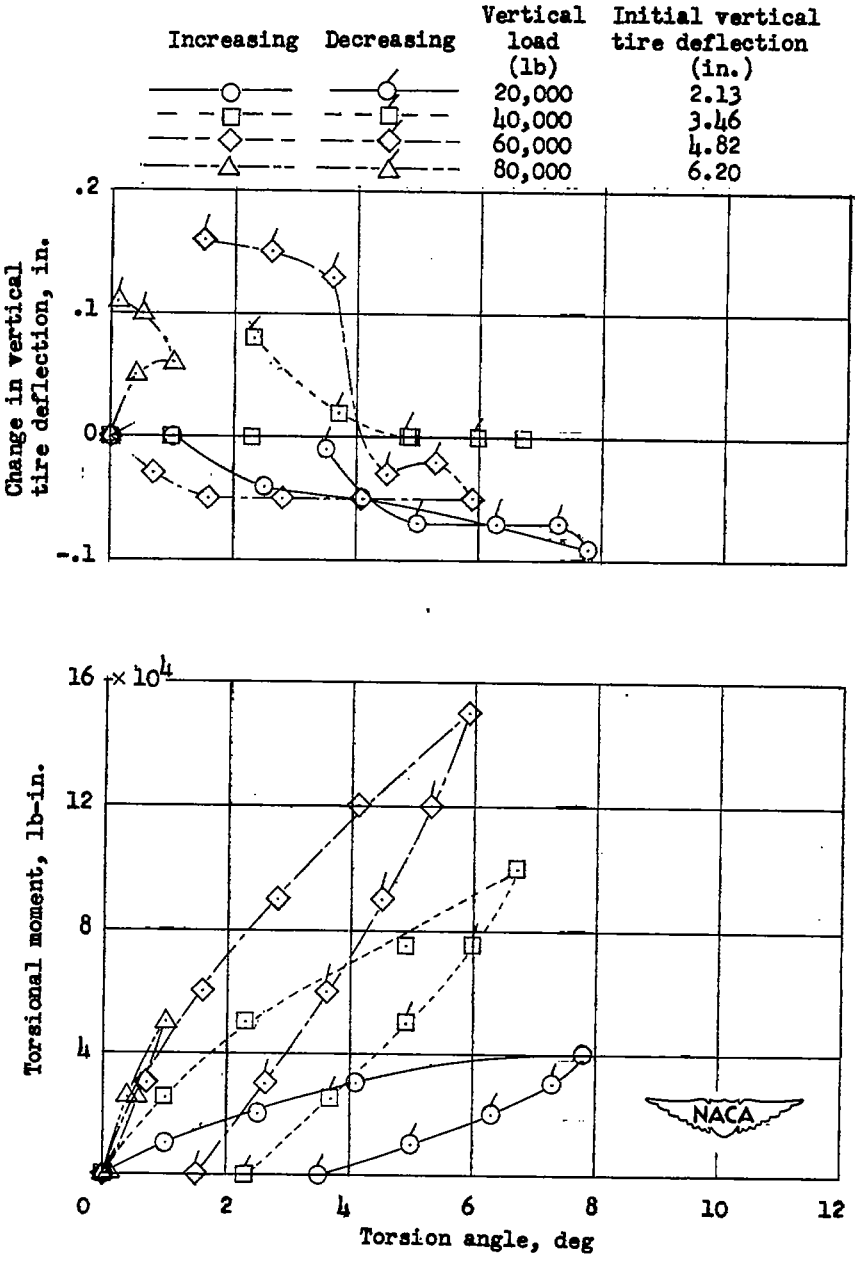

(c) Initial inflation pressure, 160 pounds per square inch.

Figure 27.- Concluded.

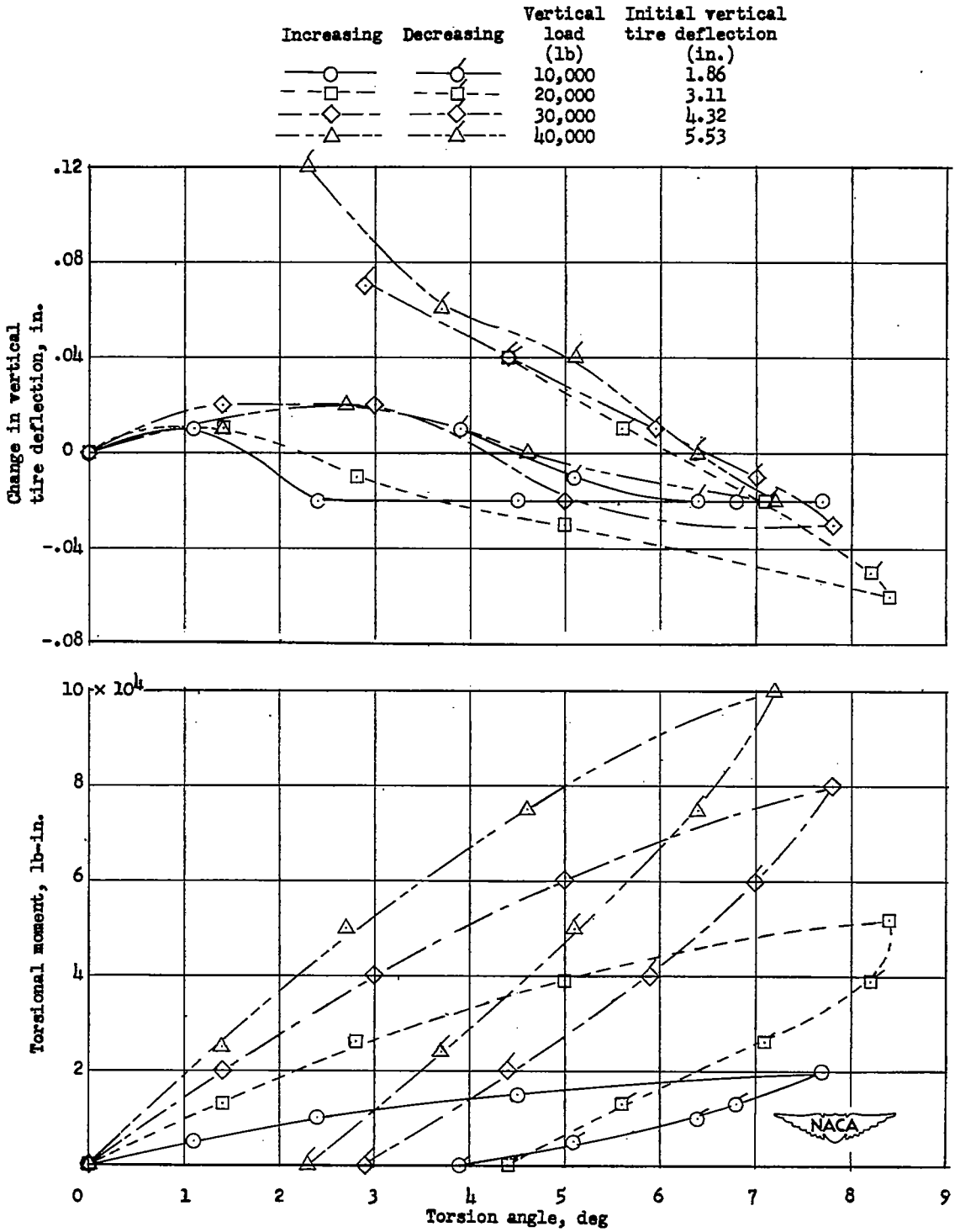

(a) Initial inflation pressure, 105 pounds per square inch.

Figure 28.- Variation with torsion angle of torsional moment and change in vertical tire deflection for different vertical loads and inflation pressures for the 45-inch, 14-ply-rating tire (tire C).

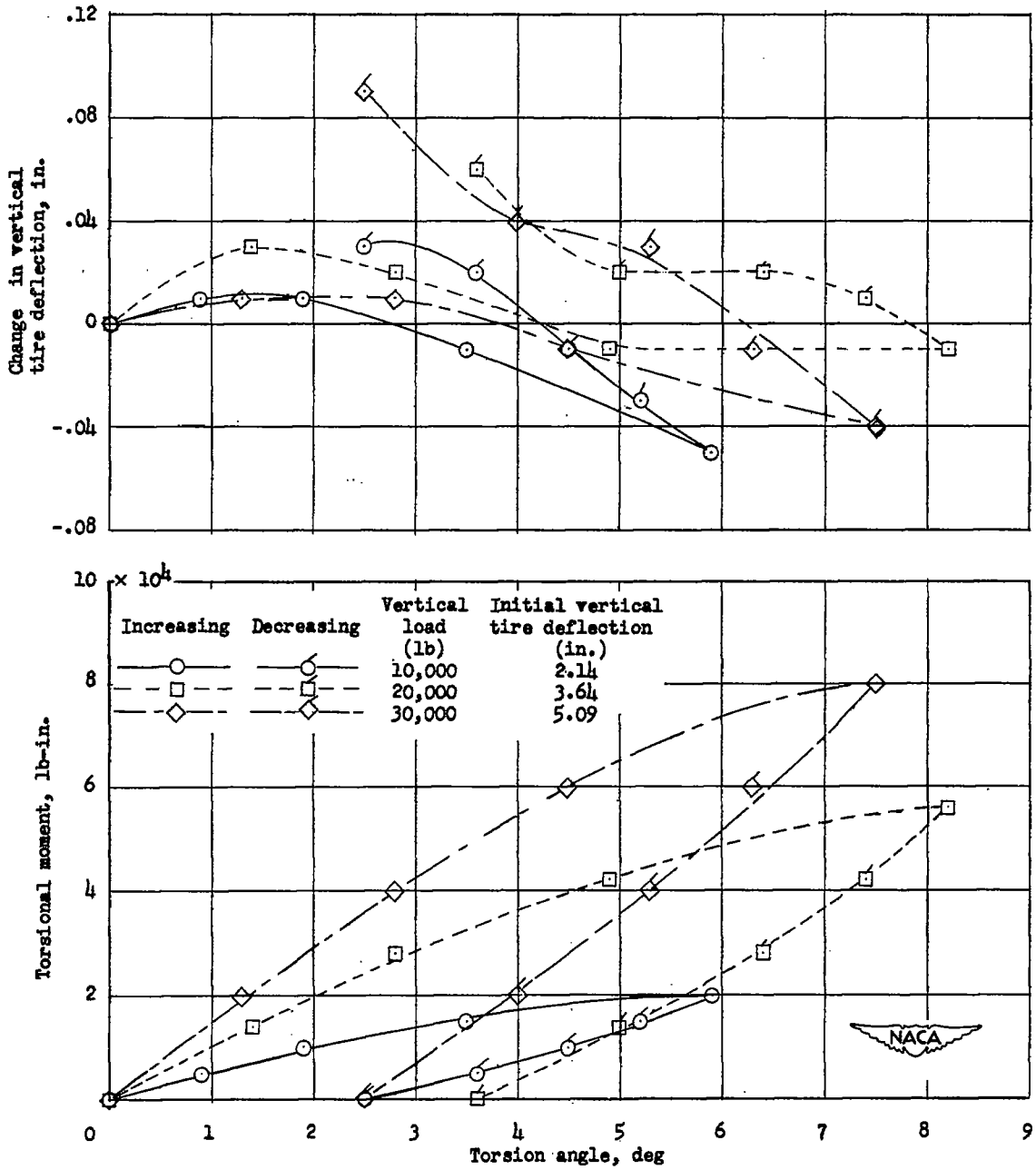

(b) Initial inflation pressure, 85 pounds per square inch.

Figure 28.- Continued.

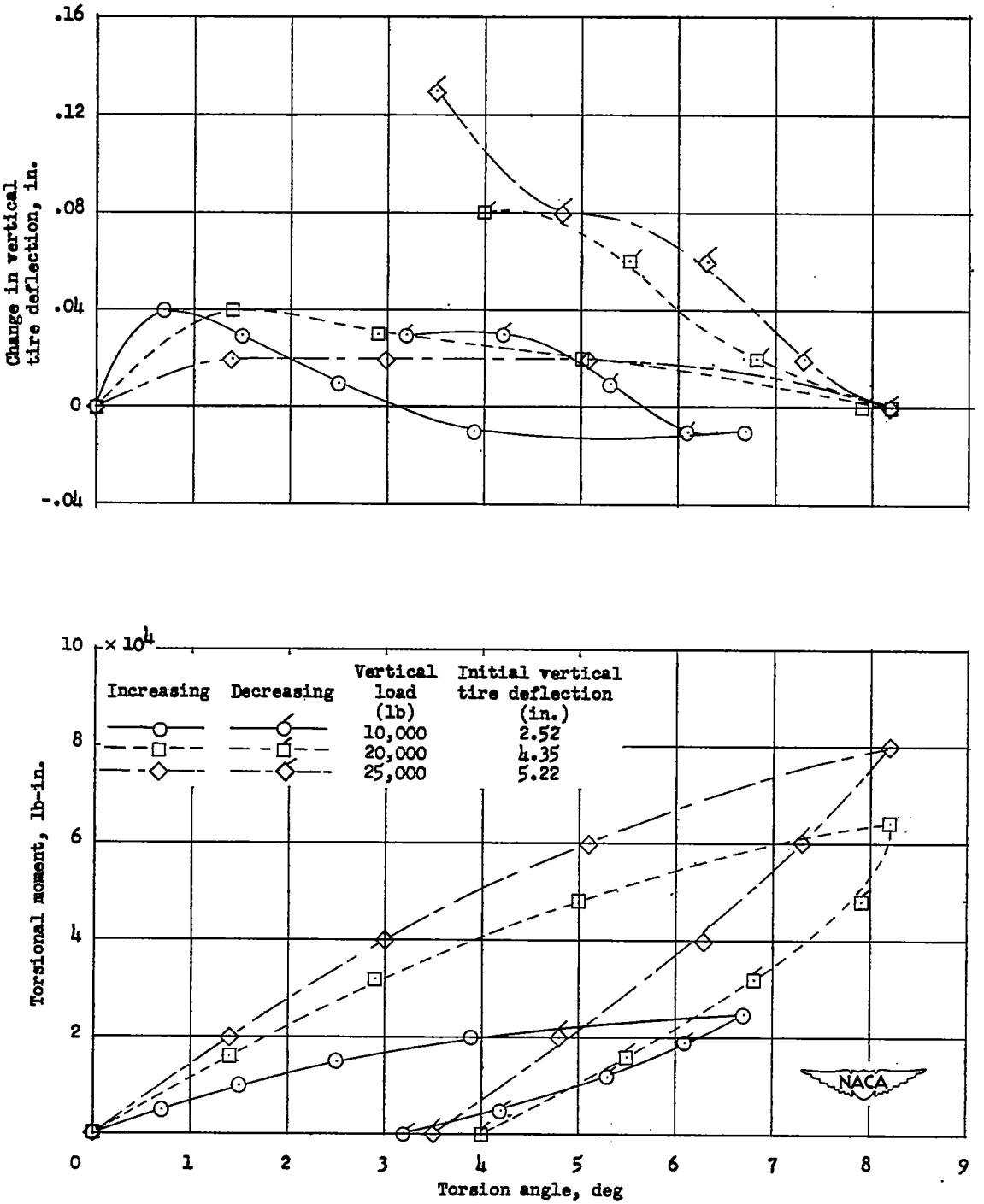

(c) Initial inflation pressure, 65 pounds per square inch.

Figure 28.- Concluded.

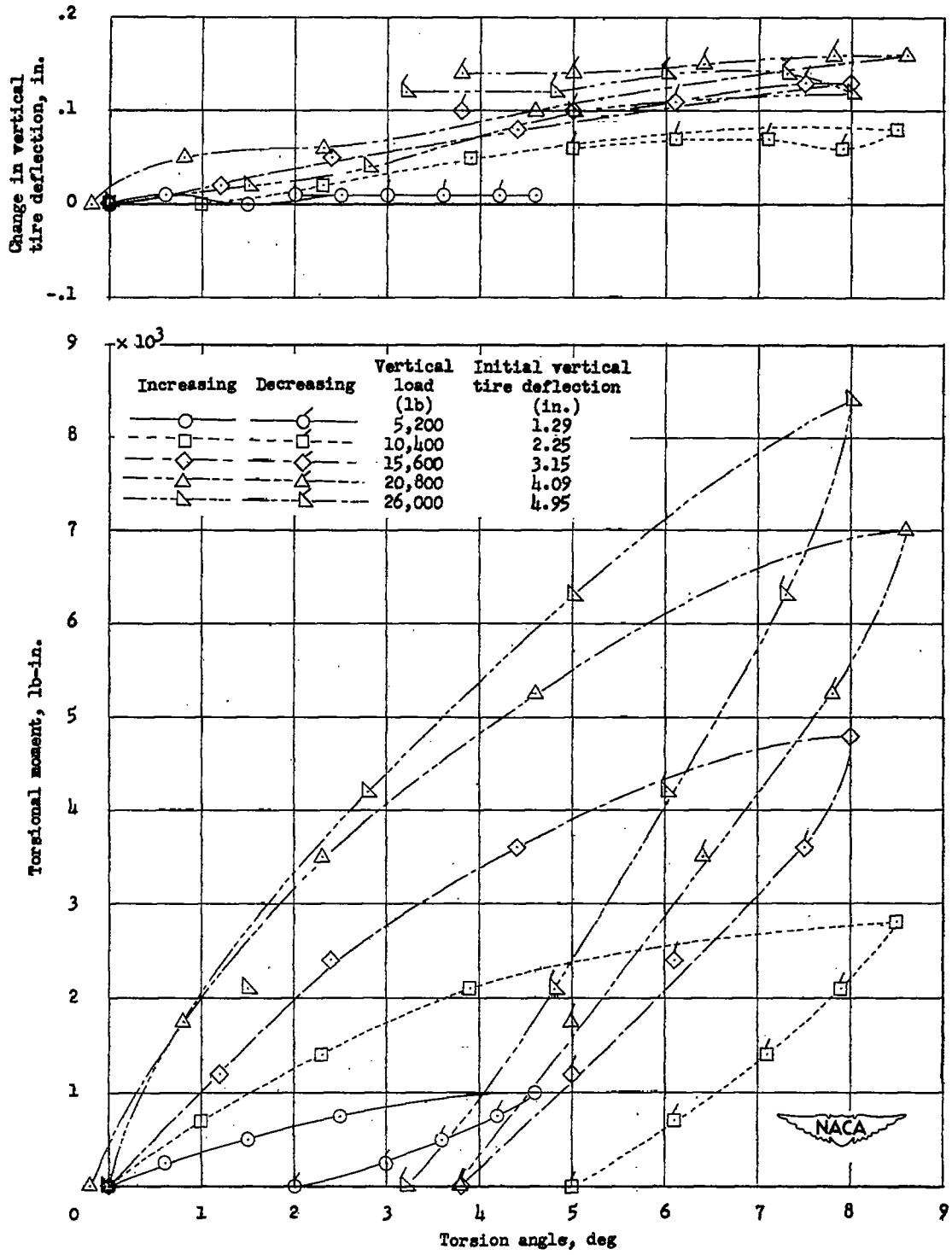

(a) Initial inflation pressure, 75 pounds per square inch.

Figure 29.- Variation with torsion angle of torsional moment and change in vertical tire deflection for different vertical loads and inflation pressures for the 44-inch, 10-ply-rating tire (tire D).

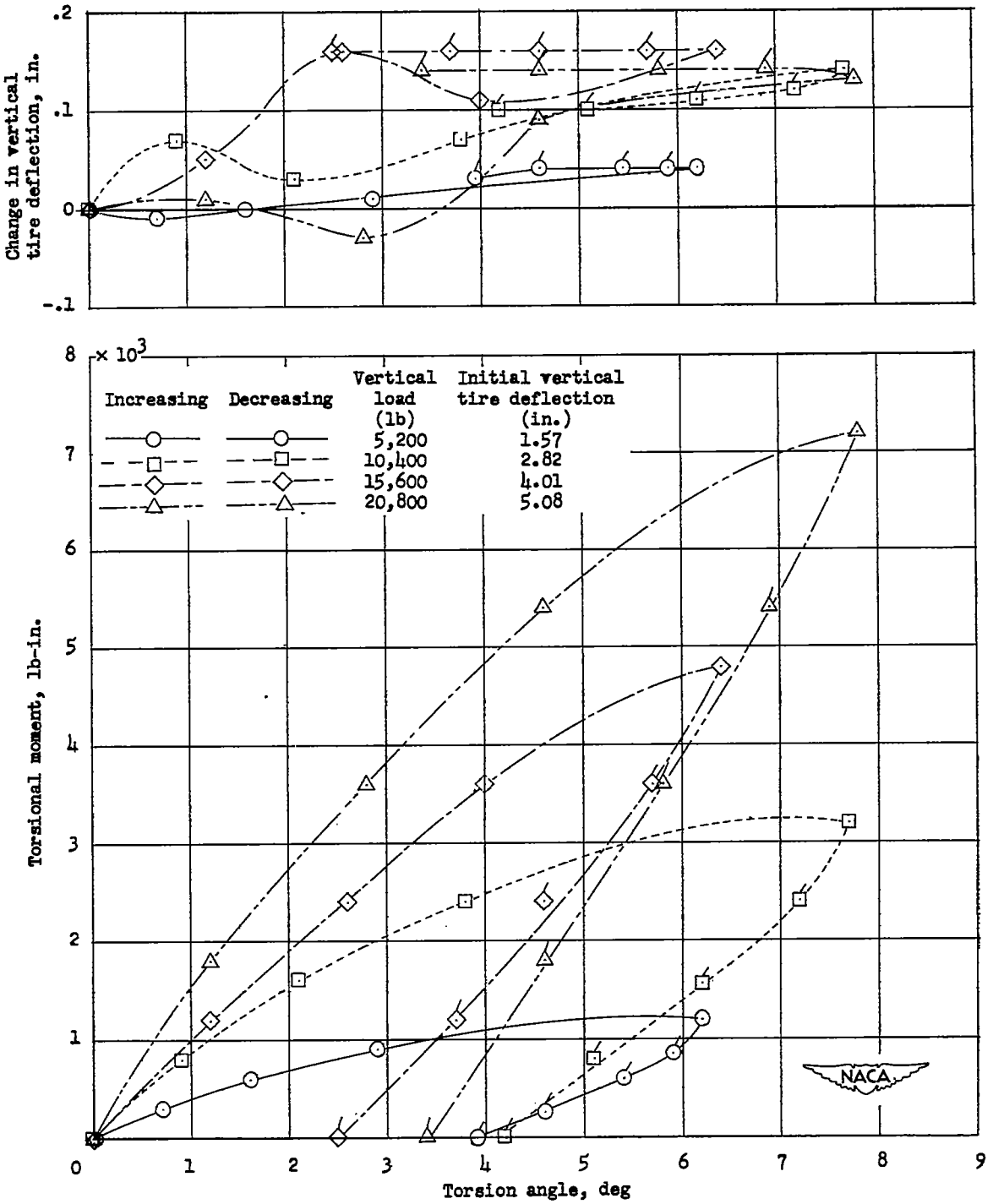

(b) Initial inflation pressure, 55 pounds per square inch.

Figure 29.- Continued.

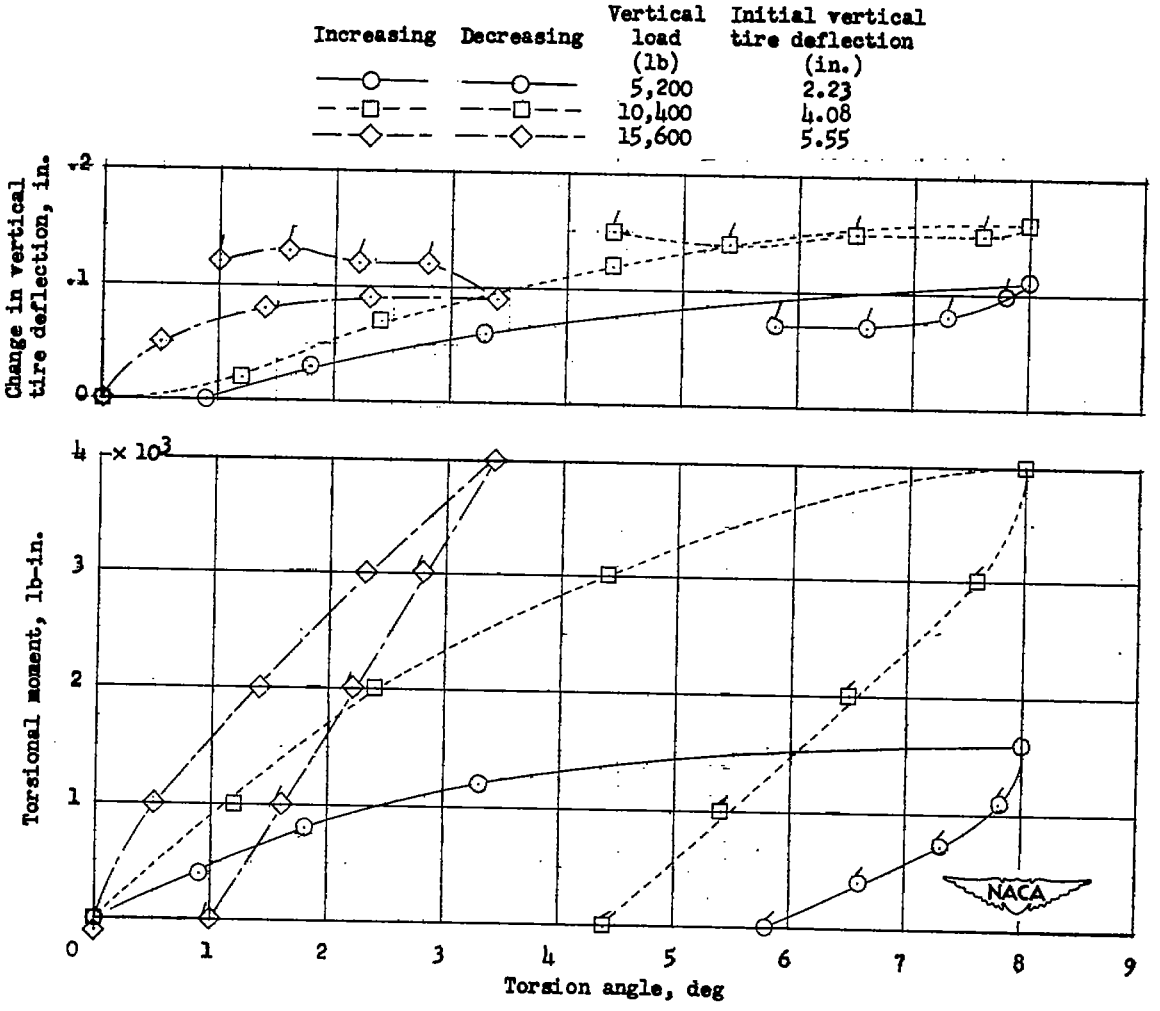

(c) Initial inflation pressure, 35 pounds per square inch.

Figure 29.- Concluded.

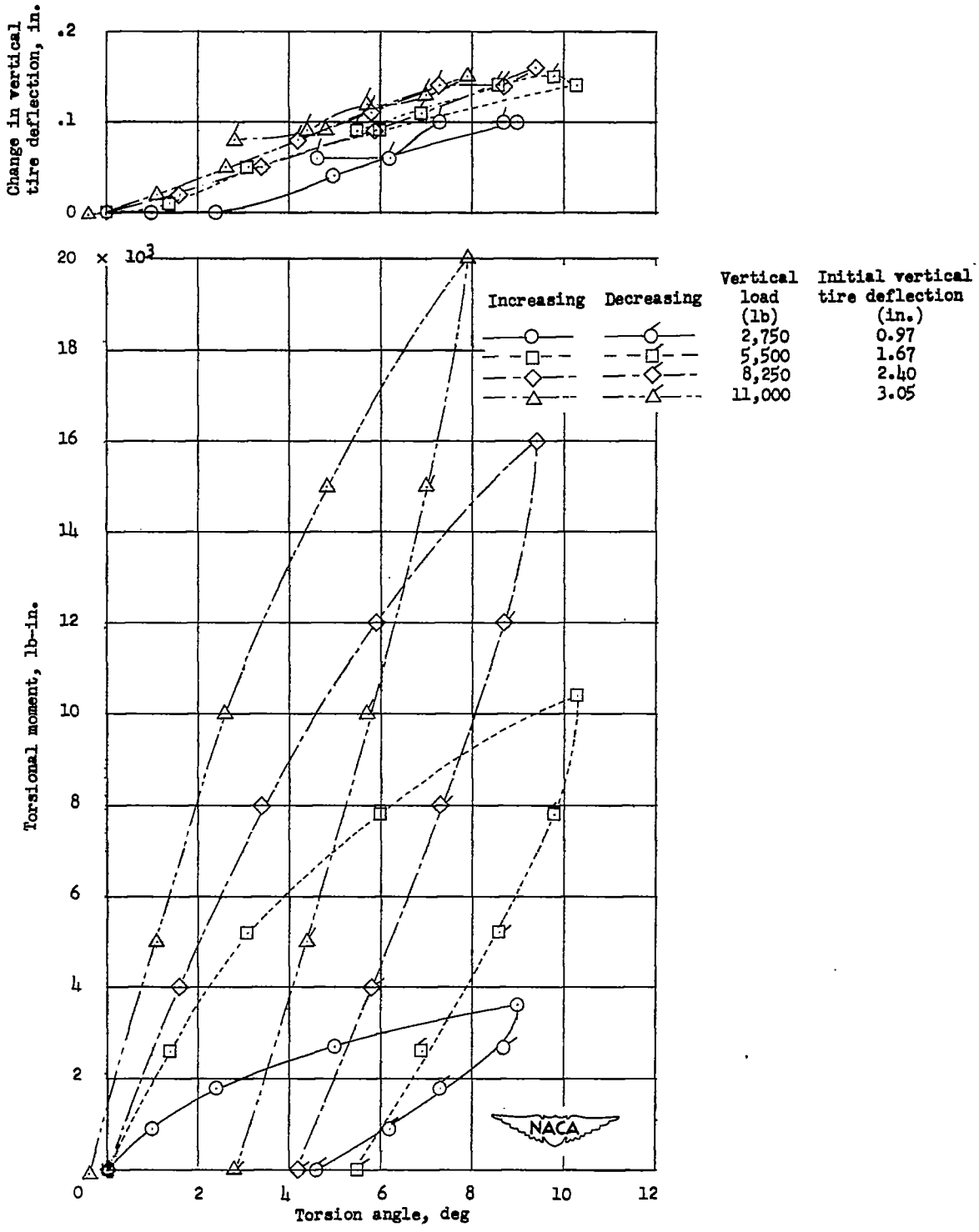

(a) Initial inflation pressure, 80 pounds per square inch.

Figure 30.- Variation with torsion angle of torsional moment and change in vertical tire deflection for different vertical loads and inflation pressures for the 27-inch, 10-ply-rating tire (tire E-2).

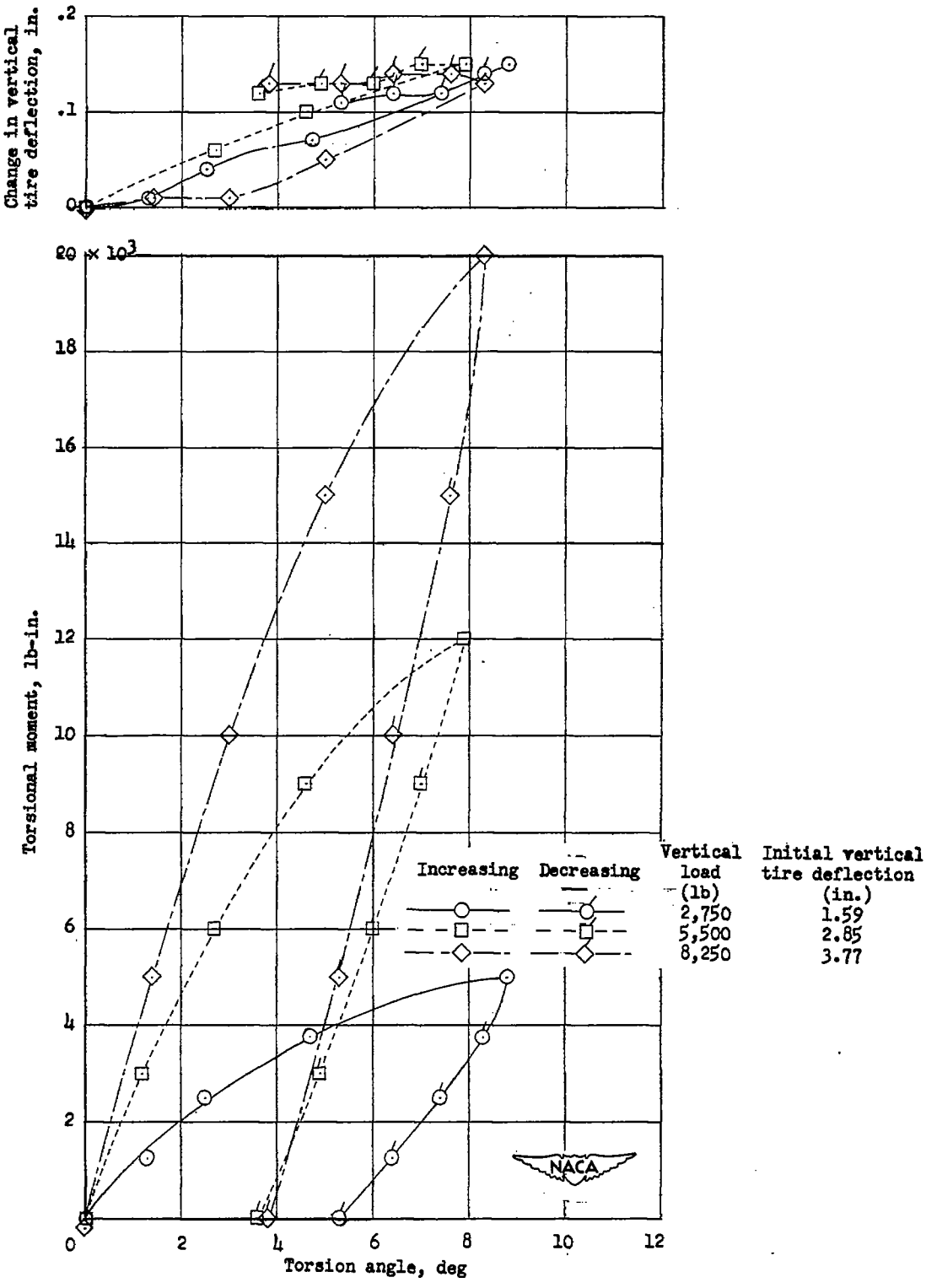

(b) Initial inflation pressure, 40 pounds per square inch.

Figure 30.- Continued.

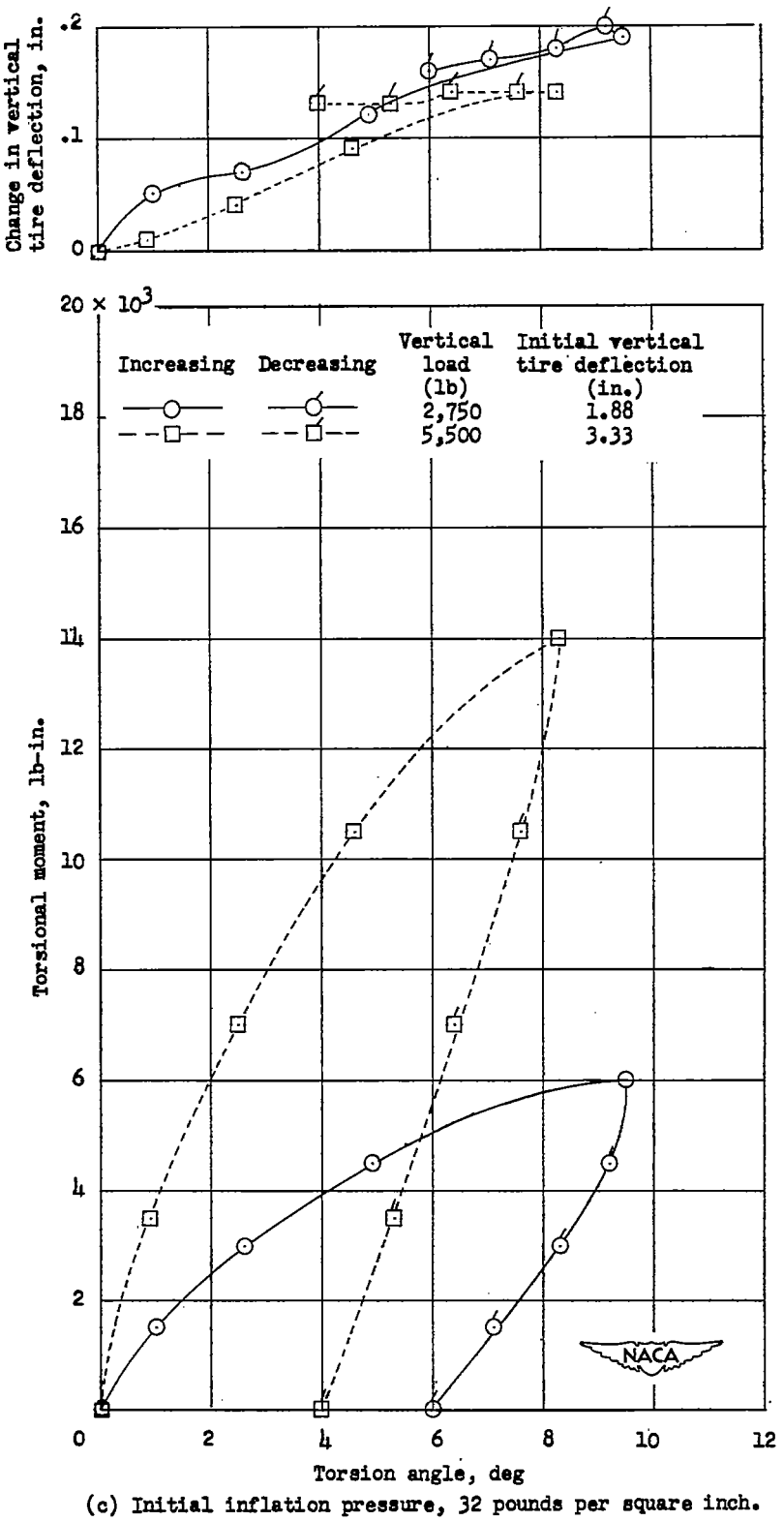

(c) Initial inflation pressure, 32 pounds per square inch.

Figure 30.- Continued.

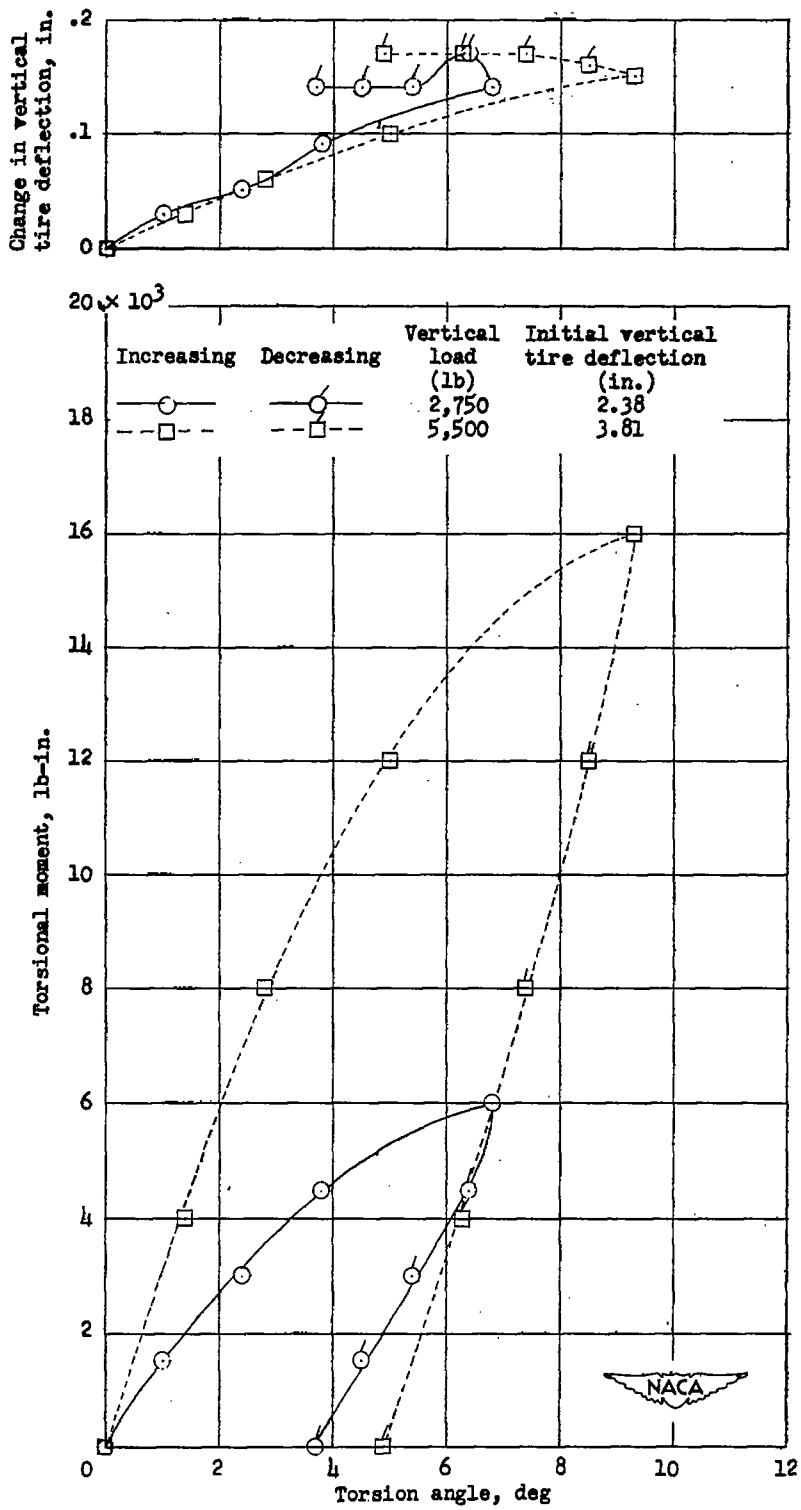

(d) Initial inflation pressure, 24 pounds per square inch.

Figure 30.- Concluded.

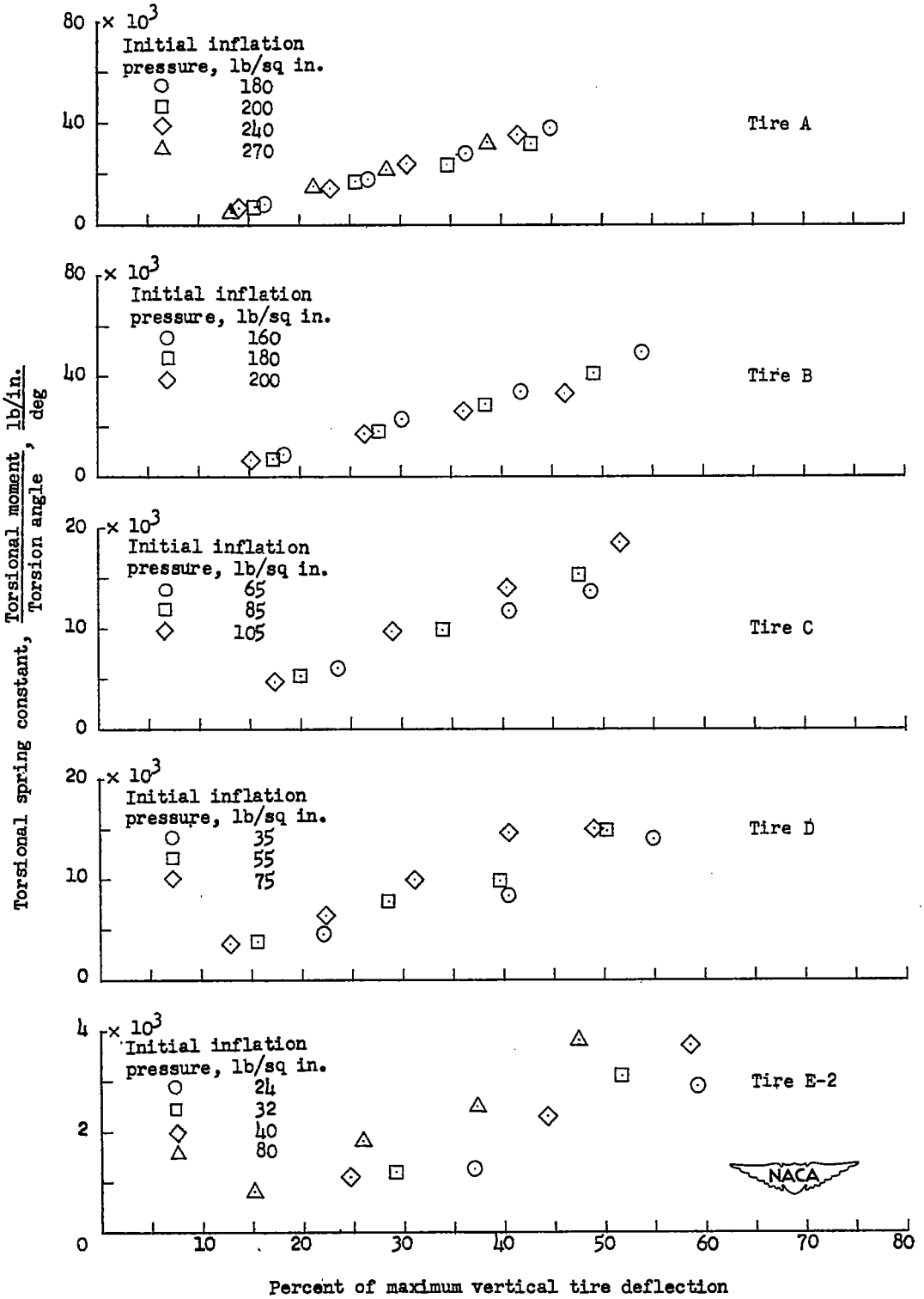

Figure 31.- Variation of torsional spring constant with vertical tire deflection and initial inflation pressure. Spring constant measured at torsion angle of 1°.

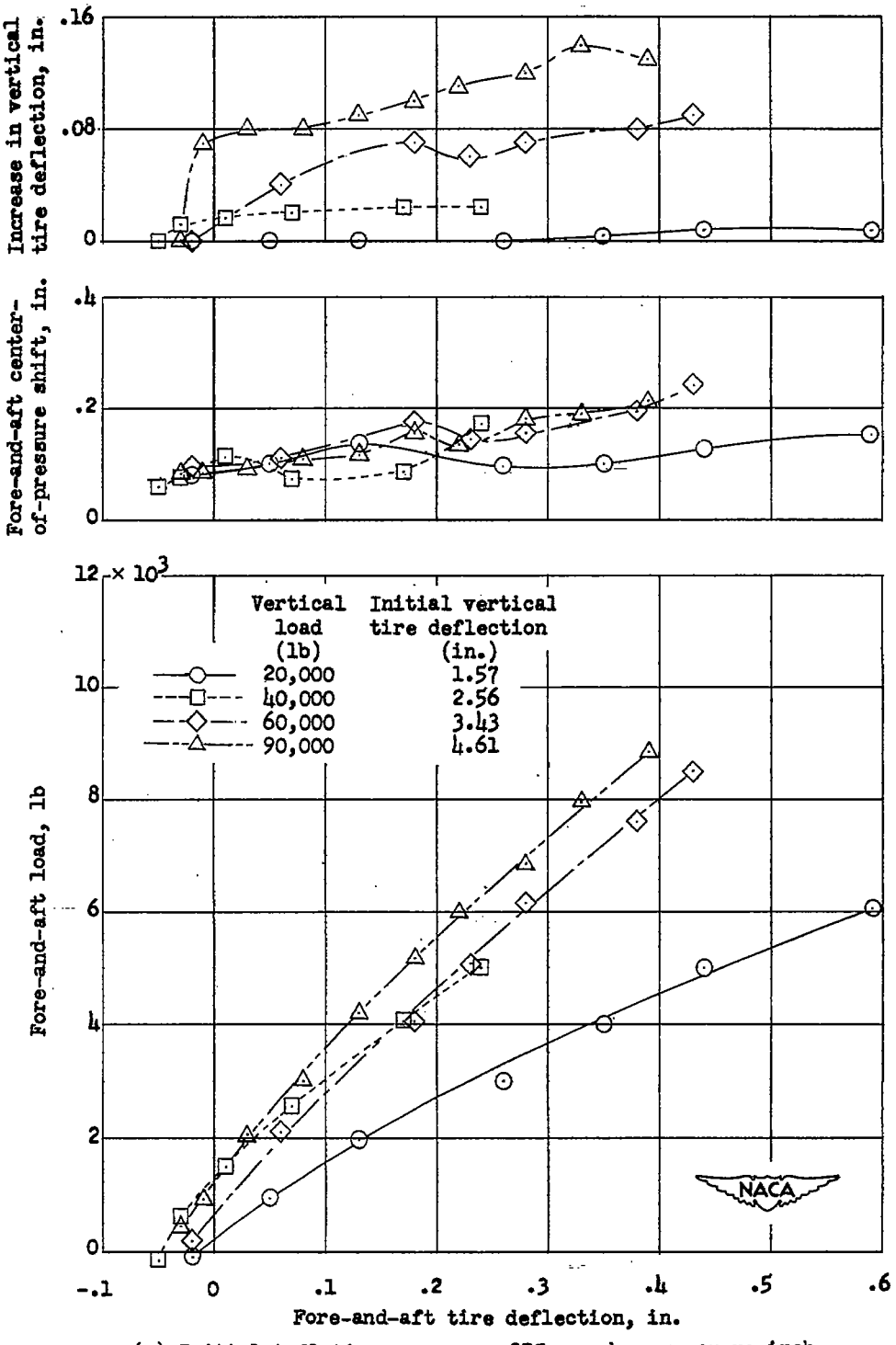

(a) Initial inflation pressure, 270 pounds per square inch.

Figure 32.- Variation with fore-and-aft tire deflection of fore-and-aft load, fore-and-aft center-of-pressure shift, and increase in vertical tire deflection for different vertical loads and inflation pressures for the 56-inch, 32-ply-rating tire (tire A).

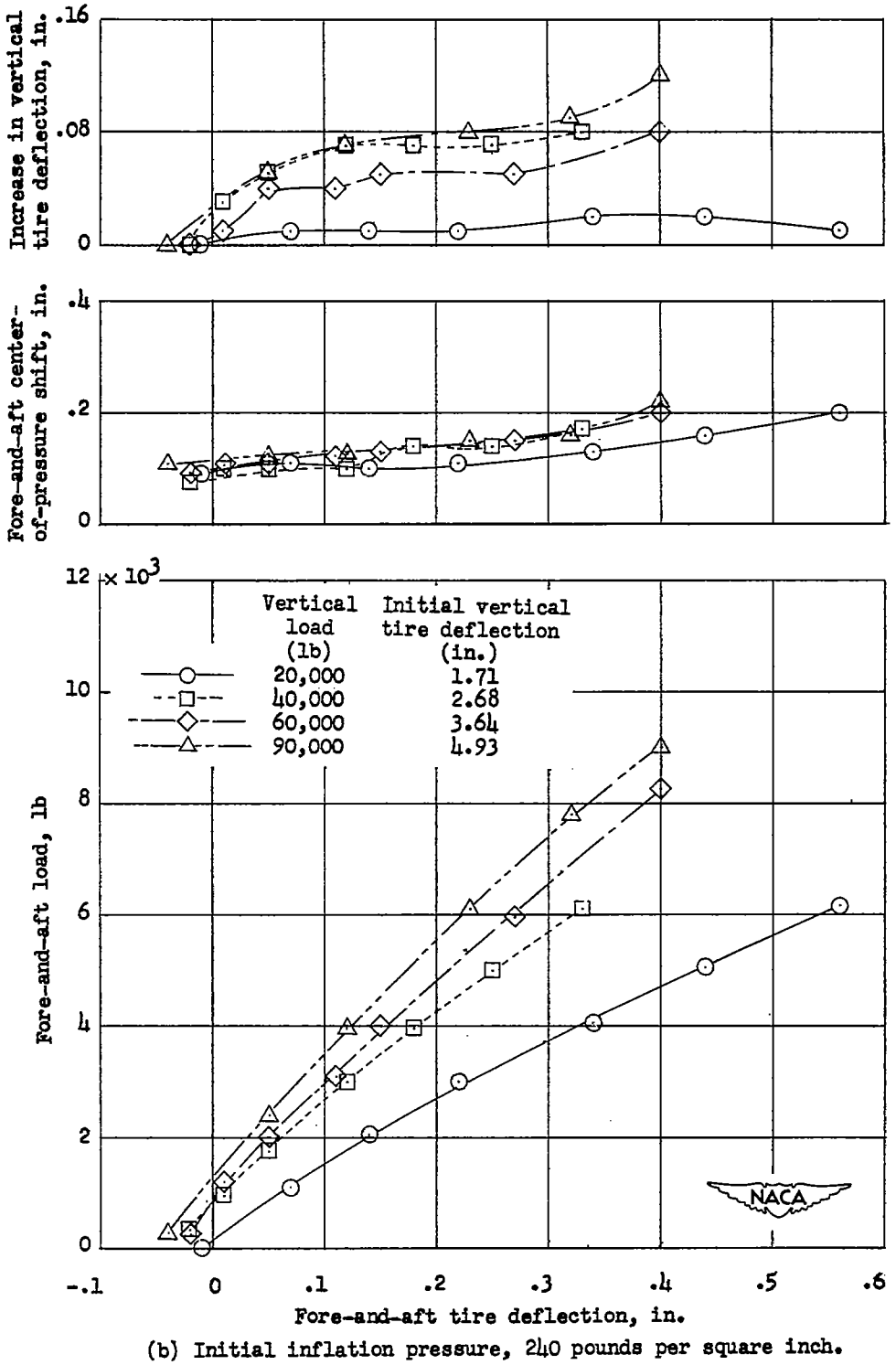

(b) Initial inflation pressure, 240 pounds per square inch.

Figure 32.- Continued.

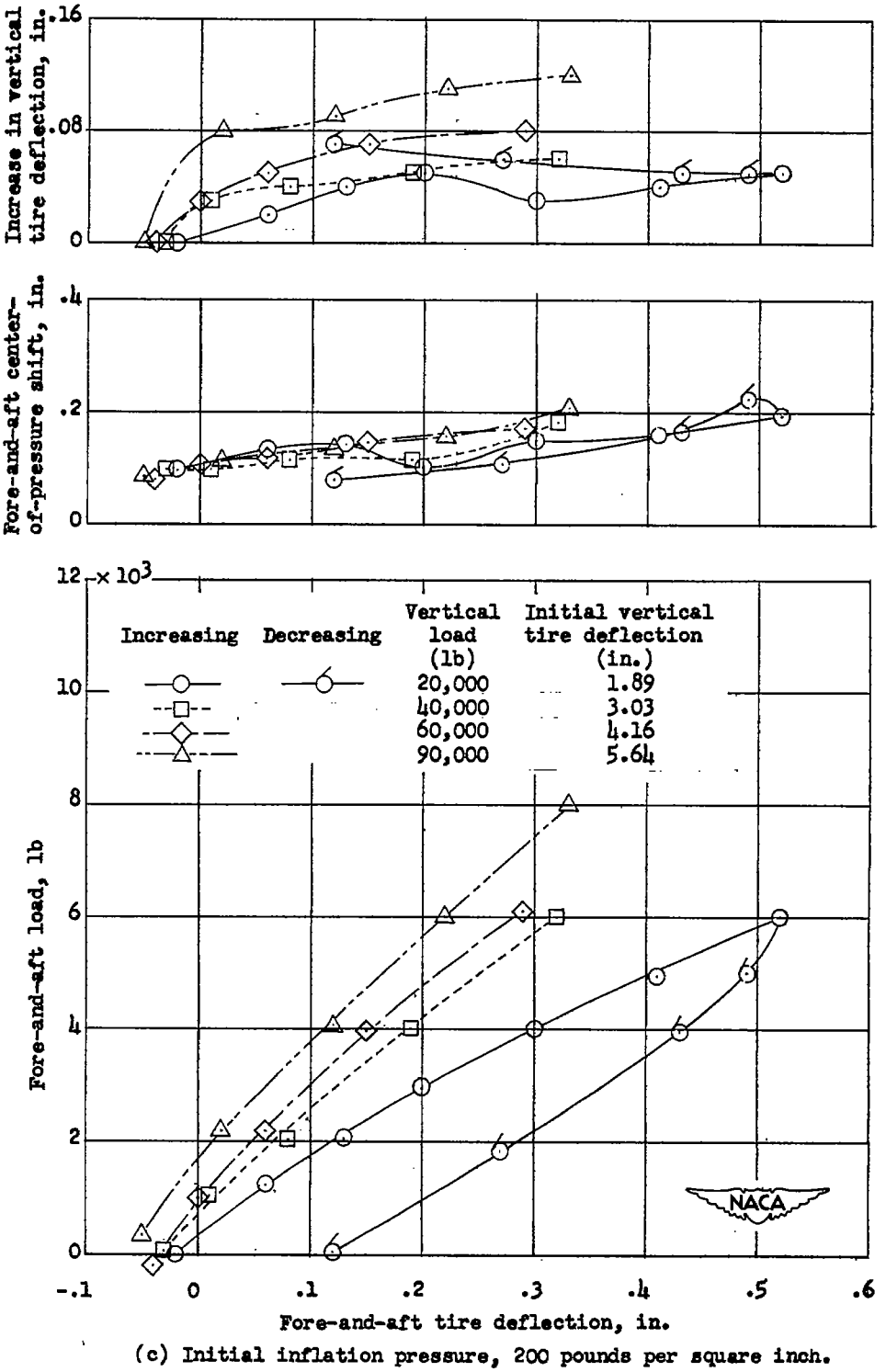

(c) Initial inflation pressure, 200 pounds per square inch.

Figure 32.- Continued.

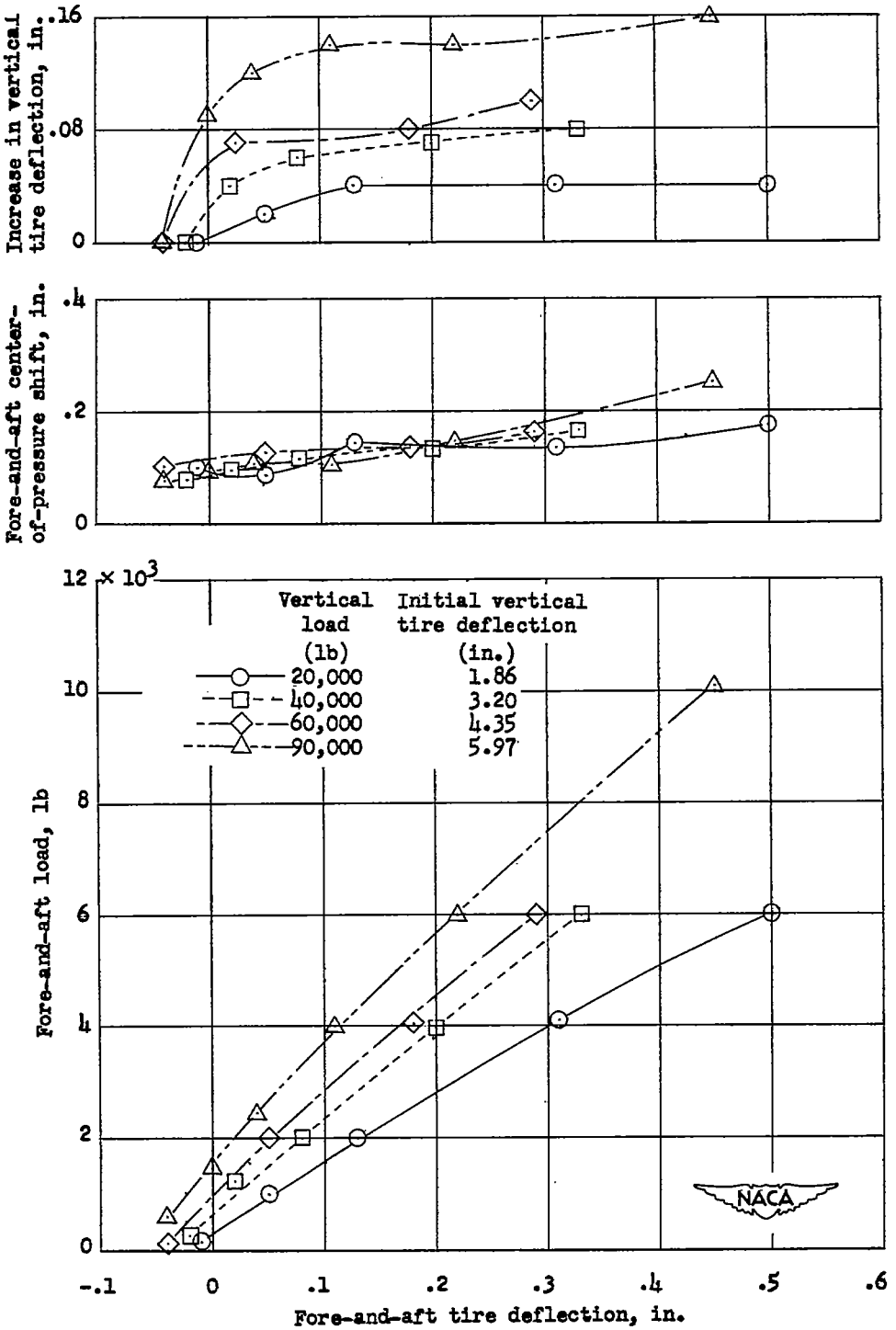

(d) Initial inflation pressure, 180 pounds per square inch.

Figure 32.- Concluded.

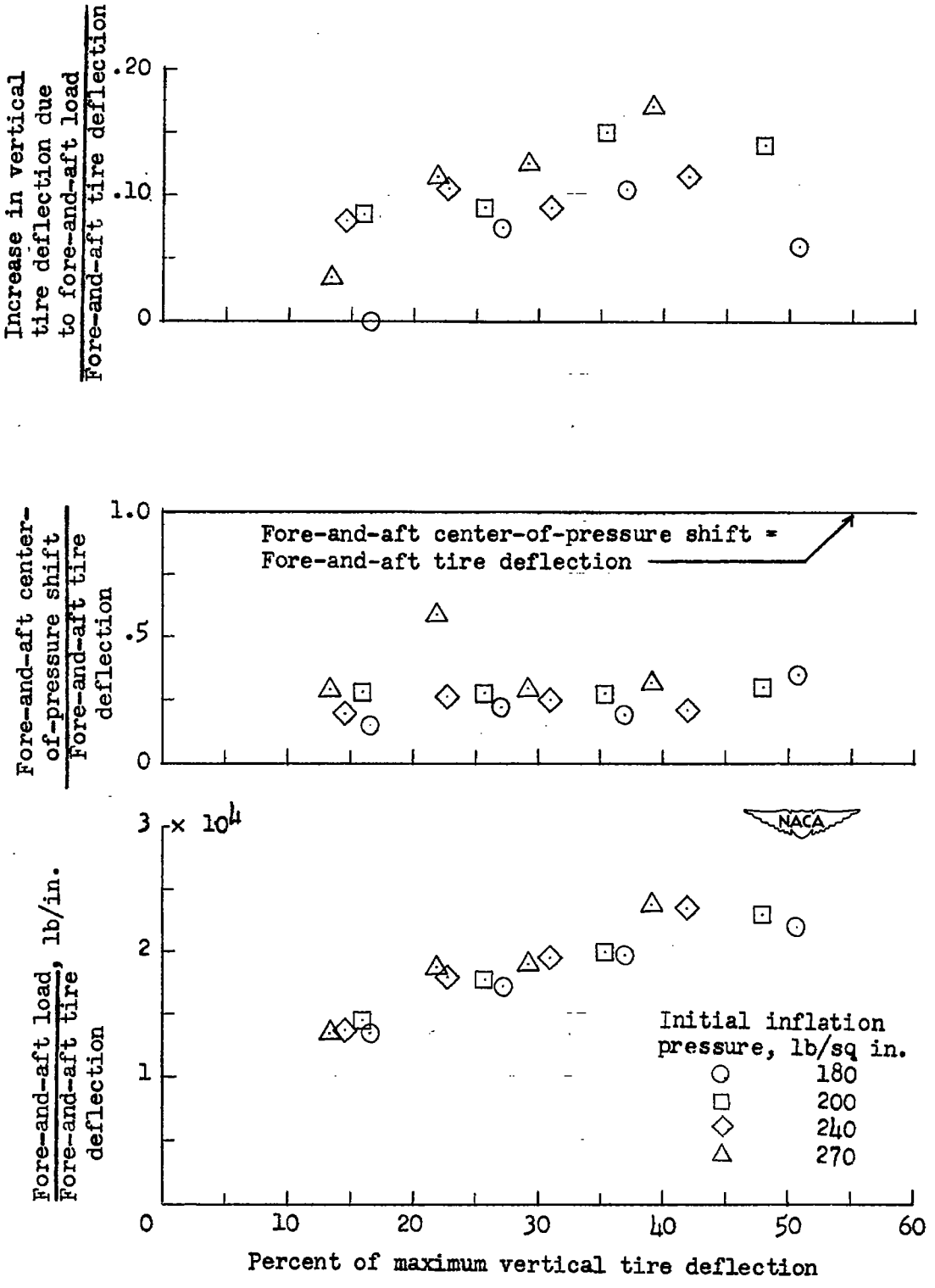

Figure 33.- Variation of fore-and-aft load tire characteristics with vertical tire deflection and initial inflation pressure for the 56-inch, 32-ply-rating tire (tire A).

NACA-Langley - 5-8-53 - 1000